Examining claims of long-range molecular order in water molecules.

Peter Spencer

Submitted in fulfilment of the requirement for the degree of Master of Philosophy

Principal Supervisor: Associate Professor Elizabeth Williams

School of Biomedical Sciences

Faculty of Health

Queensland University of Technology

Associate Supervisor: Dr Jamie Riches

School of Earth, Environmental and Biological Sciences

Science and Engineering Faculty

Queensland University of Technology

Thesis by Monograph

2018

STATEMENT OF ORIGINAL AUTHORSHIP

"The work contained in this thesis has not been previously submitted to meet requirements for an award at this or any other higher education institution. To the best of my knowledge and belief, the thesis contains no material previously published or written by another person except where due reference is made."

QUT Verified Signature

Signature

Date 31/1/18

TABLE OF CONTENTS

ABSTRACT

Water is the most common liquid on Earth and is vital for all life. It plays important roles in biomolecular, as well as a host of other, chemical interactions. The molecular structure of liquid water has been under investigation for almost a century and is influenced by a number of factors. One such factor is hydrophilic surfaces. Evidence indicates that the molecular structure of the hydrophilic surface acts as a template to the arrangement (order) of the adjacent water molecules (interface water). It has been proposed that the combination of surface structure, surface bond strength and the directional nature of hydrogen bonds cause a region of "structure" that extends into the bulk beyond that expected by the Double Layer theory.

The nature and extent of this region of "structured" water has been a matter of debate. In the past decade it has been claimed that there is strong evidence for long-range order in water adjacent to hydrophilic surfaces, even as far as 500 μm. Also, numerous bodies of research have provided evidence that magnetic fields affect the strength of hydrogen bonds and, consequently, the structural properties of liquid water.

Other research, however, indicates that the evidence supporting the claims of long-range order is misinterpreted. Alternate interpretations are presented that seem to better fit much of the data. One piece of supporting evidence is the presence of birefringence at the water-surface interface which does not have a compelling alternative explanation. This optical phenomenon is usually associated with crystalline order in mineral and osseous (bone-like) samples and appears to give strong evidence of long-range order in liquid water.

The effect of magnetic fields on hydrogen bonds is also a source of debate with much evidence on either side of the argument. However, the work by one researcher in particular, Xiao Pang-Feng, has presented what appears to be strong support for the magnetic treatment of water.

The hypothesis of this study is that, surface-induced water structure may be verified by noting the physical, optical and electrical changes at the water-surface interface, and its extent can be increased by using magnetic fields to increase hydrogen bond strength and subsequent coordination. In order to support this hypothesis multiple experiments were conducted to identify the differences between interface water and bulk water and to examine the validity of claims for and against the long-range order theory. Magnetic fields were also applied to examine the claims for and against their ability to strengthen hydrogen bonds.

Results show that previous evidence for long-range order can be attributed to factors other than molecular ordering such as a diffusion of ions from the material into the water and birefringence by reflection. No change to the molecular properties of water due to magnetic influence could be detected. Also, further reflection on some of the evidence presented to indicate magnetically structured water appears highly questionable.

An accurate understanding of the phenomenon known as “structure” in water may provide insight into how water functions in biological systems and thus provide insight into the role of water in the regulation of cellular processes such as intracellular communication and transportation.

This study is significant in that it aids scientific endeavour by clearing the path of some of the more erroneous presentations of data.

ACKNOWLEDGEMENTS

I gratefully acknowledge all the people who supported me in this project in so many ways. To my supervisors, Elizabeth Williams, Jamie Riches and Stephen Hughes, for your support and guidance and keeping me from being drawn off track by my flights of fancy. To all the technical support staff for your excellent advice and for taking an interest in my project. The following heads of discipline who have so generously given of their time and knowledge: Bill Kwiecien, Wayde Martin and Geoffrey Will. To my daughters, Renee and Briony, for your tolerance, patience and support throughout this project. Finally, I wish acknowledge my late wife, Kerry Lee, who encouraged me to pursue my crazy ideas through knowledge and research.

FIGURES

ABBREVIATIONS

3D	Three dimensional
A	Proton Acceptance
AA	Double proton acceptance
AC	Alternating Current
AFM	Atomic force microscopy
ANSTO	Australian Nuclear Science and Technology Organisation
D	Proton donation
DA	Single proton donor – single proton acceptor
DAA	Single proton donor – double proton acceptor
DD	Double proton donor
DDA	Double proton donor – single proton acceptor
DDAA	Double proton donor – double proton acceptor
DL	Double layer
EIS	Electrochemical impedance spectroscopy
E-ray	Extraordinary ray
EZ	Exclusion zone
FTIR-IRS	Fourier transform infrared internal reflection spectroscopy
H	Hydrogen
IR	Infrared
O	Oxygen
O-ray	Ordinary ray
ROI	Region of interest
SANS	Small angle neutron scattering
TOSH	Tetrahedral oxy-subhydride
VSEPR	Valence shell electron pair repulsion theory
UV Vis	Ultraviolet visual spectroscopy

CHAPTER 1

Chapter 1 INTRODUCTION

This chapter covers the background (section 1.1), context (section 1.2), purpose (section 1.3) and the significance and scope (section 1.4) of this research. Finally, section 1.5 gives an outline of the remaining chapters of this thesis.

1.1 BACKGROUND

The single water molecule may be simple but the behaviour of the liquid is complex and dynamic, particularly as it interacts with other substances. The common perception of liquid water is that it is random in its order but this is far from true. The molecular nature of liquid water has been under investigation for almost a century revealing structure, particularly at the interface of other molecules (Henniker 1949, Ling 1964, Drost-Hansen 1969, Ling, Miller et al. 1973, Lum 1998). The properties of an adjacent surface (i.e. the rigidity of the surface groups able to form hydrogen bonds as well as their areal density and lateral arrangement) greatly affect the configurational response of water molecules. Due to the cooperative and directional nature of hydrogen bonds in water a molecular network is formed. Disruption to this network by the presence of other molecules affects the arrangement of not only adjacent water molecules but has a reorienting affect further into the bulk. The region of reoriented water molecules has been observed to be distinctly different to the bulk. These differences are attributed to hydrogen bond strengths; where higher bond strengths represent greater directional (ice-like) bonds with greater ordering and reduced molecular density, and lower bond strengths represent distorted hydrogen bonds, reduced ordering and greater molecular density (Gun'ko, Turov et al. 2005). The region of increased order is regarded as structured. However, the nature and extent of the structure is unknown.

This structured region (also known as interface water) has been observed to extend more than the conventional two molecular layers beyond the adjacent surface into the bulk fluid. Indeed there has been some research reporting that structured water has been observed to extend more than 100 μm into the bulk, i.e. many layers (Yalamanchili, Atia et al. 1996, Gragson and Richmond 1998, Vogler 1998, Zheng and Pollack 2003, Zheng, Chin et al. 2006, Bunkin, Ignatiev et al. 2013).

Although structuring can be initiated by both hydrophilic and hydrophobic surfaces, the most prominent effects are found with hydrophilic surfaces

(Drost-Hansen 1969, Major, Houston et al. 2006, Jena and Hore 2010, Chai, Mahtani et al. 2012). These surfaces can be both biological and non-biological in nature. The non-biological materials include minerals, metals, polymers and hydrogels.

Various techniques have been employed to investigate not only the thickness of the interface region but also the structure or arrangement of the molecules therein. These techniques range from experimental methods such as Infrared internal reflective spectroscopy and X-ray scattering to theoretical molecular dynamics simulations. The outcome of which propose a range of structure types including ice-like tetrahedral coordination (Henao, Busch et al. 2016), a network of ring conformations (Wernet, Nordlund et al. 2004) and vortex-like structures (Higo, Sasai et al. 2001, Dickey and Stevens 2012).

From studies on hydration layers in the mineral/water interface it is quite apparent that the configuration (roughness), spacing and chemical characteristics (i.e. charge) of the surface molecules have a templating effect on the adjacent water molecules. The vertical extension of this effect has been seen to vary from a single layer on muscovite (as observed using x-ray scattering techniques (Fenter and Sturchio 2004) to 262 nm (hundreds of layers) on silicon surfaces using Fourier transform infrared spectroscopy (Yalamanchili, Atia et al. 1996). The vertical extension of this templating effect produces a region of highly ordered, low density ice-like water near the surface (Yalamanchili, Atia et al. 1996) with decreasingly ordered high and low density water extending into the bulk (Chaplin 2001, Gun'ko, Turov et al. 2005, Totland, Lewis et al. 2013). This range of order and density in the phase known as interface water may consist of numerous structural variations within the same phase.

There are multiple factors attributed to the generation of interfacial water including ionic and covalent interactions, electrostatic surface fields, Van Der Waals forces and highly directional hydrogen bonding.

In recent years there have been several studies that claim to observe structured interfacial water to distances greater than 200 μm (Zheng and Pollack 2003, Chai, Yoo et al. 2009, Chai and Pollack 2010). The predominant evidence for such claims is the physical exclusion of particles (microspheres) from the hydrophilic surface (thus it is known as Exclusion Zone – or EZ). Opponents to this claim suggest the long-range effect is caused by chemical diffusion (Schurr 2013, Florea, Musa et al. 2014, Huszar, Martonfalvi et al. 2014). However, alternate supporting evidence, in the form of observed birefringence, indicate the EZ is a liquid-crystalline state (Bunkin, Ignatiev et al. 2013, Le Bihan and Fukuyama 2016). This has yet to be addressed. It

may be that as the evidence for long-range order has opposing interpretations there may also be alternate explanations for the presence of birefringence at the water-surface interface.

Magnetic fields have been shown to affect the physicochemical properties and structure of water (Ozeki, Wakai et al. 1991, Nakagawa, Hirota et al. 1999, Chang and Weng 2006, Ghauri and Ansari 2006, Pang and Deng 2008). Many of these effects are attributed to strengthening or weakening of the hydrogen bonds and the presence of dissolved oxygen (Ozeki and Otsuka 2006). However, the topic of magnetic water treatment is controversial due to irreproducible results and experimental error (such as magnetically induced contamination).

One theory proposed by Pang (Pang 2006) suggests that hydrogen bonded closed-ring structures in the water molecules have a magnetic dipole which aligns to the external magnetic field. Once aligned, multiples of these structures maintain their alignment after removal of the magnetic field. This is proposed to be the mechanism by which magnetic fields influence the structuring of water. Experiments using infrared, Raman and UV-Visual spectroscopy techniques appear to provide strong support for this claim (Pang and Deng 2008).

Other possible mechanisms of magnetic effect include distortion of the hydration shell and/or coordination of water molecules at the water-particle/surface interface. In this case Lorentz forces are implicated whereby conductive particles passing through a magnetic field experience orientating and/or displacing force. However, this cannot be attributed to all evidence presented. Despite much research on magnetic effects on water there remains no universally agreed magnetic mechanism.

Despite the controversy, there appears to be strong evidence supporting the magnetic effect on the molecular structure of water, particularly at the interface of other particles (Fenter and Sturchio 2004). Therefore, it would seem prudent to examine what effect magnetic fields have on interface water. It is envisioned that if magnetic fields enhance interface water this will give further insights to the nature of this phenomenon. As yet, this has not been explored and will be addressed in this study.

1.2 CONTEXT

Water is essential to all life. However, it has only recently been acknowledged that in biological systems water plays more than a passive role. Indeed, it is regarded to be a major facilitator of many, if not all, intracellular activities (Chaplin 2001, Chaplin 2006, Ball 2008).

As the structuring of water at biomolecular interfaces is considered vital for intracellular function, the disruption of this structure may promote cellular dysfunction and cancer (McIntyre 2006, Pokorný 2011, Pokorný, Vedruccio et al. 2011, Abramczyk, Brozek-Pluska et al. 2014). Comprehension of water structuring due to surface interaction, and factors that influence it, may lead to discovering ways to re-establish perturbed structure in biological systems and reverse pathological dysfunction.

1.3 Purpose

This study seeks to explore claims of structuring, or long-range ordering, detected in water and determine the nature of the unusual properties exhibited. Such properties include density differences, exclusion of solutes, altered conductivity and increased molecular order. This foundational understanding is critical to further investigations into water within biological systems.

1.4 Significance, scope and definitions

Interfacial water is vital for physical and chemical interactions within cells (Chaplin 2006, Ebbinghaus, Kim et al. 2007, Ball 2008, Frauenfelder, Chen et al. 2009). However, in order to understand and make use of the properties of water in these complex environments we first need to understand it in simpler conditions. Structured interfacial water has been observed to extend further into the bulk from hydrophilic surfaces than from hydrophobic surfaces (Jena and Hore 2010). As such is the case, water adjacent to a hydrophilic environment will be the focus of this study. The complexities of biological considerations are beyond the scope of this study. This is because such issues as molecular crowding and localised hydrophilic effects (i.e. folding proteins around a hydrophobic molecule), whilst involving water, are also influenced by other factors. In the case of molecular crowding there is the factor of limited space to allow structuring as seen in less crowded environments. Also, with the folding of proteins there is a combination of hydrophobic and hydrophilic interactions. More uniform conditions would provide the preferable environment for studying water structure (Ball 2008).

1.5 Thesis Outline

The following chapters cover the literature review, experimental investigations, discussion and conclusion.

The literature review covers the history of studies on water at the hydrophilic surface interface, the theories of its structure and some of the controversies that have ensued. This section also

covers the study of the effects of magnetic fields on water and the implications such fields may have on interfacial water.

The chapters on experimental investigations detail the methods by which interfacial water was studied, the reasoning behind the studies and the outcomes of each study.

The Discussion and Conclusion chapters review the outcome of the experiments, their limitations and implications for further understanding the molecular physics of water.

CHAPTER 2

Chapter 2 LITERATURE REVIEW

Water is the most abundant liquid on Earth. The structure of a single water molecule is well understood. However, there is considerable controversy in what is understood to be the "arrangement" of water molecules within the liquid phase and particularly those adjacent to other surfaces. Liquid water cannot be considered a simple liquid in which molecules can be represented as particles with spherical or non-directional interaction. The geometric constraints imposed by the hydrogen bonds impact properties such as density, heat capacity and compressibility, thereby causing liquid water to not correspond in a linear fashion to temperature as expected in a simple liquid (Ball 2008) (Nilsson and Pettersson 2015) (and references therein).

An example of this is seen in that the density of water increases with decreasing temperature until a maximum density is reached at 277 K (4°C). With further cooling the density decreases. To further highlight the complex nature of water multiple states have been identified. Like many substances water has three basic phases; solid, liquid and gas. However, within the liquid and solid phases there are multiple variations that have significantly different molecular structures, and therefore properties, to others within the same phase. Figure 2-1 depicts a phase diagram of water in which the solid, liquid and gaseous phases are represented by different colours. Within the solid phase (blue region) are several subdivisions denoted by roman numerals. These represent the different crystal structures. For instance, ice Ih is the most commonly found form of ice and has a hexagonal lattice structure, ice II has a rhombohedral crystal cell structure and the unit cell of ice III forms tetragonal crystals. The prominent factors affecting the phase differences, and structural variations, are temperature and pressure (Lyapin, Stal'gorova et al. 2002).

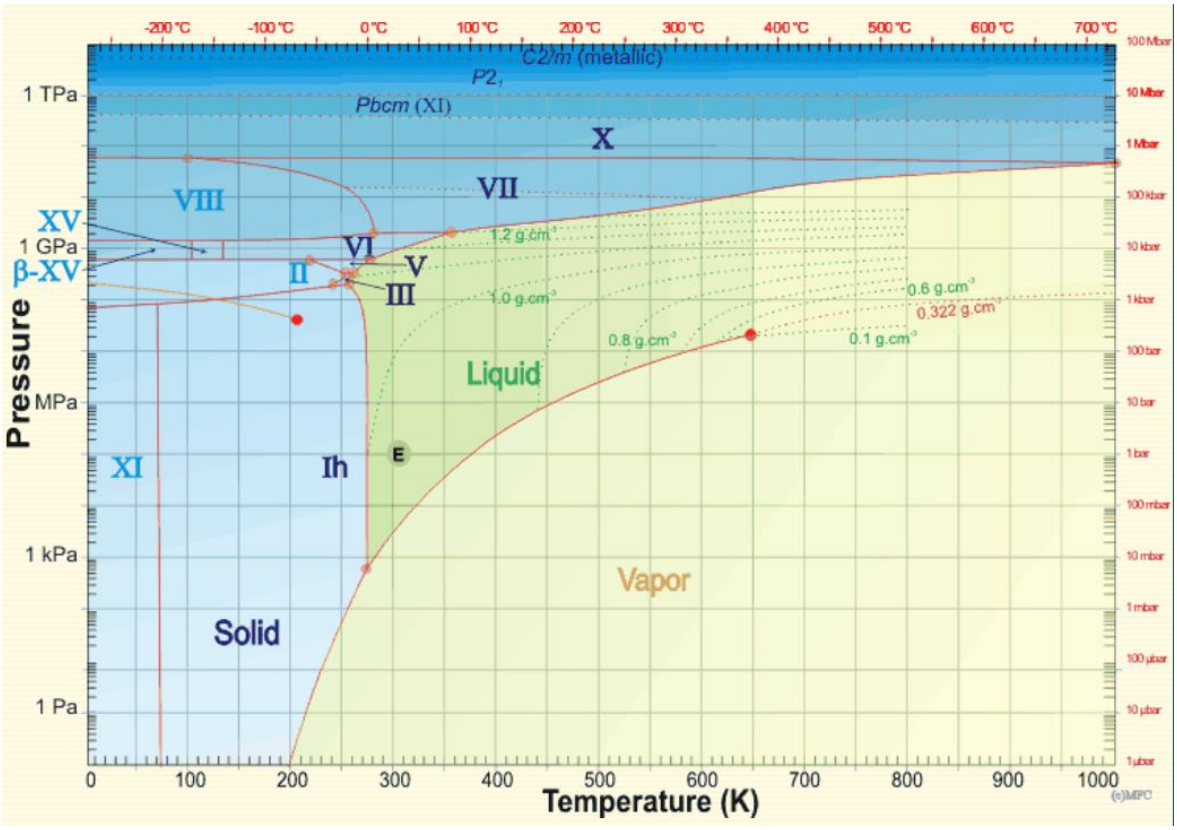

Figure 2-1 Water Phase diagram.

Reproduced from Chaplin (2017 d). Subdivisions within the solid phase are denoted by Roman numerals according to their crystal structures. Red lines denote distinct phase boundaries. The vertical axis (pressure) has a logarithmic scale as the required pressures vary over more than ten orders of magnitude.

There are, however, other factors that can affect the molecular arrangement (and therefore structure) of a liquid, namely adjacent interface properties. Such interfaces are the liquid-gas, liquid-liquid (such as oil and water) and liquid-solid interfaces. It is important to note that water is an associative liquid in that changes made to one region (i.e. the interface) may extend to affect the molecular arrangement of other regions. The distance to which this effect extends has been a matter of discussion for decades.

2.1 Water Structure

A review by Henniker (1949) identifies W. B. Hardy as the first to introduce the concept that although the radius of structuring influence of a single molecule may be small (the diameter of the molecule), strain on one molecule may be transmitted from molecule to molecule, thereby effecting a realignment of molecules to a distance of hundreds of microns (Hardy 1912). Thus it is theorised that a single layer of water molecules linearly bonded (via hydrogen bonds) to a solid surface may have a polarising effect within the liquid to considerable distances, thereby forming a distinctly different layer of water between the influencing surface and bulk water

(uninfluenced water). It is worth noting that apolar (i.e. hydrophobic) surfaces also induce structure by limiting hydrogen bonding to the surface. This reorienting of the water molecules has a "knock on" effect where molecules further from the surface are also reoriented (Fenter and Sturchio 2004, Ball 2008, Jena and Hore 2010).

More recently, this concept of long-range influence was taken up by Gilbert Ling noting that molecular arrangements at the surface interface of biological macromolecules can profoundly affect biological activity further from the initiating surface (Ling 1964, Ling 1965, Ling 2003). Here Ling postulates that all water in living cells does not exist as a single physical state but "exists reversibly in more than one metastable cooperative states in the course of its normal physiological activity." (Ling 1965). He proposes that water molecules in living cells form dynamic polarised multilayers oriented on surfaces of cellular proteins. Indeed, other researchers propose that intermolecular communication and transport within the biological cell depend on not just the water but the structure of the water in the interface region (Peter, Pethig et al. 1981, Pokorný 2004, Pokorný, Vedruccio et al. 2011, Mills, Orr et al. 2013). Similarly, it is proposed that the region known as interfacial water facilitates most, if not all interactions within the cell (Chaplin 2001, Jasnin, Moulin et al. 2008, Ball 2008 a, Mills, Orr et al. 2013). As the structure (i.e. molecular arrangement) of interface water differs to that of bulk water, it may be that bulk water is unable to facilitate the same interactions as interface water. It has been proposed, therefore, that the type and proportion of water within the cell (interfacial or bulk) will affect intermolecular functionality, and therefore the health of the cell (Pokorný 2011, Abramczyk, Brozek-Pluska et al. 2014). This seems to be supported by the use of Nuclear Magnetic Resonance to detect cancer. In this method, the spin echo nuclear magnetic resonance of the spin lattice and spin-spin relaxation times of water molecules in normal tissue are compared with that of malignant tissue. It has been found that there is a significant increase in relaxation times in malignant tissue samples compared to normal tissue. Such greater motional freedom has been interpreted as reduced structure (i.e. reduced constraining forces associated with structure) within the cell water (Damadian 1971, Damadian, Zaner et al. 1974). It is also found that cancer cells are more hydrated than noncancerous cells (McIntyre 2006) with a greater volume of bulk water compared to interface water (Abramczyk, Brozek-Pluska et al. 2014). In other words, bulk water appears to be less constrained in its molecular movement and orientations than interface water.

With the above in mind it is apparent that understanding the nature of interfacial water may be of great significance to understanding intracellular activities and its effect on the general health of the cell.

In order to understand what is meant by “structure” in interfacial water we begin with a single water molecule. Figure 2-2 depicts a water molecule showing the angled arrangement of the hydrogen atoms around the oxygen atom, the distance between the oxygen and hydrogen atoms, the polarity and charge difference between the two elements and the general shape of the electron cloud. This is considered the most thermodynamically stable arrangement but variations in the physical values occur due to bonding with other molecules.

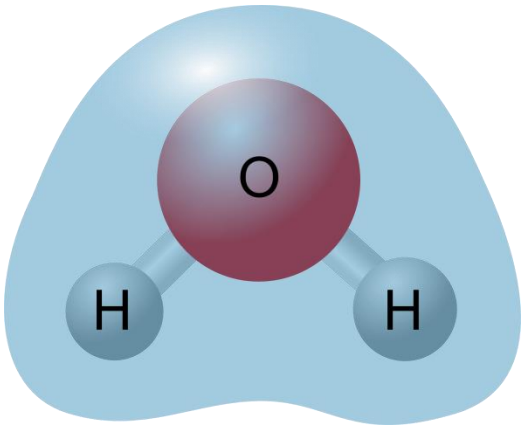

Figure 2-2 Water molecule with electron cloud depicted.
The oxygen (O) atom is red, hydrogen (H) atoms white and electron cloud green. In thermally stable conditions of liquid water the O-H length is around 0.991 Å and the H-O-H angle ~105.5°. These values vary in different hydrogen-bonded environments and when the water molecules are bound to solutes and ions. (Chaplin 2017 b).

Figure 2-3 is a depiction of the electron cloud surrounding the water molecule from an angled view. Here we can see that the charged volumes, where hydrogen atoms bond, are concentrated in specific locations around the molecule.

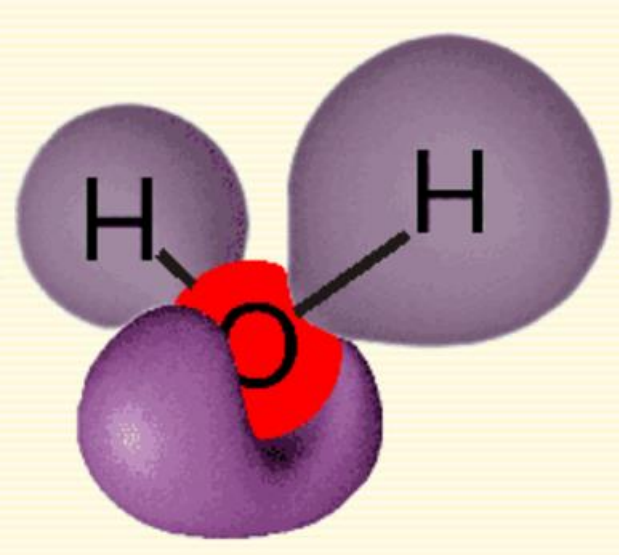

Figure 2-3. Angled view of electron cloud surrounding a water molecule.
A depiction of the shape of the electrons surrounding a single water molecule. The upper electrons are located relatively evenly around the hydrogen (H) atoms and lower electrons are more distinctly located below the oxygen (O) atom and away from the H atoms. Reproduced from Chaplin (2017 b) Water structure and science.

The reason for the configuration of the water molecule is made clear by understanding the electron orbitals involved. An oxygen atom has 8 electrons in total, 6 of which are valence electrons available for bonding. The Lewis dot structure diagram below (figure 2-4) shows a simple, 2-dimensional representation of bonding 2 hydrogen atoms to an oxygen atom to form water.

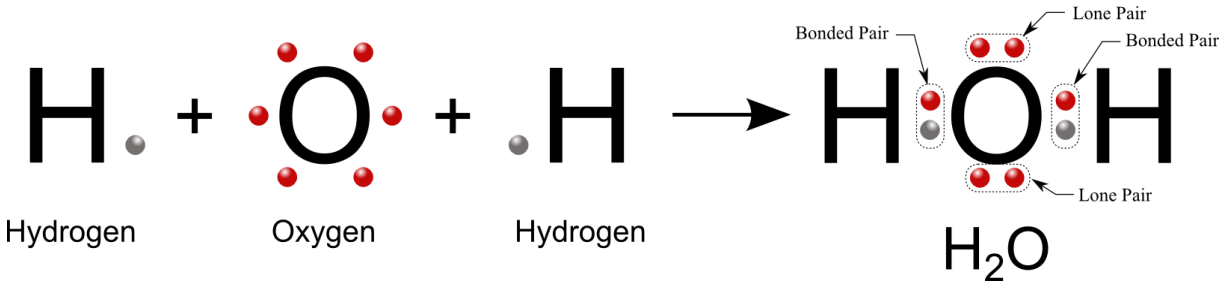

Figure 2-4. Lewis dot structure diagram of the formation of water.
Hydrogen (H) atoms combining with an oxygen atom (O) to form water. Bonds are formed when electrons from the hydrogen atom (grey spheres) pair with electrons from the oxygen atom (red spheres). The remaining electrons from the oxygen atom form lone pairs (right hand side).

Here we see the electrons from the hydrogen atoms bonding to electrons in the oxygen atom leaving the remaining 4 electrons to form non-bonded, lone pairs.

The geometry (3-dimensional configuration) of the water molecule is determined by the electron orbitals of the central oxygen atom. Figure 2-5 represents the oxygen atom showing electron shell orbitals. An orbital is a simple way to represent the most probable location of electrons within their given electron shells.

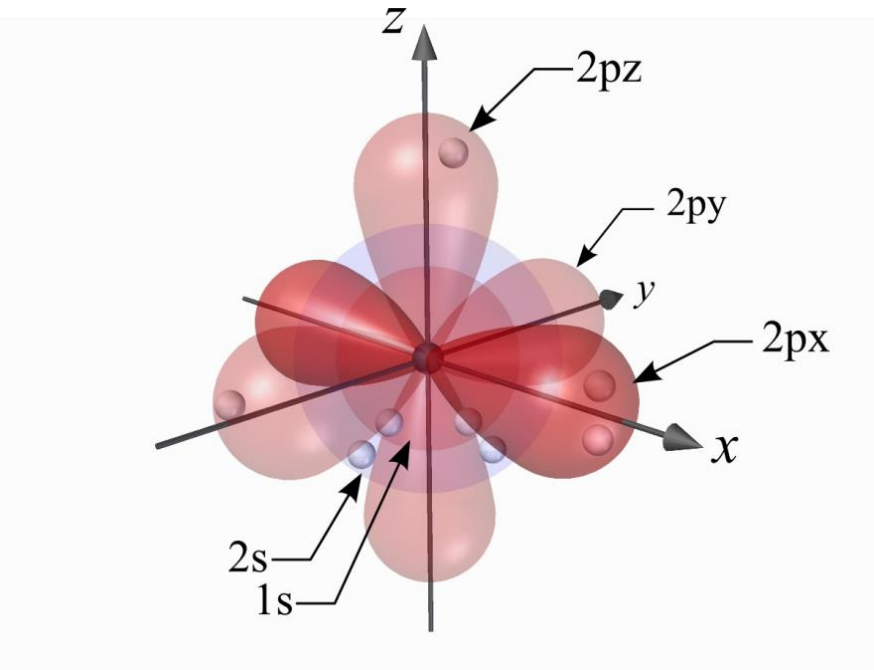

Figure 2-5. Electron orbitals of an oxygen atom.
All orbitals are centred around the nucleus (central black sphere). The spherical 1s and 2s orbitals have 2 electrons each. The 2p orbitals are shaped as shown and oriented around the x, y and z axes. One of the p orbitals has 2 electrons ($2p_x$ – darker red) and the other 2p orbitals have only 1 electron each ($2p_y$ and $2p_z$).

Here we see the electrons located around the central nucleus. The spherical 1s orbital has the lowest energy and is completed (or filled) with two electrons. The 2s orbital is also spherical with higher energy and is also filled with two electrons. Each of the 2p orbitals are similar in form to a three dimensional figure-8 and are aligned along the x, y and z axes as shown. Note that only the $2p_x$ orbital (darker red) is filled with two electrons while the $2p_y$ and $2p_z$ orbitals are unpaired. In this situation the electrons in the three 2p orbitals combine with the 2s orbital to form four hybridised $2sp^3$ orbitals in a tetrahedral configuration (figure 2-6). This is because according to Valence Shell Electron Pair Repulsion theory (VSEPR) the electrons will arrange themselves around the central atom so there is minimum repulsion between them.

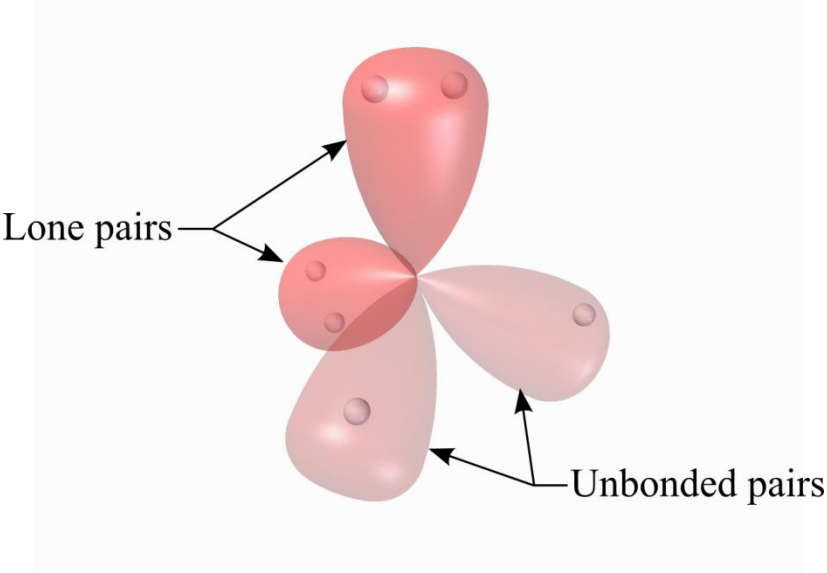

Figure 2-6. Arrangement of valence electrons of an oxygen atom.
Two of the hybridised sp^3 orbitals have 2 electrons (darker red), forming lone pairs, while the remaining 2 have only one electron.

However, two of the $2sp^3$ orbitals only have one electron in each while the other two form lone pairs. It is these single-electron orbitals that form covalent bonds with hydrogen atoms to complete the electron complement of the orbitals as shown in figure 2-7.

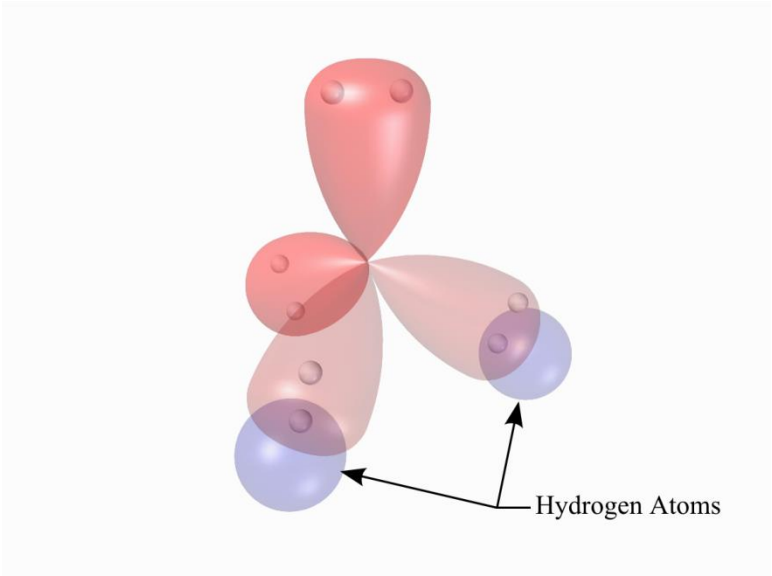

Figure 2-7. Water molecule orbitals with hydrogen atoms (blue spheres).

However, lone pairs have greater repulsion force than bonded pairs. This causes the lone pairs to extend further from the nucleus and the bonded pairs to move closer together as shown in figure 2-8.

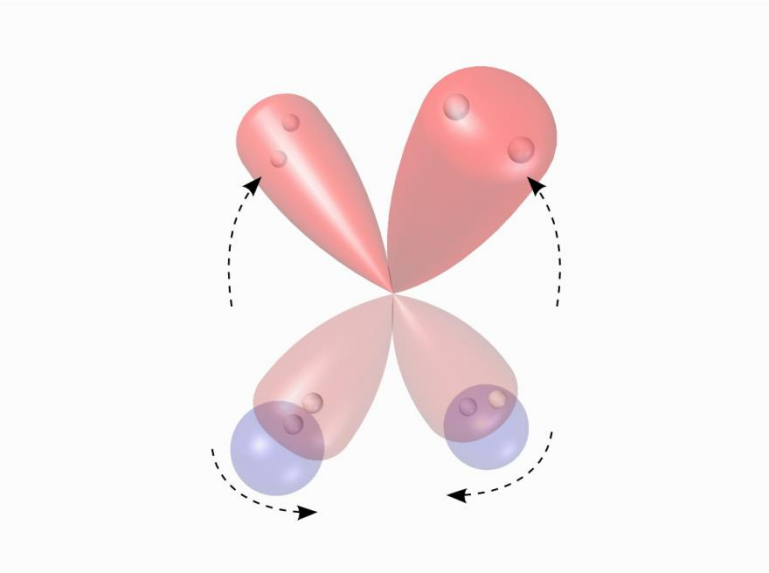

Figure 2-8. Final arrangement of water molecule orbitals.
The non-bonded pairs (darker red) extend further from the nucleus and the bonded pairs move closer together.

With this altered configuration the positive and negative charges are concentrated at opposite ends giving the molecule its polarity. This also explains why there are four points at which the hydrogen atoms bond one molecule to another. These are known as hydrogen bond points.

It is because of these hydrogen bonding points (and the molecular geometry) that water, without interference from thermal perturbations, tends to form a hexagonal lattice at 0° C and ambient air pressure (see figure 2-9).

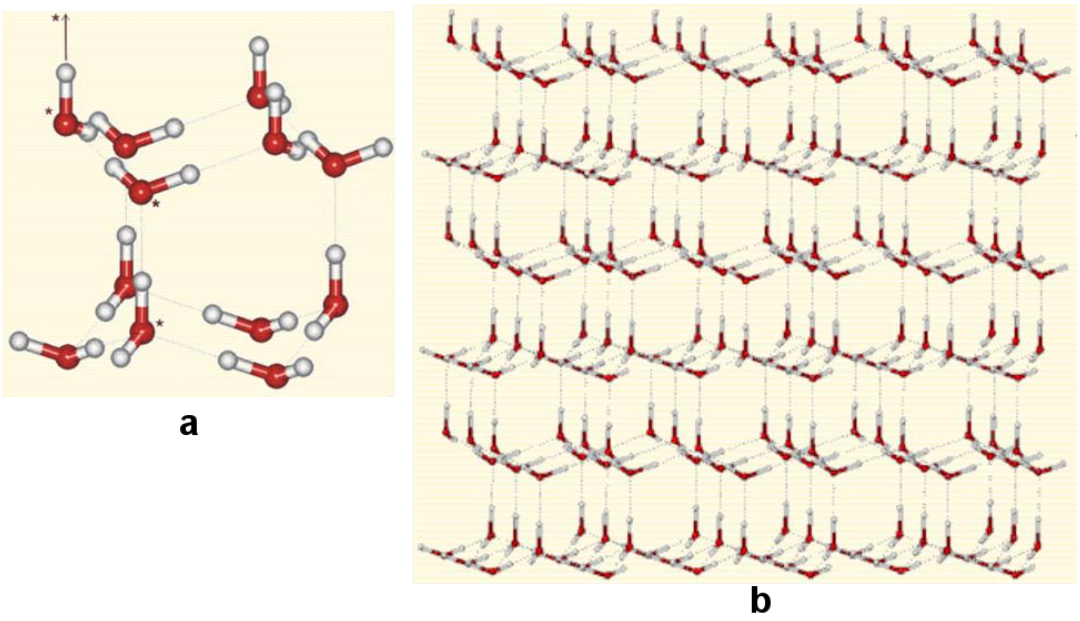

Figure 2-9. Hexagonal arrangement of ice lattice.
Linked hexagonally arranged water molecules (a) comprise a single unit of the ice lattice (b). Reproduced from Chaplin (2017 c), Hexagonal Ice.

In the presence of thermal perturbations, however, (i.e. in liquid phase) Chaplin (1999) proposes that alternate configurations are formed. Such configurations contain cage-like formations (clathrates) or clusters of various sizes and shapes yet within a dynamic network (Stillinger 1980, Gragson and Richmond 1998, Head-Gordon and Hura 2002, Ebbinghaus, Kim et al. 2007, Clark, Cappa et al. 2010). Figure 2-10 shows a few examples of the proposed possible cluster formations.

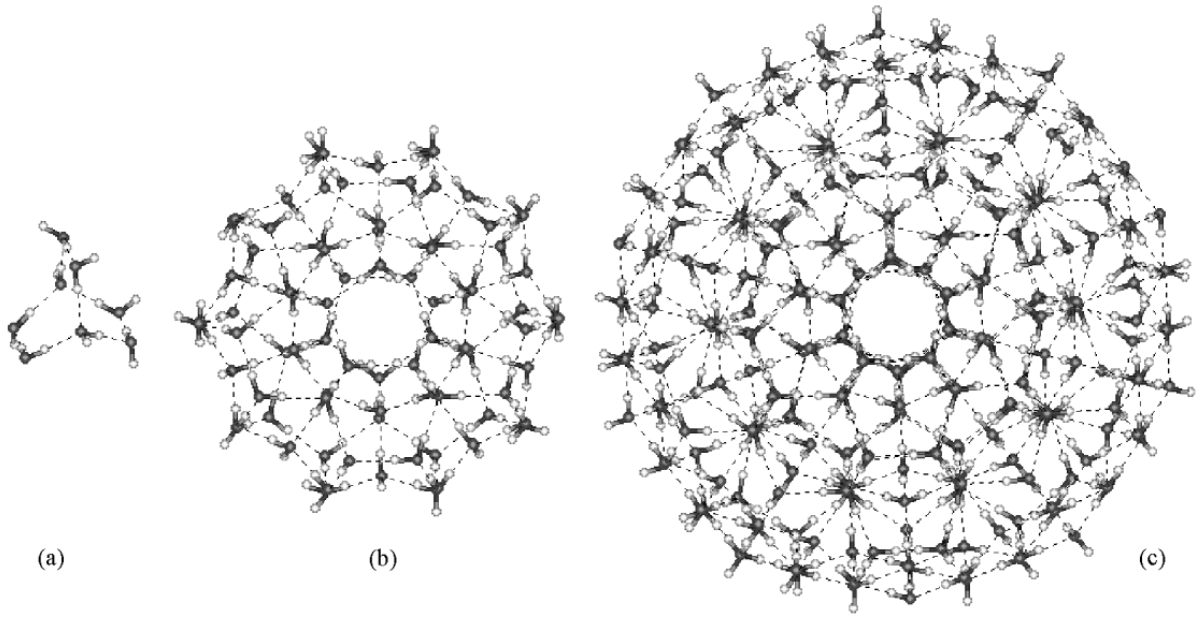

Figure 2-10. Water clusters.
(a) A small but relatively stable octamer $(H_2O)_8$, (b) twenty octamers may come together to form an open structure centred on a water dodecahedron, (c) structure (b) may expand further to contain 280 water molecules forming an icosahedral cluster. Reproduced from Chaplin (2001).

According to Chaplin, the directionality and relative weakness of the hydrogen bond causes the clathrates and other structures to break due to disruption by thermal vibration and then quickly form other formations. This produces a fluctuating molecular network (Chaplin 1999). Structures of this nature have been considered responsible for the heat capacity of water (Benson and Siebert 1992). However, direct observation of such structures is yet to be produced.

Kim, Boehm et al. (2013), using a cantilever-based optical interfacial force microscope, observed large sawtooth-like oscillatory forces generated by confined water under lateral modulation between two hydrophilic surfaces. These were attributed to chain-like water structures in the nanoscopic space between the two surfaces with an estimated viscosity to be 10^8–10^{10} times greater than that of bulk water. Similarly, force microscopy experiments by Major, Houston et al. (2006) and Li, Gao et al. (2007) reveal viscosity several orders greater than the bulk between hydrophilic surfaces less than 2 nm apart. This has been attributed to increased tetrahedral ordering of the liquid and (in these cases) large numbers of hydrogen bonds to the surfaces.

Segtnan, Sasić et al. (2001) investigated the statistical analyses of near-infrared spectra of water at a band centred around 1450 nm at temperatures between 6° and 80 °C. They found that the wavelengths of 1491 and 1412 nm account for more than 99% of the spectral variation. These are seen to represent two major water species with stronger, linear hydrogen bonds and

weaker bifurcated hydrogen bonds, respectively. Whilst this does support the view that liquid water is a dynamic network of weakly bonded, high density and strongly bonded, low density structures it does not give indication of the form of these structures. This is somewhat consistent with the view of Benson and Siebert (1992) who propose a simple two-structure model of liquid water. However, it should be noted that Segtnan, Sasić et al. also identified evidence of a third species of structuring located at 1438 nm, whose concentration was relatively constant as a function of temperature. It is their view that the "simple" two-state model of water structure is inadequate to account for waters properties.

The above experimental and simulation results do not necessarily confirm the existence or form of clathrate structures in liquid water but they do highlight the structuring tendency owing to hydrogen bonds. The tendency of water to form structure is of particular interest at the interface of a gas or solid. Although there is a significant difference between the molecular structuring at the water-air and water-solid interface this study focusses on the effect initiated at the water-solid interface, particularly hydrophilic interfaces. It is here that other factors come into play such as the electrical properties of the surface, arrangement of hydrogen bond sites and surface configuration. As water adheres readily to surfaces with polar molecules these surfaces are labelled as hydrophilic (water loving). Surfaces with non-polarised molecules are labelled as hydrophobic (water fearing). The degree of hydrophilicity is demonstrated by the contact angle a droplet makes with the surface.

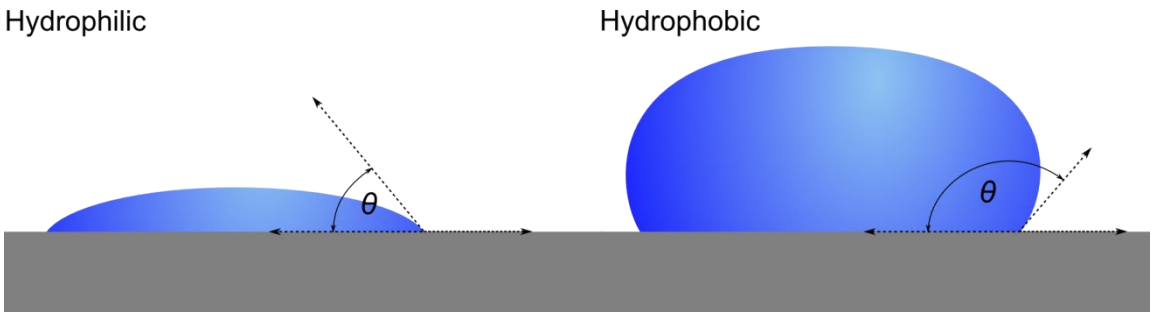

Figure 2-11 Hydrophilic and hydrophobic contact angles.
The hydrophilic surface (left) exhibits a low contact angle with the water droplet (θ<65°), whilst the hydrophobic surface (right) exhibits a much higher contact angle (θ>65°). Surface: grey; Water droplet: blue.

According to Vogler (1998), hydrophobic surfaces exhibit a contact angle greater than 65° and hydrophilic surfaces have a contact angle less than 65° (see figure 2-11). It is these hydrophilic surfaces that have recently been the centre of much interest and controversy. In particular, the question of how far a hydrophilic surface can influence the molecular arrangement of water from the nucleating surface into the bulk fluid. More than just the molecular arrangement, there

is also considerable interest in a possible long-range ordering influence beyond the double layer (Drost-Hansen 1969, Vogler 1998, Shelton 2014, Nilsson and Pettersson 2015, Henao, Busch et al. 2016).

It should be noted that water structuring is not necessarily always due to hydrogen bonding. In biological systems, macromolecular crowding within a cell can confine water between bilayer surfaces 1-3 nm's apart. In these circumstances Ji-Xin, Sophie et al. (2003), using coherent antistokes Raman scattering microscopy, observed that even though water molecules have enhanced ordering they are oriented with their dipoles opposed to the lipids and even more weakly hydrogen bonded than the bulk. However, as Ball points out, such ordering would be expected of any liquid owing to such a densely packed environment and lateral ordering due to surface structure. This is likely to lead to the disruption of hydrogen bonding (Ball 2008)(and references therein).

There is also the hydrophobic effect where water molecules near a non-polar (hydrophobic) surface tend to "turn back" in order to maximise hydrogen bonding. This creates an increase in strength of the hydrogen bonding adjacent to a hydrophobic surface such that they form a more ice-like arrangement (Gragson and Richmond 1998). According to Wiggins and Van Ryn (1986) water molecules adjacent to a hydrophobic surface or moiety of a solute are in a state of higher energy that those further away from the surface because they are unable to make bonds on that side. Due to the cooperative nature of hydrogen bonds, weak bonding is transmitted through several layers of water molecules by a configurational rearrangement. The hydrophobic effect extends to a distanced roughly equal to van der Waals-dispersion force but is an order of magnitude stronger (Israelachvili and Pashley 1982).

Here we see that hydrogen bonding, whether associated with a hydrophilic or hydrophobic surface, is considered the "main player" when it comes to long-range effects.

2.2 HYDROGEN BONDING

In the Double Layer (DL) principle (also called the Electrical Double Layer, EDL), as a charged (e.g. negatively charged) surface, particle or molecule is introduced to a fluid it is then surrounded by a layer of counter ions (e.g. positively charged). This initial layer will then be surrounded by a layer of oppositely charged (e.g. negatively charged) ions, thereby electrically screening the initial layer. As the bond strength between the second and first layers is less than that of the surface and first layer, this second layer is more able to move under the influence of electrical attraction and thermal motion. According to these principles the distance to which a

molecule can exert attractive or repulsive forces will only be to the extent of the two surrounding charged layers (see figure 2-17).

The forces acting on water molecules are a combination of long-range and short-range forces (Eisenberg and Kauzmann 2005). The long-range forces act over distances greater than ~ 3 Å and consist of electrostatic, induction and dispersion forces. At these large separations electrostatic forces predominate. These arise from permanent electric moments of the molecules and the interaction of their dipoles. It is because of this dipole interaction that the orientation of the molecules will determine whether the electrostatic forces are attracting or repelling.

In contrast, induction forces are invariably attractive. In this case the permanent dipole moment of one molecule will induce a dipole moment of another. Thus the molecules will reorient (rotate) in order to produce stronger attraction force between them.

Dispersion forces, also called London forces, arise from the correlated movement of electrons in neighbouring molecules. Put simply, at a given instant, the configuration of electrons of one molecule will result in an instantaneous dipole moment. This dipole moment induces a dipole moment in another interacting molecule.

Short-range forces dominate when water molecules approach within about 3 Å as is the case with liquid water and ice. These forces can be attributed to a combination of electronic overlap repulsions and electron delocalisation. The electronic overlap repulsion arises from a tendency of the electrons of one molecule to avoid those of another molecule. However, the repulsive energy is dependent on the orientation of the molecules. Delocalisation (or distortion) refers to the deformation of the charge cloud and exchange of electrons that takes place when a water molecule bonds to the O-H group of another molecule. This greatly increases the binding energy.

The hydrogen bond is considered to arise from electrostatic binding energy. Here, the term “hydrogen bond” refers to the specific association of the hydrogen atom of one molecule with the lone pairs of electrons of another. The hydrogen bond tends to be linear in configuration which results in the maximum electrostatic binding energy. This is seen in the arrangement of water molecules in ice. However, the hydrogen bond is weaker than covalent bonds and tends to bend and break under thermal agitation as seen in liquid water. It is noted that the term “break”, when referring to hydrogen bonds, is not entirely accurate as “distort” may be more appropriate (Eisenberg and Kauzmann 2005) (pages 246-249). Thus the “broken” bond reorients the water molecule causing other associating molecules (in a liquid) to compensate for the rearrangement.

Thus the tendency of the arrangement (or structure) of molecules in liquid water is to be dynamic in nature.

Water molecules bind to the molecules of a surface at angles governed by the hydrogen bonds. As these bonds are highly directional in nature they contribute to waters variety of geometrically arranged networks (Stillinger 1980). It is important to note that the hydrogen bond does not chemically change the interacting molecule.

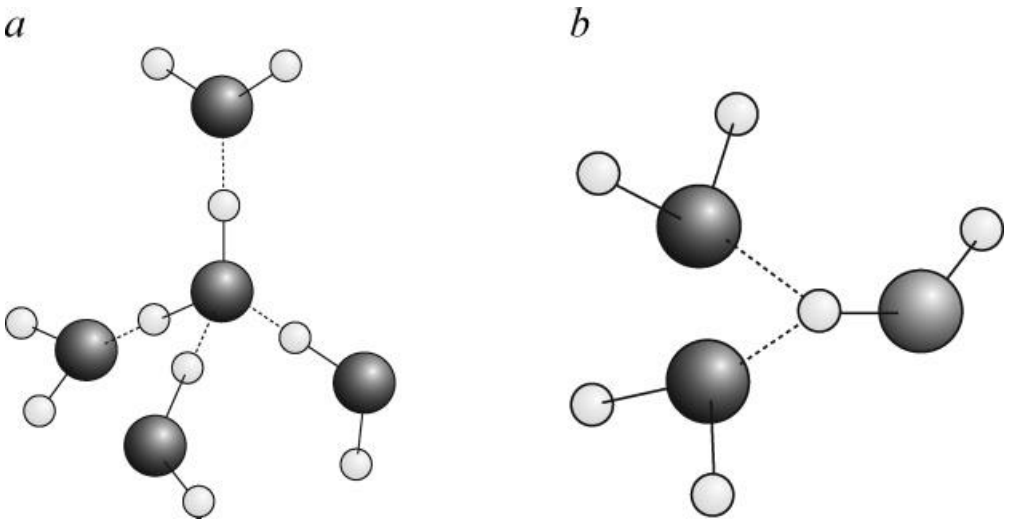

Figure 2-12. Hydrogen bonding coordination geometry.
Hydrogen bonding (dashed lines) forming tetrahedral coordination geometry (a) and bifurcated hydrogen bond (b) where two molecules weakly bond to the same hydrogen atom. Reprinted with permission from P. Ball (2008). Copyright 2008 American Chemical Society.

Figure 2-12a depicts a tetrahedral arrangement of hydrogen bonded water molecules where the bonds are directionally aligned with the covalent bond of the hydrogen atom. Such linear bonds are considered to be the strongest (Hakala, Nygård et al. 2006), however bond bending is possible resulting in decreasing bond strength with greater deviation from the bond alignment. Figure 2-12b depicts a situation where the bond angle is bent to the extent that it is only half that of the linear bond thereby allowing a second, weaker bond. This bifurcation of the hydrogen bond allows two water molecules to attach to the same hydrogen atom (as shown). It is proposed that such bifurcation of hydrogen bonds plays a key role in the mobility of water molecules in the liquid state (Geiger, Sciortino et al. 1991). Figure 2-13 indicates how a molecule with all hydrogen bonds occupied can accept an additional (5^{th}) bond thereby

dislodging an already established bond. This in turn demonstrates how bonded water molecules maintain mobility in the liquid state.

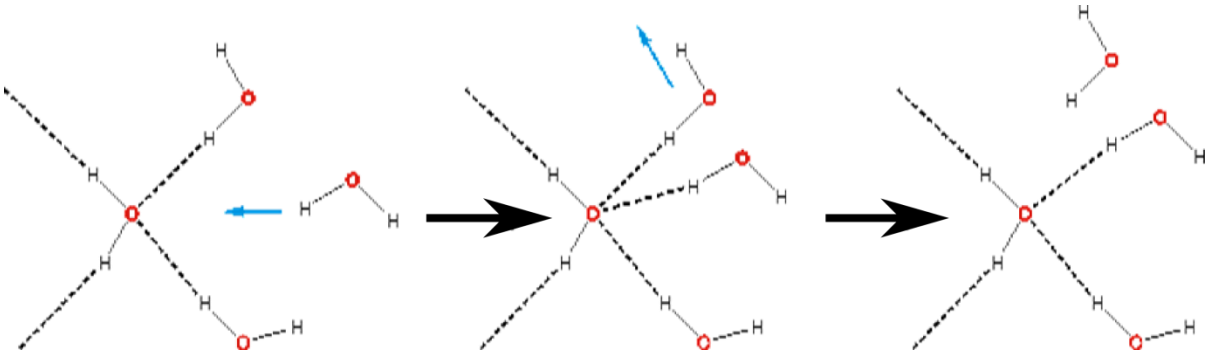

Figure 2-13. An example of hydrogen bond bifurcation.
An existing hydrogen bond (left) is added to by the intrusion of an additional water molecule (middle) replacing the original bond (right). Reproduced from Chaplin (2018).

Such arrangements as shown in figure 2-13 are very dynamic and require the breakage of two hydrogen bonds; one in the formation of the bifurcated arrangement and another to allow the inclusion of the new bond. Other hydrogen bonds affected by these changes may require rotation, bending or stretching thereby changing the hydrogen bond network.

In the liquid phase, although the tetrahedral molecular arrangement depicted in figure 2-12a indicate four hydrogen bond sites, it is not necessary that all four sites are occupied (Ball 2008) (and references therein). Additionally, two hydrogen atoms can be bonded to the oxygen atom of the same molecule (Chaplin 2017 a).

Frank and Wen (1957) postulate that hydrogen bonds are formed in a cooperative and anti-cooperative manner such that when one bond forms others will be encouraged to form. Equally, when one bond breaks, whole clusters will "dissolve". Also, the hydrogen bonds form as a result of either a proton donation (D) or proton acceptance (A) or variations thereof (Sun 2009). In this case proton donation and acceptance refers to the bonding of a hydrogen atom from one water molecule to another. Figure 2-14 indicates variations of proton donation (D) and acceptance (A) bonds.

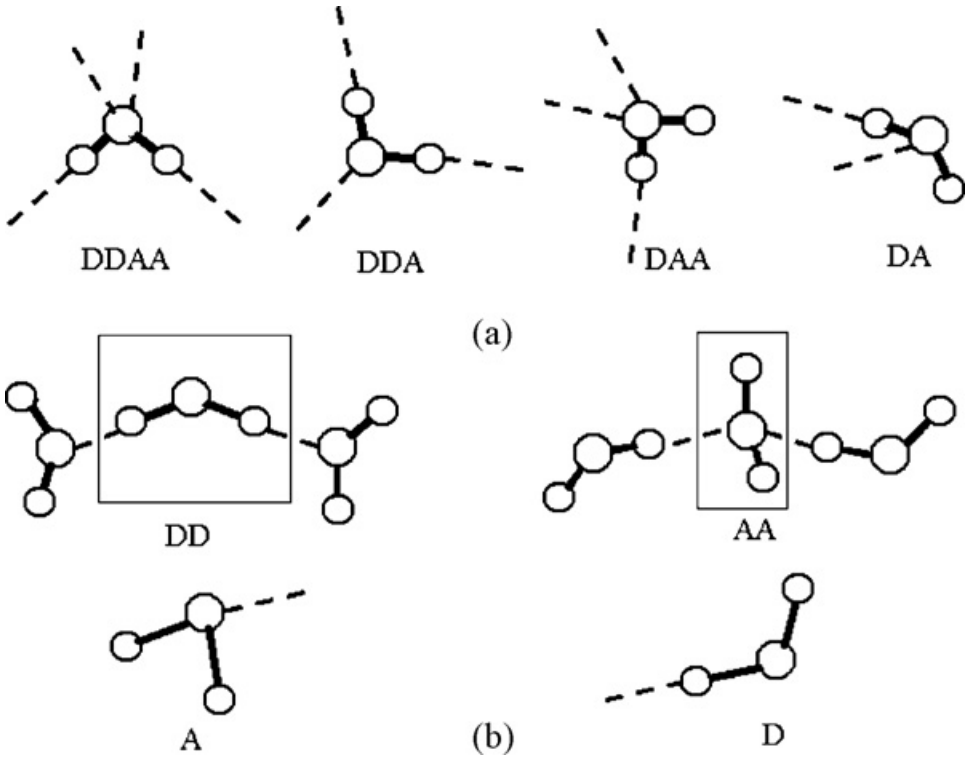

Figure 2-14. The local bonded network variations for a water molecule.
D = proton donation, A = proton acceptance. Hydrogen bonds are drawn in a dashed line. At ambient conditions bonds DDAA, DDA, DAA, and DA are likely to form (a), bonds DD, AA, A and D are unlikely at these conditions (b). Reprinted from Vibrational Spectroscopy 51(2): 213-217. Sun, Q. (2009). "The Raman OH stretching bands of liquid water." Copyright 2009 with permission from Elsevier.

Simulations by Bartha and Kapuy et al. (2003) indicate that as a molecule donates a proton (e.g. Figure 2-14b – D) there is an increase of electron density in the lone pair region. This will then encourage further hydrogen bonding in this region. Also, a molecule accepting a hydrogen bond (e.g. Figure 2-14b – A) will decrease electron density around the lone pair region. This will encourage further bond donation but discourage further acceptance. The cooperative response can also be described as acceptance of one hydrogen bond encouraging the donation of another, such as single donor – single acceptor (DA). The anti-cooperative response can be described as the acceptance of one hydrogen bond discouraging acceptance of another, such as double acceptor (AA). Theoretical studies propose that under ambient conditions the main local hydrogen bonding motifs for a water molecule can be classified as DDAA (double donor–double acceptor), DDA (double donor–single acceptor), DAA (single donor–double acceptor), and DA (single donor–single acceptor) as shown in figure 2-14 (Sun 2009).

2.3 ASSOCIATED STRUCTURING AND LONG-RANGE CORRELATION

Fenter and Sturchio (2004) reviewed investigations into the structure and distribution of water at the mineral-water interface using high-resolution x-ray scattering techniques. These investigations indicate a layer of structuring occurs in the adjacent water molecules that correlate to the structure of the mineral. Yalamanchili, Atia et al. (1996) found similar results using internal reflection Fourier transform infrared spectroscopy (FTIR-IRS). They found ice-like structure (tetrahedral coordination) in water molecules at the mineral surface decreasing in significance further with distance from the surface. Maccarini (2007) reviewed select research on solid/water interfaces using x-rays and neutron reflectometries, and sum frequency generation spectroscopy. In this work it is noted that there is ordering of water molecules at the solid surface interface into layers parallel to the surface. This is particularly the case in hydrophilic surfaces as they are able to form hydrogen bonds with the contacting water molecules. However, there is debate on the nature of the organisation. Hodgson and Haq's review (2009) identifies structure at the water-metal interface but note distinct differences in molecular arrangement with different metals. The above examples provide strong evidence indicating that the molecular arrangement of hydrophilic surfaces forms a template for the structuring of adjacent water with subsequent diminishing of order further from the surface. To further support this idea it has been found that the aggregation of clusters in dilute solutions suggests such structuring is initiated by the foreign molecules. It is very interesting to note that such cluster aggregation leads to the formation of macroclusters (~ 0.5–1 μm) (Samal and Geckeler 2001). From this we can see that a structuring influence of an adjacent surface extends beyond that predicted by the double-layer principle.

The nature of the structured interface water is not entirely clear but not for want of investigation. Drost-Hansen (1969, 1973) reviewed many experiments and came to the following conclusions; 1/ interface (vicinal) water is differently structured to bulk water, and 2/ the structural difference extends tens to thousands of molecular diameters. He also notes that anomalous thermal differences (expressed as abrupt changes) between vicinal and bulk water may indicate higher order phase transitions at the interface. He interprets these transitions as indications of stabilised structures near the interface, possessing specified thermal stability limits. He also notes that interface water may possess liquid-crystalline characteristics.

The structure of water at hydrophilic interfaces has been the subject of much scrutiny for several decades but with relatively little progress to show for it (Ball 2008). However, some of the properties of interfacial water have been determined and include greater viscosity, structuring and density (Korson, Drost-Hansen et al. 1969, Damadian 1971, Allan and Norman

1973, Damadian, Zaner et al. 1974, Gragson and Richmond 1998, Vogler 1998, Gun'ko, Turov et al. 2005, Chaplin 2006, Goertz, Houston et al. 2007, Milischuk and Ladanyi 2011, Yoo, Paranji et al. 2011, Bunkin, Ignatiev et al. 2013).

Alternately, Takei and Mukasa et al. (2000) investigated the density and surface tension of water in the small pores of silicas by comparing the adsorption and desorption isotherms in pores of different volume and radii. Their results indicate that interfacial water exhibits a 12 to 16% decrease in density and surface tension within silica pores with a pore radius between 1.55 and 3.90 nm with the density increasing further from the silica surface.

In addition to the physical properties of interfacial water there are also distinct electrical differences such as increased permittivity (Park, Choi et al. 2006, Sistat, Kozmai et al. 2008). Electrical Impedance Spectroscopy (EIS) measures the electrical potential within a system by passing an alternating current (a.c.) of known frequency and small amplitude through it. The phase difference and amplitude of the concomitant electrical potential that develops across the system is then measured. In EIS the interface between an electrode and a solution is referred to as the "double layer". This layer is electrochemical in nature and consists of a layer of ions adsorbed to the surface of the electrode with an additional "diffuse layer" further from the surface into the solution (Coster, Chilcott et al. 1996). The electrical properties of the interface layer are distinctly different to that of the bulk solution, particularly in that they exhibit greater capacitance (storage of electrical charge) at lower a.c. frequencies.

Long-range molecular orientation correlation has been observed using hyper-Rayleigh light scattering and is proposed to result from molecular rotation-translation coupling in acoustic phonons (Shelton 2014). In other words, excitations in one region of water have long-range (>200 nm) effects through re-ordering molecular orientation/structure. This is consistent with theoretical considerations of Fröhlich and Pokorný (Fröhlich 1975, Pokorný 2011). Indeed, much consideration of long-range order in water has been either theoretical or by use of molecular dynamics simulations (MD). Such investigations have found that bound water (interfacial water) has a cooperative orientational effect on the movements of adjacent water molecules (Besseling 1997, Ebbinghaus, Kim et al. 2007, Mills, Orr et al. 2013). Some studies propose they create large vortex-like structures (Higo, Sasai et al. 2001, Dickey and Stevens 2012).

A review by Fenter and Sturchio (2004) highlights the interaction between hydrophilic mineral surfaces and water. It is noted that since the net bonding strength to a water molecule is fixed, a water molecule with one strong hydrogen bond will have weaker hydrogen bonding strength in

its other interactions. In the context of hydration layers, this produces a compact hydration layer with weak interaction with fluid water, thereby producing fewer subsequent layers. Conversely, weaker bound water at mineral surfaces produces more subsequent interfacial water layers. Also, due to non-bonded oxygen atoms at the mineral surface the weaker mineral-water bond may only be possible with a dissociative bond. That is, the water molecule is broken in order to create the bond. The result of this dissociation may be localised protonation and deprotonation as protons are separated from the initial interface layer and shared through the subsequent layers. It may be that the localised net charge due to proton concentrations plays a supporting role in subsequent hydrogen bonds.

In contradiction to Fenter and Sturchio, Chaplin (2001), in regards to the formation of water clusters states that "The substantial cooperative strengthening of hydrogen bonds in water is dependent on long-range interactions. Breaking one bond weakens those around whereas making one bond strengthens those around and this, therefore, encourages the formation of larger clusters, for the same average bond density. A weakly hydrogen-bonding surface restricts the hydrogen-bonding potential of adjacent water so that these make fewer and weaker hydrogen bonds. As hydrogen bonds strengthen each other in a cooperative manner, such weak bonding also persists over several layers. Conversely, strong hydrogen bonding will be evident at distance."

Whatever is the case, the nature of long-range order in water still remains inconclusive (Ball 2008, Sun 2009).

2.4 LONG-RANGE ORDER CONTROVERSY

The extent to which hydrophilic surfaces affect the structuring of water is another area of much interest. As mentioned previously changes in water density and surface tension due to surface interaction has been observed as far as 4 nm in silica pores, equating to 11 – 14 molecular layers (Takei, Mukasa et al. 2000). This is consistent with the 3-5 nm structural modifications found by Etzler and Fagundus in silica gels and porous glasses (Etzler and Fagundus 1987), force measurements between mica sheets (Israelachvili and Adams 1978) and a structural component of the disjoining pressure of quartz plates at distances <6 nm as noted by Peschel and Belouschek et al. (1982).

Conversely, infrared internal reflective spectroscopy studies revealed tetrahedrally coordinated structure as far as 262 nm from a silicon surface (Yalamanchili, Atia et al. 1996). Nuclear

magnetic resonance studies indicate a highly ordered surface-induced water structure extending to micrometres from the initiating hydrophilic surface (Totland, Lewis et al. 2013).

Ultraviolet Visual Spectroscopy (UV Vis) was used to indicate a change in the UV absorption properties of water adjacent to a number of hydrophilic surfaces to a distance of 150 µm. These substances included Nafion 117, NaCl, KCl and LiCl (Chai, Zheng et al. 2008).

Recently, Pollack and co-workers reported to have observed macromolecular phenomena in the water-hydrophilic surface interface extending distances of several hundred microns. Using a microscope they observed latex microspheres in suspension moving away from the hydrophilic material, Nafion (Zheng and Pollack 2003, Huszar, Martonfalvi et al. 2014). It is claimed that interfacial water at hydrophilic surfaces has a distinct physical effect whereby solutes are propelled considerable distances (hundreds of micrometres) from the hydrophilic surface (Zheng and Pollack 2003, Huszar, Martonfalvi et al. 2014). Figure 2-15 shows an example of this physical effect where 1 µm diameter carboxylated polystyrene beads are excluded from a Nafion (hydrophilic polymer) surface over a period of 300 seconds.

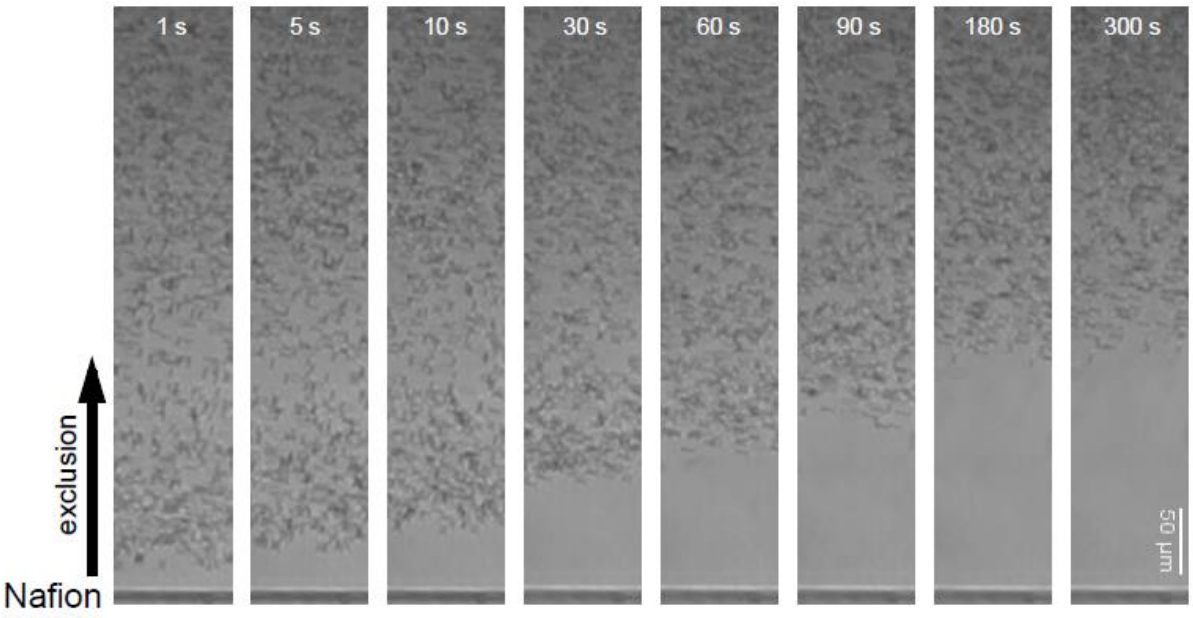

Figure 2-15. Microspheres excluded from a Nafion surface.
1 µm diameter carboxylated polystyrene beads excluded from a Nafion surface (bottom of each image) over a period of 1 to 300 seconds. Reproduced from Huszar, Martonfalvi et al. (2014).

It is this distinct physical effect that has led to the title "Exclusion Zone water". Another prominent phenomenon is a distinct separation of charge in the EZ water. Figure 2-16 shows variations in pH values in water close to a Nafion surface over time using pH sensitive dye. The

red colouring indicates a pH <3 close to the Nafion surface increasing towards neutrality further away (Chai, Yoo et al. 2009). This may also indicate a higher concentration of protons/positive charge diffusing from the Nafion material over time. It is also worthy of note that a clear region can be detected directly adjacent to the Nafion surface where it appears the dye is excluded. Investigations using microelectrodes indicate that this EZ region appears to be negatively charged (Klimov and Pollack 2007). Klimov and Pollack postulate from their experiment that the charges are held in their respective regions by the formation of a stabilised matrix, although they acknowledge further experimental evidence is required. It may be important to note here that EZ's are not necessarily negatively charged. Experiments by Chai, Mahtani et al (2012) show that EZ's near the charged surfaces of some metals are positively charged, particularly zinc and aluminium. Again, the reason for this charge separation is not clear.

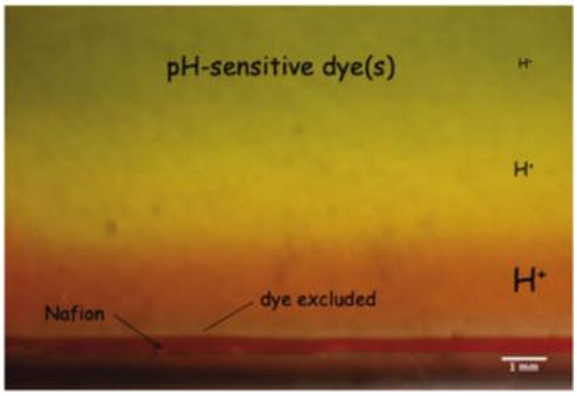

Figure 2-16. Changes in pH of water over time.
Image of water containing pH sensitive dye adjacent to a Nafion surface taken 5 minutes after the solution was added to the Nafion. Colours indicate a lower pH close to the Nafion surface, tending toward neutrality at increasing distance from the surface. Reprinted with permission from Chai, Yoo et al. Copyright (2009). American Chemical Society.

There is much debate as to the cause behind the properties of the EZ. Pollack (2013) proposes that this hydrophilic effect acts as a template to the adjacent water molecules inducing an ordered, liquid-crystalline structure. This idea is not without support; Ling (Ling 2003) proposed an Association-Induction hypothesis whereby intracellular water is polarised in multilayers by inductive effects at hydrophilic interfaces. He claims that this polarised water is responsible for the size-dependent distribution (exclusion and inclusion) of solutes within the cell.

There are, however, alternate arguments for the properties of EZ water. Huyghe, Wyss et al (2014) propose that the EZ can be generated by a combination of ion exchange and diffusiophoresis. In their study, Nafion is used as the hydrophilic material similar to many of

Pollack and co-workers experiments. They note that Nafion has an ample supply of exchangeable protons ready to exchange with cations in the solution. Such an exchange would create an inhomogeneous distribution of ions (salt gradient) in the liquid. According to the DL theory (described above), a charged particle in an electrolyte solution would attract counter-ions (oppositely charged) via the influence of the local electric field. In a homogeneous solution it would be expected that the distribution of ions and counter-ions would be symmetrical around the particle. This would lead to a homogeneously distributed hydrostatic pressure with no fluid flow as shown in figure 2-17.

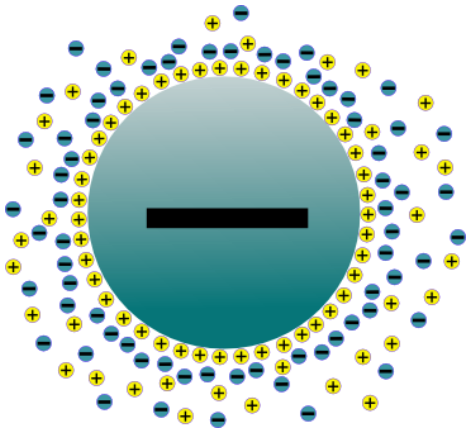

Figure 2-17. Even distribution of ions around a charged particle.

However, with the introduction of a proton donor like Nafion the resulting inhomogeneous charge distribution would produce an asymmetrical arrangement of ions around the particle as shown in figure 2-18. In an effort to balance ions and counter ions a fluid flow results, propelling the particles away from the Nafion surface.

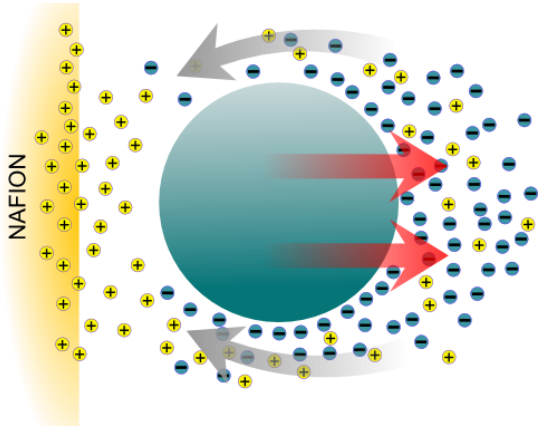

Figure 2-18. Depiction of particle propulsion due to diffusiophoresis.
Uneven distribution of ions near Nafion surface produces an ion flow (grey arrows). The resulting fluid flow propels the particle away from the Nafion surface (red arrows).

Oehr and LeMay (2014) theorise that the observed EZ water may comprise tetrahedral oxy-subhydride structures (TOSH). They argue that such structuring may account for a number of the properties it exhibits. These include, light absorbance at specific infrared wavelengths, its negative potential in water and ethanol, a maximum EZ light absorbance at 270nm ultraviolet wavelength, the ability of dimethyl sulphoxide to form an EZ but not ether, and the transitory nature of EZ's derived from melting ice.

Oehr and LeMay also propose that some water molecules at the surface of ice may not have all their hydrogen bonds occupied and therefore may be more susceptible to rupture and formation of H^+ ions. Such rupturing may be caused by the addition of specific wavelengths of infrared, visible or ultraviolet light. The energy required for this disruption may be relatively low due to anharmonic vibration of the hydrogen bond of an excited water molecule in the liquid state (Bakker and Nienhuys 2002). Figure 2-19 illustrates the process of molecular restructuring after the ejection of protons (H^+).

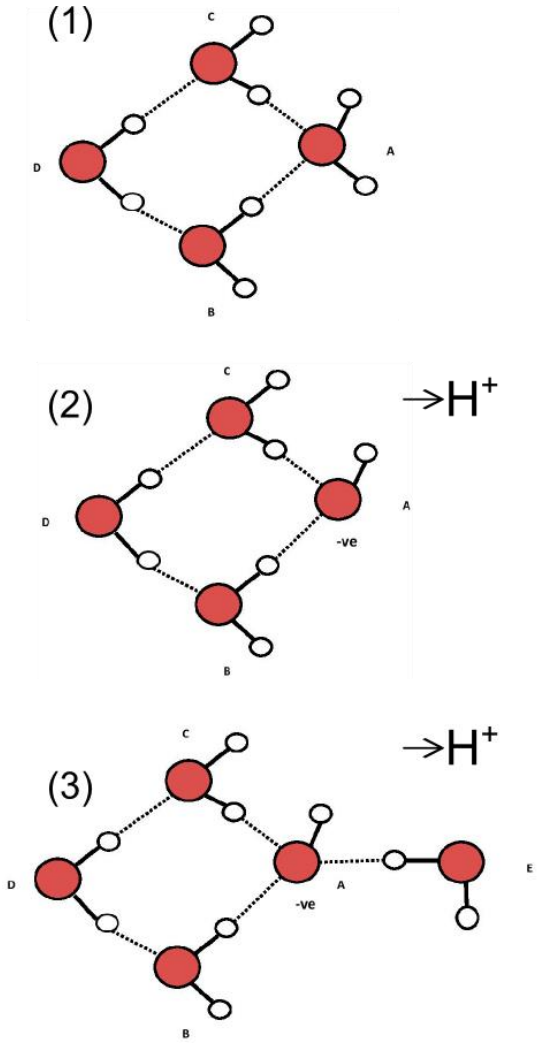

Figure 2-19. Process of molecular disruption and rearrangement due to disassociation of proton (H+). Oxygen atoms are red, hydrogen atoms are white, covalent bonds are solid black lines, hydrogen bonds are dashed black lines. Reproduced from Oehr and LeMay (2014).

Figure 2-19-1 depicts the molecular arrangement found in standard ice with molecule A, located at the surface, having two non-hydrogen bonded hydrogen atoms. Figure 2-19-2 shows molecule "A" ruptured after the absorption of a photon of sufficient energy producing an OH^- function group and an ejected H^+. Figure 2-19-3 shows the newly formed hydroxyl species from figure 2-19-2 hydrogen bonding with a new non-ice water molecule "E". This new structure (molecules ABCE) contains a tetrahedral (OH^-) $(H_2O)_3$ core with an H_4O^- sub-core (i.e. molecule A). It also highly absorbs infrared light at both ~3436 nm and ~2907 nm. This closely matches the wavelengths observed in water-derived EZ's (Oehr and LeMay 2014) and references therein. This is also proposed to be the most stable of the possible variants of $(OH^-)(H_2O)_4$ (Novoa, Mota et al. 1997) (page 7845). The negative charge of water derived EZ's may be due to this negatively charged specific hydroxy-tetrawater isomer. The protons then accumulate outside this region to form the positively charged region as seen in figure 2-16.

Oehr and LeMay also propose an alternate TOSH structure similar to that mentioned above as shown in figure 2-20. The difference here is that hydrogen bond strengths around oxygen atom "A" can be increased through resonance, thereby making all bonds around "A" equal in strength.

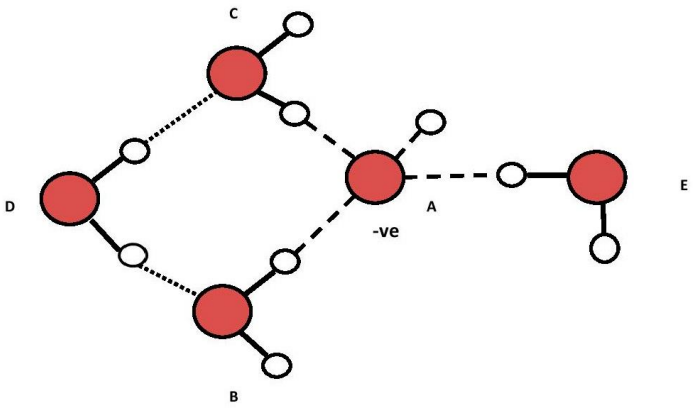

Figure 2-20. Variation of structure in figure 2-19-3.
Hydrogen bond strengths around "A" made equal by resonance (dark dashed lines). Reproduced from Oehr and LeMay (2014).

Noting that EZ's derived from melting ice are transitory in nature Oehr and LeMay postulate that an anchoring feature containing OH functional groups is required to stabilise the TOSH sub-clusters. These anchors are permanently present in hydrophilic materials but temporary in melting ice.

Other suggested mechanisms for excluding microbeads from the hydrophilic surface-water interface include (a) the dissolution of the hydrophilic gel where polymer strands diffuse out of the material and push out the microbeads; (b) an entropic brush mechanism where surface-bound elastic polymer strands extend from the hydrophilic material keeping the beads away; (c) the formation of a distinct phase (equilibrium process) from the material surface growing into the water; (d) chemical gradient (non-equilibrium process) mechanism where a mechanical force is generated by a physical-chemical gradient near the edge of the Nafion surface. These proposed mechanisms were investigated by Huszar, Martonfalvi et al (2014). They found that the hydrophilic material did not diminish in volume or undergo shape deformation even when it was soaked in buffer for several days. Therefore the dissolution mechanism (a) was discarded as a possible cause of EZ's. In the same study atomic force microscopy (AFM) was used to investigate the presence of polymer strands in the EZ near the Nafion surface but none were found. Therefore mechanism (b), the entropic brush mechanism, was also discarded. In support of this conclusion similar experiments were performed using a hydrophilic monolayer containing COOH groups (Zheng, Chin et al. 2006) and metal surfaces to generate EZ's (Chai,

Mahtani et al. 2012). Although EZ regions were found adjacent to certain metal surfaces they were not as extensive as that found near hydrophilic polymers. Thus it may be a reasonable assumption that EZ's are not necessarily due to the presence of polymer strands emanating from the polymer proper.

Furthermore, to investigate mechanism (c), an optical tweezer was employed to suspend some of the microbeads near the Nafion surface before, during and after the formation of the EZ. The laser was then turned off thereby releasing the microbeads. It is proposed that if the beads were now surrounded by a distinct phase of water (in equilibrium) they would remain motionless as there would be a lack of flow within the EZ region. However, when the beads were released (laser turned off) many were seen to move away from the anchor point to the EZ boundary. This suggested there was indeed a flow (non-equilibrium process) from the Nafion surface to the EZ boundary. The prospect that the EZ was derived from a chemical gradient was further supported by observing that the size of the EZ diminishes to be undetectable within 2 hours. Furthermore, the EZ remained diminished after washing the Nafion sample over several hours (Huszar, Martonfalvi et al. 2014).

The most likely source of the chemical gradient was believed to be the high concentration of H^+ ions found in Nafion. This view is similar to the diffusiophoresis process proposed by Huyghe, Wyss et al (2014) above.

The conclusion drawn from these investigations was that the EZ is not a quasi-static build-up of a highly ordered water phase (as proposed by Pollack above) but rather a non-equilibrium phenomenon coupled to a diffusion-driven material transport mechanism.

There is, however, one EZ phenomenon that requires further investigation, observed birefringence (polarised double refractive index) (Pollack, Cameron et al. 2006, Bunkin, Ignatiev et al. 2013, Pollack 2013, Le Bihan and Fukuyama 2016). This has been used to support the argument for the presence of a crystalline structure.

Birefringence is responsible for the double refraction phenomenon whereby light is refracted and polarised in two directions as it passes through certain crystalline mediums. This gives a double view of anything seen through a birefringent material (see figure 2-21).

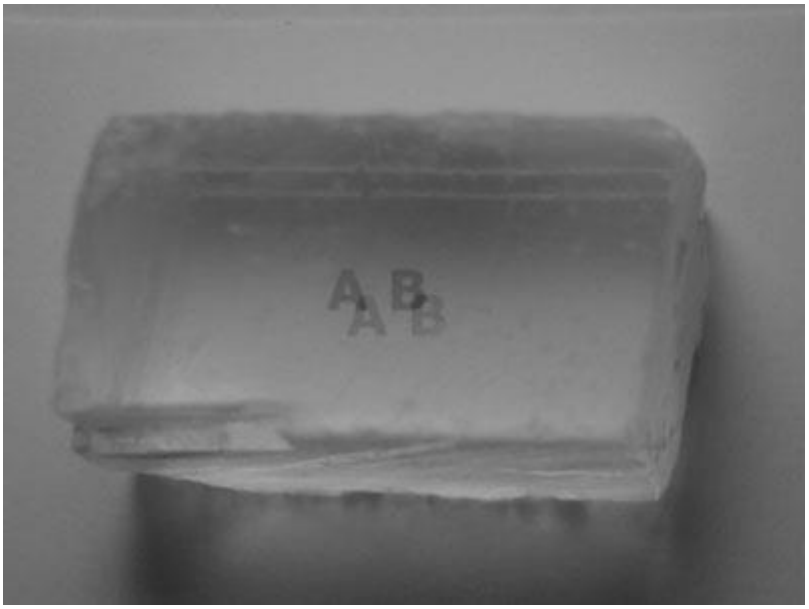

Figure 2-21. A sample of calcite crystal.
A double-refracted view of the letters "A B" viewed through calcite. Reproduced from Walker (2004).

The two light rays emerging from the birefringent material are called the "ordinary ray" (o-ray) and the "extraordinary ray" (e-ray). The o-ray is refracted in a typical manner according to Snell's Law of refraction in which the ratio of the sine of the angle of incidence to the sine of the angle of ordinary refraction is a constant when passing between two media. The e-ray does not follow this law but its refraction angle is dependent on the axis of the aligned molecules in the media.

Birefringence is detected using polarised light microscopes which utilise crossed polarising filters known as the polariser and analyser (figure 2-22).

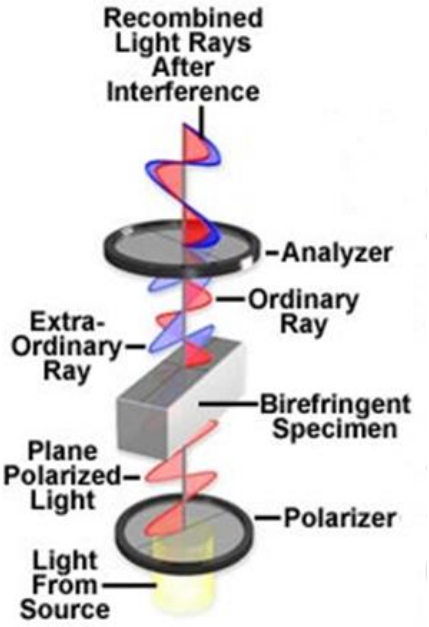

Figure 2-22. The process of polarised microscopy.
Reproduced from Robinson and Davidson (2000)

In figure 2-22 it can be seen that light is polarised before passing through the birefringent sample/specimen. From the birefringent sample the light is doubly refracted into the o-ray and e-ray, which are oriented perpendicular to each other. Both the refracted rays are then recombined in the second polarised filter (analyser) oriented perpendicularly to the first polarised filter.

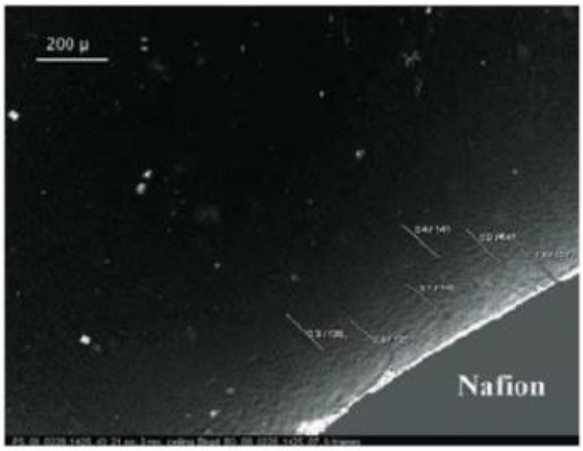

Figure 2-23. A birefringent zone adjacent to Nafion surface.
Birefringent zone (bright region) extending approximately 200 µm from a Nafion surface, seen as light and dark fringes. The Nafion sample is covered by grey. Reproduced from Le Bihan and Fukuyama (2016).

Figure 2-23 shows the EZ near a piece of Nafion to be birefringent, expressed as a region of light and dark fringes, using a polarised light microscope. Such birefringence in liquid water is purported to indicate crystallinity in the EZ. This is interpreted as long-range order within the liquid phase.

2.5 MAGNETISATION OF WATER

Magnetic fields have been utilised in the treatment of water for several years to purify (Ambashta and Sillanpää 2010), de-scale (Coey and Cass 2000) and even disinfect water (Biryukov, Gavrikov et al. 2005). It is believed that magnetic fields affect the morphology of crystalline precipitates (Higashitani, Kage et al. 1993, Gehr, Zhai et al. 1995, Madsen 1995, Barrett and Parsons 1998, Holysz, Szczes et al. 2007).

Magnetic fields are also reported to affect the size, strength, configuration and stability of water molecule clusters thereby changing the physicochemical properties of liquid water (Hosoda, Mori et al. 2004, Chang and Weng 2006, Cai, Yang et al. 2009). These effects are expressed in terms such as increased viscosity (Ghauri and Ansari 2006, Cai, Yang et al. 2009), changes in refractive index (Hosoda, Mori et al. 2004), increased melting temperature (Inaba, Saitou et al. 2004), increased rate of vaporisation (Nakagawa, Hirota et al. 1999), enhanced adsorption (Ozeki, Wakai et al. 1991), changes in electrolyte conductivity (Holysz, Szczes et al. 2007) and decreased conductivity of pure water (Szcześ, Chibowski et al. 2011).

A number of these effects have been observed to remain in liquid water for many hours after initial exposure to magnetic fields (Coey and Cass 2000, Szcześ, Chibowski et al. 2011, Silva, Queiroz Neto et al. 2015, Mahmoud, Yosra et al. 2016).

Molecular dynamics simulations have indicated that magnetic fields (up to 10 Tesla) enhance hydrogen bonding causing an increase in size (~0.34%) and stability of water clusters (Chang and Weng 2006). This appears to be supported by work by Inaba, Saitou et al. (2004). However, other research has indicated that magnetic fields may collapse large clusters producing smaller clusters with stronger (more resistant) intracluster hydrogen bonds (Toledo, Ramalho et al. 2008).

It is important to note that the reported effects on hydrogen bonds are inferred from experimental and simulation evidence and are not conclusive. Indeed, the topic of magnetised water remains controversial due to lack of reproducible results (Smothers 2001, Knez and Pohar 2005, Toledo, Ramalho et al. 2008).

A review by Baker and Judd (1996) investigates numerous claims and reports on the effectiveness of magnetic treatment of water as an anti-scaling measure. Their view is that magnetic fields do not specifically affect the intermolecular forces of water molecules but rather the particulates in the water. They note that the more successful results are obtained with magnetic fields orientated orthogonally to the flow within recirculated systems. This implies that Lorentz forces acting on particulates in the water may be responsible for the results rather than the water itself. That is, forces are exerted on charged particles passing through the magnetic field. Baker and Judd do not specify what effects the force will exhibit but it may likely involve displacement and orientation with the acting field. It may be that uniformly oriented particles will affect the development of crystal shape and size. Charge is likely induced by passing the conductive particles (ions) through the magnetic field.

Their review notes some of the proposed mechanisms behind the magnetic affect and these are divided into four categories:

a. Intra-atomic effects (e.g. changes in electron configuration).
b. Contamination effects (due to magnetically-enhanced dissolution).
c. Inter-molecular/ionic effects (e.g. changes in coordination of water with ions).
d. Interfacial effects (e.g. distortion of the double layer).

Regarding the intra-atomic effects, these involve intra-ionic transfer of electrons. However, this has been argued to likely be very short-lived and would not explain the memory effect.

Contamination effects are the proposed contributor to several experiments where magnetically-enhanced corrosion creating Fe^{2+} ions which retard the growth rate of calcite scale deposition. However, this conclusion could not account for the results of other experiments where the treating magnets were not exposed to the solutions.

Regarding intermolecular/ionic effects, it has been proposed that the magnetic field, and resulting Lorentz force, initiate a stabilising influence on water molecules at the particle-water interface. The result of which is a more stabilised co-ordination of water molecules which do not exchange in the bulk solution. This is proposed to explain the memory effect.

However, Baker and Judd prefer the interfacial effects mechanism. Here it is proposed that the magnetic field (Lorentz force) causes an isotropic distortion of the diffuse layer, displacing co- and counter ions, leading to a change in the charge distribution within the electrical double layer.

However, it is noted that the effects involving Lorentz forces may not account for reported magnetic treatment of stationary water. Also, they note that no universally agreed mechanism for magnetic treatment exists (Baker and Judd 1996)(and references therein).

Contrary to Baker and Judd's view there appears to be support for the effect of magnetic fields on water interfaces. Ozeki, Wakai et al. studied the effect of differing magnetic intensities on water adsorption to solid surfaces and found that increasing the field strength increased water adsorption. They attribute the apparent stabilisation of water under magnetic field to "a kind of magnetic transition or to a structural change." Their view is that "the magnetic anisotropy of a water molecule might induce magnetically a cooperative orientation of water molecules in a two-dimensional cluster." (Ozeki, Wakai et al. 1991). This is consistent with the findings of Higashitani and Oshitani (1998) and Holysz, Szczes et al. (2007).

Further work by Ozeki provides even stronger support for the existence of a stabilised coordination of water molecules at an interface. Evidence from infrared and Raman spectroscopy indicated quasi-stable structures in magnetically treated water. These appear to be oxygen clathrate-like hydrate and developed water networks. It is interesting to note that the effect is not due to the magnetic field alone but in combination with dissolved oxygen and relative motion of water in a magnetic field. Their results clearly show increases in IR

absorption peaks as a result of increased magnetic field and oxygen content. The issue of contamination is ruled out by degassing the samples using ultrasonication and then retesting. The same sample, once degassed, did not yield the new peaks found in the previous magnetic treatment. They conclude that the magnetic effect on water is real but transient, forming oxygen clathrate-like hydrates and promoted hydrogen-bonded networks (Ozeki and Otsuka 2006).

Pang provides a theoretical mechanism for water magnetism based on proton conductivity in ice and the proposed presence of closed hydrogen-bond chains (Pang 2006). He proposes that the ring-like structure of water molecules in ice provides a conduit for the migration of protons. With the transfer of charge through these closed rings a dipole is created acting like "small magnets". Such structures are proposed to exist in the liquid water as well but in much less number. The alignment of such dipoles to an external magnetic field results in a redistribution of the liquid water molecules rather than change to their chemical nature. Pang also acknowledges that the magnetic affect will be relatively small owing to the small number of appropriate ring-like structures in liquid water.

It should be noted that the migration of protons in ice is temperature-dependent and decreases with increased heat, i.e. the ice melts thereby destroying the conducting structures. Also, any structuring of molecules in liquid water (i.e. clathrates) will be very short-lived and, according to Pang's theory, any magnetic affect is unlikely to be sustained.

There appears to be experimental support for the Pang's theory provided by Shelton (2014). Here Hyper Rayleigh Scattering techniques were used to identify long -range correlation of water molecules. This is in opposition to the belief that intermolecular correlations in liquids extend only a few molecular diameters. Shelton proposes that these long-range correlations result from rotation-translation coupling in acoustic phonons (i.e. ultrasonic waves) in the liquid. Although such a vortex-like structure is only marginally similar to Pang's ring-like structure the presence of a magnetic dipole is likely present in both structures. Molecular dynamics simulations on water by Higo, Sasai et al. (2001) predict the presence of a "site-dipole field'' which is defined as "the averaged orientation of water molecules that pass through each spatial position". In simulating bulk water large vortex-like structures of more than 10 Å in size were observed. Such coherent patterns were seen to persist longer than 300 ps. Similar molecular dynamics simulations of water confined between surfaces predict vortex-like structures that are dependent on the distance from the surface and the nature of the surface, i.e. whether is hydrophilic or hydrophobic (Higo, Sasai et al. 2001, Dickey and Stevens 2012). Furthermore, quantum electrodynamics investigation by Emilio Del, Alberto et al. (2013) predict the presence of coherence domains. These are regions of electromagnetic fields confined

within ensembles of water molecules. The structure of these ensembles is vortex-like thereby producing magnetic dipoles. These dipoles are predicted to be aligned by external fields (i.e. magnetic and electric).

As seen above much of the support for Pang's theory comes from theoretical sources. Although the rotation-translation coupling proposed by Shelton seems to provide experimental support it is noted that this phenomena is induced by an external influence, i.e. acoustic phonons. Therefore it is not likely to be intrinsic to the structuring properties of water molecules.

Lee, Jeon et al (2013) noted in their study of magnetically treated water that the concentration of gas within the water significantly affected their results. This is consistent with the findings of Ozeki and Otsuka above. Similarly Szcześ, Chibowski et al. (2011) reported changes to gas concentrations in their studies and attributed the changes to magnetic treatment of water. And as noted above, the morphology of crystalline precipitates are also reported to be affected by magnetic fields. With these examples in mind it may be that the magnetic treatment of water does not directly affect its molecular structure alone but rather how it interacts with other substances (e.g. gases, mineral ions and electrolytes).

A more recent review of studies on magnetic force treatment of water and aqueous solutions from the past decade concludes that a consistent theory of the field mechanism action is still lacking (Chibowski and Szcześ 2018). However, Chibowski and Szcześ note that the recent literature furthers the view that the mechanism of magnetic water treatment is based on changes in the structure of water via changes in hydrogen bonding in intraclusters and between interclusters. An additional mechanism for magnetically enhanced precipitation of minerals from solution is also presented. This theory considers the presence of prenucleation clusters existing in solution under ambient conditions. These consist of short chains of the constituent ions which are aligned and polarised by a magnetic field. Following this the clusters promote crystal formation and precipitation. These prenucleation clusters are called Dynamically-Ordered-Liquid-Like Oxy-anion-Polymers (DOLLOP).

From the above literature, it would appear that not all evidence supports the view that magnetic fields promote coordination of interfacial water molecules. However, it is theorised that if such coordinating effect do occur they can be evidenced as increased macromolecular phenomena. That is, evidence of interfacial ordering (structure) may be enhanced by the application of magnetic fields.2.6 Summary and Implications

Liquid water is a very dynamic substance with multiple phases resulting from a wide variety of possible molecular configurations. Evidence indicates that the molecular configuration of hydrophilic surfaces influence the configuration of liquid water. The bound water (adhered to a hydrophilic surface) appears to have a structuring effect on adjacent water molecules that perpetuates a considerable distance into the bulk, well beyond that which is expected by the Double Layer theory. This region is known as interfacial water and has properties significantly different to that of bulk water.

The molecular structure of liquid water is very difficult to determine and current understanding relies heavily on molecular dynamics simulations and theoretical interpretations of experimental data. There are, however, some reports of replicable, observable structuring.

Magnetic fields are also reported to affect the structuring of clusters in liquid water by strengthening hydrogen bonds thereby changing its physicochemical properties (Chang and Weng 2006, Ozeki and Otsuka 2006, Holysz, Szczes et al. 2007, Cai, Yang et al. 2009, Szcześ, Chibowski et al. 2011). There also appears to be strong evidence that magnetic fields specifically affect the coordination of hydrogen bonds at the water-particle (or ion) interface (Ozeki, Wakai et al. 1991, Ozeki and Otsuka 2006). If such is the case magnetic fields may also influence the structure of interfacial water by enhancing it. Any change to the properties of interfacial water due to a magnetic influence may give a clue as to the nature of its structure.

CHAPTER 3

Chapter 3 RESEARCH DESIGN

The following experiments investigate previously published reports of evidence of EZ's. Also examined are claims of changes to the properties of water due to magnetic fields. This is to establish a baseline from which to detect change in the extent of the EZ and investigate its basis and how it is modulated.

3.1 EXPERIMENT 1; NEUTRON RADIOGRAPHY

Objective

The objective of this experiment is to examine the claim that interface water is; 1/ greater in density, and 2/ extends hundreds of microns into the bulk (Drost-Hansen 1969, Chai, Zheng et al. 2008, Chai, Yoo et al. 2009, Das and Pollack 2013).

Contrary to the claim of increased density of interfacial water and the distance to which it extends, investigations into the density of water in small silica pores shows a decrease of density extending only as far as 5 μm as mentioned earlier (Peschel, Belouschek et al. 1982, Takei, Mukasa et al. 2000). Although it is unlikely that this experiment can examine such small regions it is likely that at least the claim of long-range density difference can be ruled out. It is sufficient to say that both of the above claims show a difference in density of interface water even if there is contradiction in whether it is increased or decreased.

A similar experiment was conducted using neutron radiography to visually indicate density differences between supercritical and subcritical water (Takenaka, Sugimoto et al. 2013). Their results showed clear variation in neutron beam intensity between the two types of water. This indicates that changes to the molecular structuring of liquid water (and therefore density differences) can be detected using this technique.

Materials and method

This experiment was conducted at the Australian Nuclear Science and Technology Organisation (ANSTO) with the aid of Dr. Klaus-Dieter Liss. Neutron radiography was used to detect changes in density of water adjacent to hydrophilic surfaces. This technique is the neutron analogue to X-ray radiography and has traditionally been used to image hydrogenous materials inside metallic or ceramic objects.

The instrument used was the Dingo radiography imaging station at the Australian Nuclear Science and Technology Organization (ANSTO). The neutron flux varies between 4.75 x 10^7 neutrons cm^{-2} s^{-1} for a L/D ratio of 500 and 1.15 x 10^7 neutrons cm^{-2} s^{-1} for a L/D ratio of 1000 (L/D = Length of collimator and Diameter of aperture opening). The area of the detector is 5 cm × 5 cm with 2000 pixels × 2000 pixels and therefore the pixel size is 5×10^{-2} m/2000 = 25 µm. A Siemens test object was placed in the field of view and a 12 s exposure obtained (figure 3-1). From this image the instrumental resolution was judged to be better than 100 µm and was considered adequate to detect an EZ extent of at least 200 µm (Zheng, Chin et al. 2006, Chai, Yoo et al. 2009, Das and Pollack 2013).

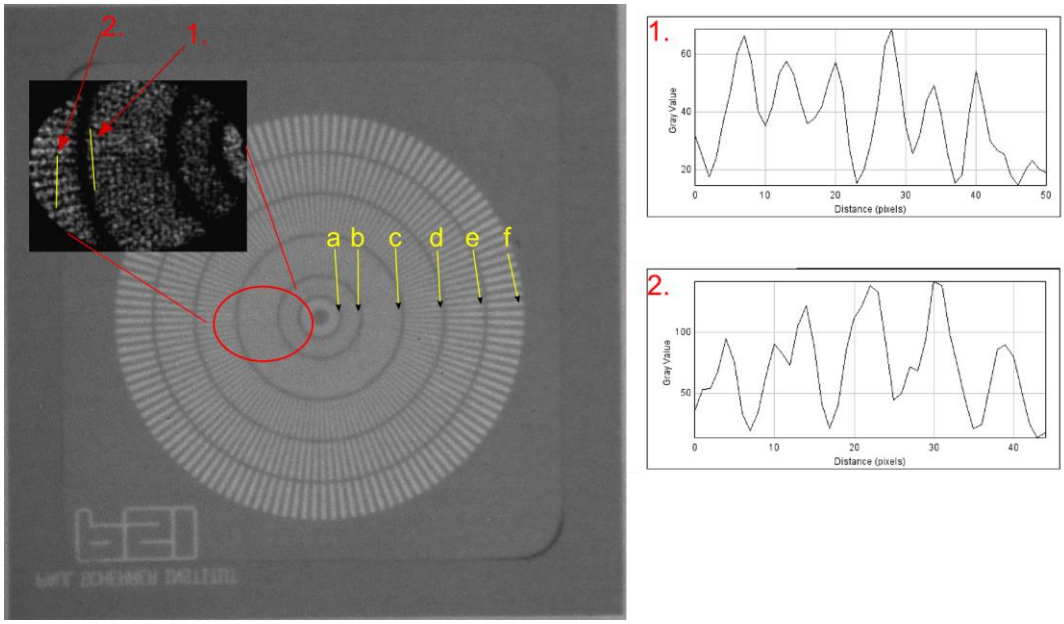

Figure 3-1. Neutron radiograph of radial test object.
The spacing of the radial lines at the edge of the first circle out from the central dot is 25 µm (a), then 50 µm (b), 100 µm (c), 200 µm (d), 300 µm (e) and 400 µm (f). The test object shows that the resolution is marginally better than 100 µm as indicated by profile plot 1 of the contrast-enhanced insert showing detectable, evenly spaced lines in this region. This profile plot is consistent with the more pronounced profile plot 2.

For this experiment, a sample cell normally used on the small angle neutron scattering (SANS) instrument (QUOKKA) was used (figure 3-2). The cell has a 2 mm gap between quartz glass plates and two ports in the top of the cell to allow the admission of liquids and samples. A syringe with hypodermic needle was used to fill the cell with distilled water. Two strips of Nafion, a sulfonated tetrafluoroethylene based fluoropolymercopolymer developed by DuPont, were inserted into the SANS cell, as seen in figure 3-2. The temperature of the apparatus was 21° ± 1 °C. The Nafion (Fuel Cells Etc.; Texas, USA) used in these experiments was 0.43 mm thick and 1-2 mm in width.

Figure 3-2. The 2 mm QUOKKA cell placed on the DINGO platform. Two strips of Nafion inserted into the cell forming a "V" shape.

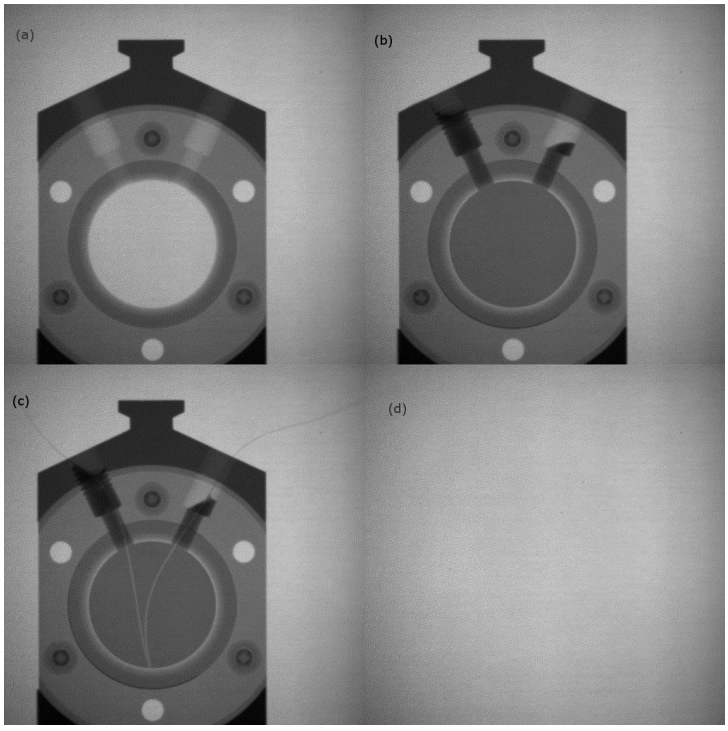

Figure 3-3. Samples of Neutron Radiography images used for processing. (a) Empty cell (no water). (b) Cell with water. (c) Cell with water and 2 strips of Nafion. (d) Bright image (no cell)

A series of 100 images were taken under different conditions, namely; with no cell in the field of view, with an empty cell (figure 3-3a), the cell filled with distilled water (figure 3-3b) and then

with two strips of Nafion inserted to form a "V" (figure 3-3c). The images were taken at 12 second exposures with a 1.8 second read out.

Images were loaded into ImageJ for analysis. Each stack of 100 images was averaged to produce a single image. The experiment of interest involved two strips of Nafion inserted into the cell filled with distilled water. The natural logarithm of the image of the cell filled with distilled water was subtracted from the image of the cell filled with distilled water and added Nafion strips. This produced an image showing only the Nafion, as demonstrated by equations (1-3), where μ_q represents the neutron attenuation coefficient of the quartz, μ_w the attenuation coefficient of the water, μ_n the attenuation coefficient of the Nafion and μ_i the attenuation coefficient of interfacial water, x_q the thickness of each quartz window, x_w the thickness of the water, x_n the thickness of the Nafion and x_w the thickness of the interfacial water in the direction of the neutrons, I_0 the initial intensity of neutrons and I intensity of the neutrons after they have passed through the cell.

With only water: $I_1 = I_0 e^{-(2\mu_q x_q + \mu_w x_w)}$ (1)

With the added Nafion strips $I_2 = I_0 e^{-(2\mu_q x_q + \mu_w x_w + \mu_n x_n + \mu_i x_i)}$ (2)

$\ln(I_1) - \ln(I_2) = \mu_n x_n + \mu_i x_i$ (3)

Neutrons are attenuated (intensity decreased) by materials and this attenuation varies depending on the material that it passes through. An increase in the density of a material will increase the number of atoms the neutrons interact with, thereby increasing the attenuation. This is demonstrated in the study by Takenaka, Sugimoto et al. (2013) where neutron radiography provided clear visual distinction between supercritical and sub critical water.

The equations above assume there are three materials present – quartz glass, water and Nafion with the addition of interfacial water. The subtraction process described, strips out the water and the glass, with the residual being the contribution of the Nafion and any density changes to the adjacent water (interface). If the natural logarithm of image 3-3c is subtracted from image the natural logarithm of 3-3b the signal is the attenuation coefficient of the Nafion multiplied by the thickness of the Nafion. This is the same technique used in digital subtraction angiography to remove background anatomy to enhance the contrast media pattern. The resulting image should contain only the Nafion signal and any water density enhancement effect – if it exists.

Figure 3-4 shows the scan of the cell with water only extracted from the cell with Nafion strips and water. Line profiles were taken close to the convergence of the two strips.

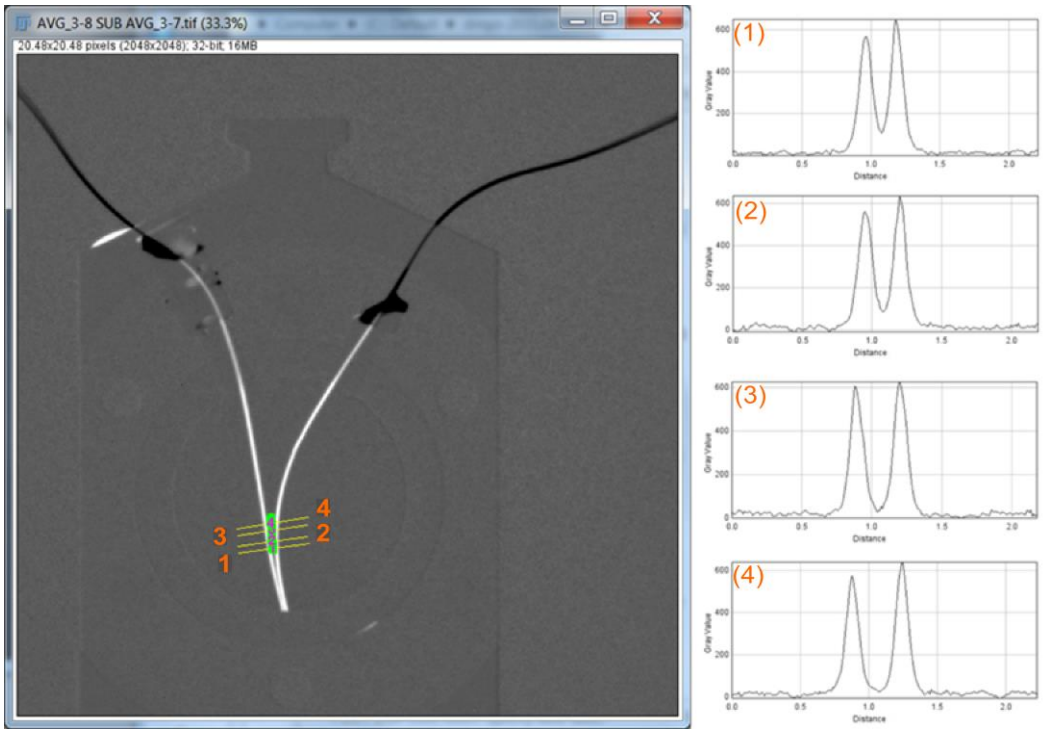

Figure 3-4. Processed neutron radiography image showing cell with distilled water and Nafion strips subtract cell with distilled water only.
(Figure 3-3, c Subtract b). Analysis profiles (yellow and numbered) cross the material strips. Profile plots 1-4 on the right hand side.

It was expected that a denser region of EZ water would nucleate from the Nafion surface as per experiments by other researchers (Zheng, Chin et al. 2006, Chai, Yoo et al. 2009). In these experiments the EZ extended to ~300 µm. Therefore, with a pixel size equating to 25 µm the expected density difference would be evident over 12 pixels either side of the material strips. Therefore, a visible difference of increased pixel values spanning ~24 pixels was expected. The arrangement of the two Nafion strips in a "V" formation was intended to create a synergistic effect where the visible difference (increased pixel values) due to EZ formation could at least be doubled, creating an EZ region large enough to be identified between the strips (see figure 3-5).

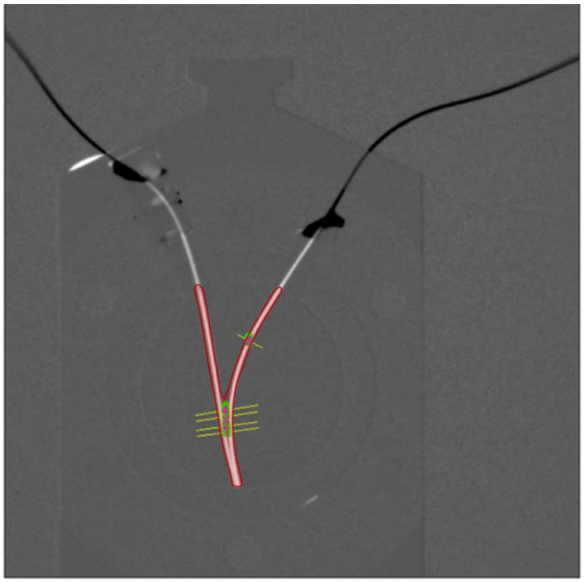

Figure 3-5.Neutron radiography image showing cell with water and Nafion strips. Red region indicates expected area of density difference.

Results

Figure 3-6 shows the result of subtracting the natural logarithm of the water-filled cell with and without two strips of Nafion. Figure 3-7 shows a 3D surface plot of the rectangular ROI shown in figure 3-6. The 3D representation is based on the relative pixel values and makes the differences more distinct.

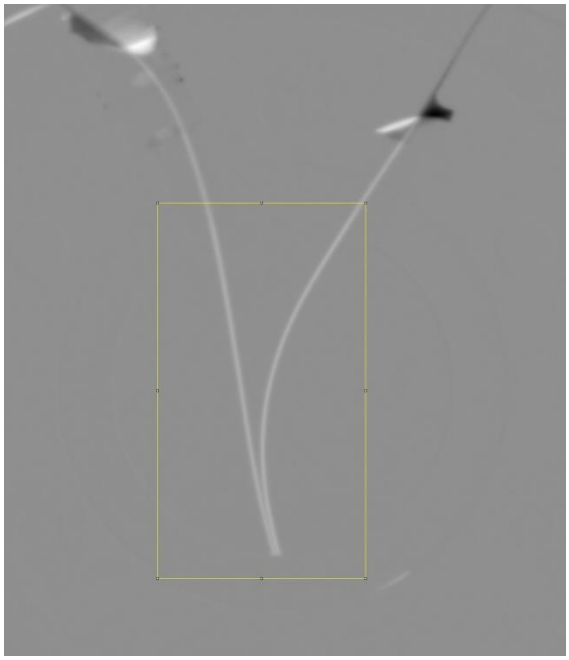

Figure 3-6. Processed neutron radiography image.
Produced by subtracting the natural logarithm of the distilled water -filled cell with and without two strips of Nafion. The yellow outline shows the region of interest (ROI) for creating a 3D surface plot (see figure 3-7).

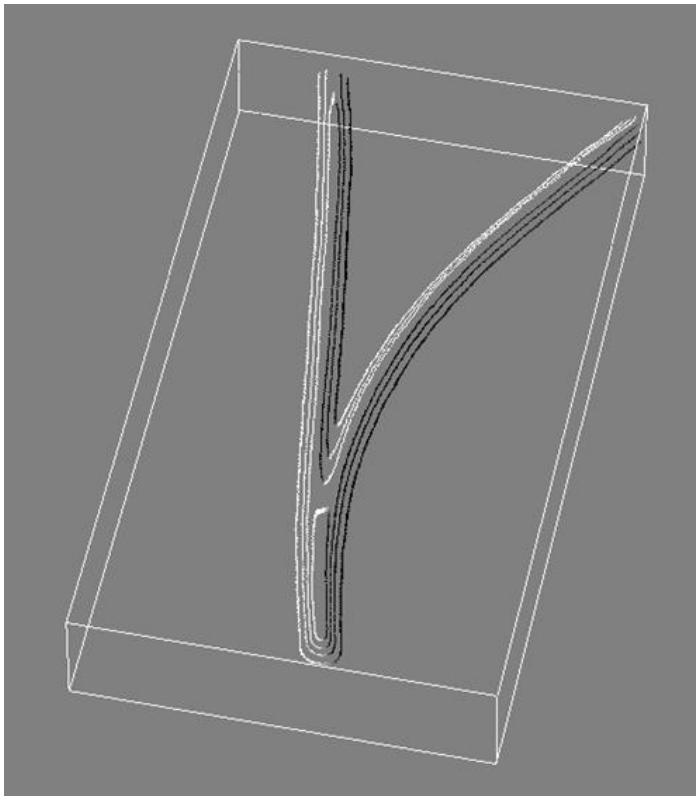

Figure 3-7. 3D surface plot of Nafion strips.
A 3D representation of the relative pixel values from the ROI shown in figure 3-6.

3.2 EXPERIMENT 2; PH VARIATION

Objective

It has been claimed that water adjacent to the hydrophilic surfaces such as Nafion is highly structured, and that this structuring of the water molecules causes a mechanical effect that excludes micro-particles and solutes from the surface to distances up to 500 μm (Zheng and Pollack 2003, Zheng, Chin et al. 2006, Chai and Pollack 2010, Das and Pollack 2013). Thus the region is called the Exclusion Zone. An alternate explanation is that the EZ is caused by a diffusion of ions (protons or hydrogen ions H+) from the hydrophilic polymer Nafion (Musa, Florea et al. 2013, Schurr 2013, Florea, Musa et al. 2014, Huszar, Martonfalvi et al. 2014).

As protons are diffused into the surrounding water it will become more acidic. This experiment seeks to test the claim that Nafion diffuses protons into water by comparing the local pH values of Nafion with other hydrophilic materials used by Pollack and associates.

Materials and method

A range of samples of hydrophilic materials were fully immersed in water in identical containers over a period of days and the pH levels were recorded intermittently. All experiments were performed at ~23°C with ambient room lighting. Samples were sealed with a plastic lid between pH recordings to reduce the amount of atmospheric CO_2 absorbed. The hydrogels (agar and agarose) were selected for their hydrophilicity, the metals (zinc and aluminium) were selected as they were used in experiments by other researchers (Chai, Mahtani et al. 2012) and Nafion was included as it was the predominant material used in EZ experiments.

The samples consisted of: agar (2%; weight: 0.8 - 1.28 g; size: 1.5 – 2 cm diameter masses; Difco, Maryland, USA;); agarose (5%; weight: 0.7 – 1.2 g; size: 1.5 – 2.5 cm diameter masses; California, USA), Nafion 117 sheet (0.2 mm thick; weight: 0.058 – 0.108 g; Fuel Cells Etc.; Texas, USA), aluminium foil (purity: >99.9%, thickness: 0.0254 mm; weight: 0.0025 - 0.0053 g; ESPI Metals, Oregon, USA), and zinc wire (diameter: 0.508 mm, purity: >99.9%; weight: 0.06 – 0.08 g; length: ~2.5 cm; ESPI Metals, Oregon, USA). All control samples were filtered deionized water (10 ml) obtained from an Elix® 100 Water Purification System supplier.

The pH measurements were performed using a pH probe (Sentix 940-3; WTW, Xylem Analytics Australia) and reader (Multi 3430; WTW, Xylem Analytics Australia). All samples were mixed by swirling the container before measurements were taken. This was to ensure an even distribution of any diffused ions throughout the sample rather than localised pH variations in proximity to the sample surface.

Results

The changes to the pH values of each sample were measured (Figures 3-8 to 3-12). Only Nafion showed a significant change (decrease) in water pH (figure 3-8). By contrast, the other substrates did not significantly alter water pH.

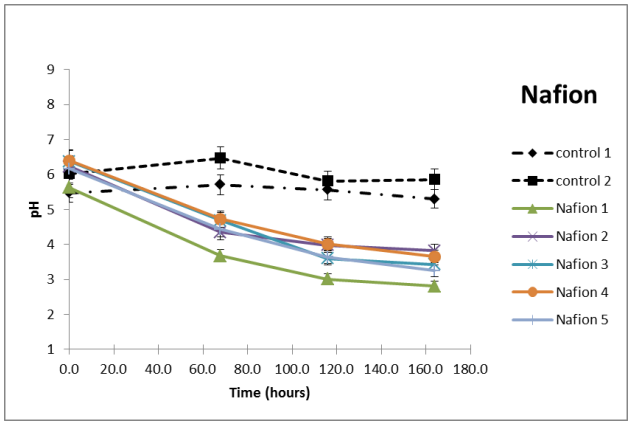

Figure 3-8. pH change of water samples containing Nafion over time.
The control samples are water only. Independent replicate samples are denoted as Nafion 1, Nafion 2, Nafion 3, Nafion 4, and Nafion 5.

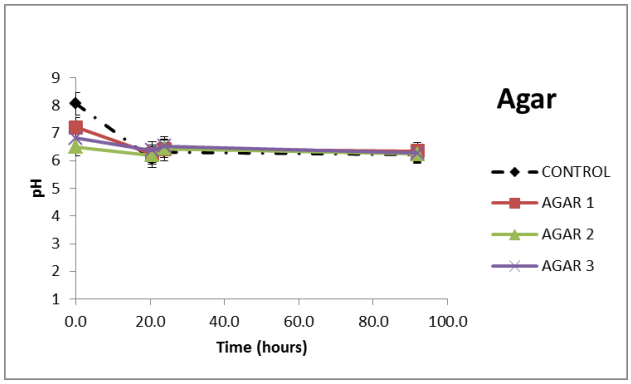

Figure 3-9. pH change of water samples containing 2% agar over time.
Control sample is water only. Independent replicate samples are denoted as Agar 1, Agar 2, and Agar 3.

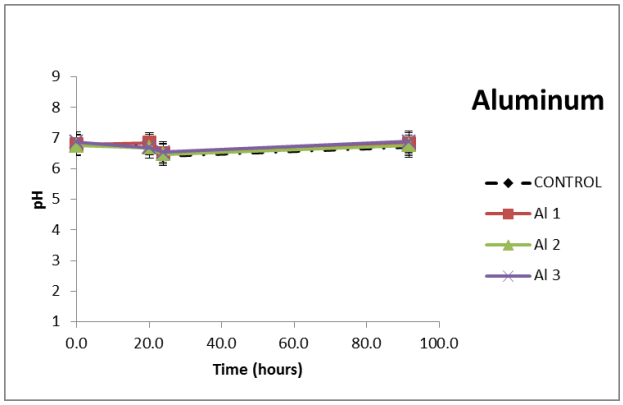

Figure 3-10. pH change of water samples containing aluminium over time.
Control sample is water only. Independent replicate samples are denoted as Al 1, Al 2 and Al 3.

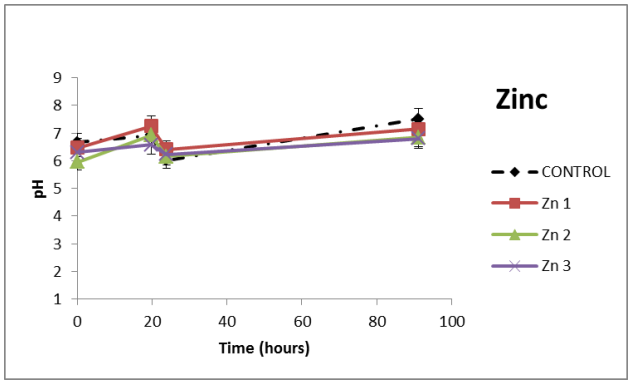

Figure 3-11. pH change of water samples containing Zinc over time.
Control sample is water only. Independent replicate samples are denoted as Zn 1, Zn 2 and Zn 3.

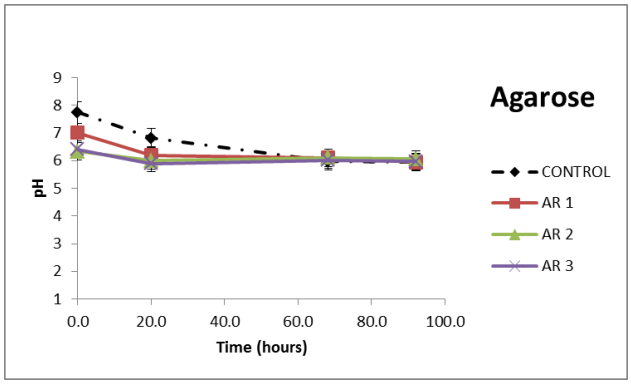

Figure 3-12. pH change of water samples containing 5% agarose over time.
Control sample is water only. Independent replicate samples are denoted as AR 1, AR 2 and AR 3.

3.3 Experiment 3; Birefringence.

Objective

The purpose of this experiment is to determine whether birefringence is indicative of an ordered interfacial layer of water at the sample surface.

Background

Water is known as an isotropic liquid. That is, the properties of the liquid, such as molecular orientation, are the same in all directions. In contrast, the properties of anisotropic materials or liquids differ in some directions, creating a more distinct alignment within their molecular arrangement. In transparent or translucent materials and liquids the level of isotropy affects light as it passes through, particularly how it is diffracted. With anisotropic materials such as crystals, light is often diffracted in two planes. That is, the diffracted rays emerge polarised in

two different directions. This is known as birefringence. A good example of a birefringent crystal is calcite (see figure 3-13).

Figure 3-13. Calcite crystal displaying distinctive double refraction of underlying image. (Summers 2015).

In this example it is clear that the image underneath is transmitting through the crystal, emerging as two separate images. When viewed through a polarised filter one of the images "disappears" as it is blocked by the filter. When the same filter is turned another 90° the first image is filtered out and the second becomes visible. This indicates that the emerging rays are polarised and oriented at 90° to each other. The two types of rays emerging from birefringent materials are known as "ordinary" and "extraordinary" rays. The extraordinary rays are refracted whilst the ordinary rays pass through the sample unchanged (Wahlstrom 1954).

A useful tool to investigate birefringence in crystalline materials is a polarised light microscope (figure 3-14).

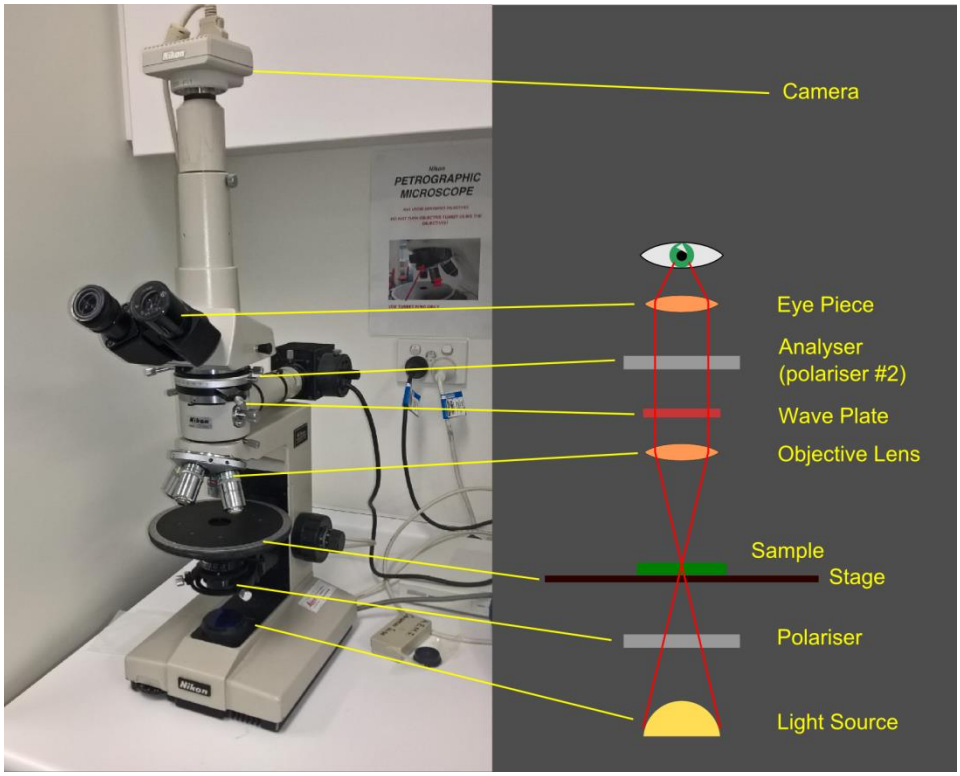

Figure 3-14 A typical polarised light microscope.

Notice from figure 3-14 that the incident light is first polarised before passing through the sample. Finally it passes through a second polarised filter (Analyser). In typical use the Analyser is set at 90° to the Polariser. This effectively filters out the initial light from the Polariser. It is only the reoriented light from a crystalline sample that will pass through to the Eye-Pieces. An important part of this microscope is the Gypsum Plate also known as a Retardation Plate or Wave Plate. This component typically consists of a birefringent or crystalline material and is used to recombine the out-of-phase, polarised light rays passing through a birefringent sample. When viewing birefringent samples the resulting image is usually brightly coloured due to the interaction of the two alternately polarised light rays.

Weakly birefringent materials, however, do not produce a brightly coloured final image. In order to enhance detection of weakly birefringent samples a technique was devised by Newton, Haffegee et al. (1995). In this method the wave plate is reoriented from its typical angle of 45° from the initial polariser to that of ~7.5°. This enhances the intensity contrast and colour contrast of structures with lower optical path difference and different orientation relative to that of the conventional 45° orientation. Figure 3-15a depicts the resulting image in comparison with the typical 45° orientation (3-15b) and the polarised light image without the wave plate (3-15c).

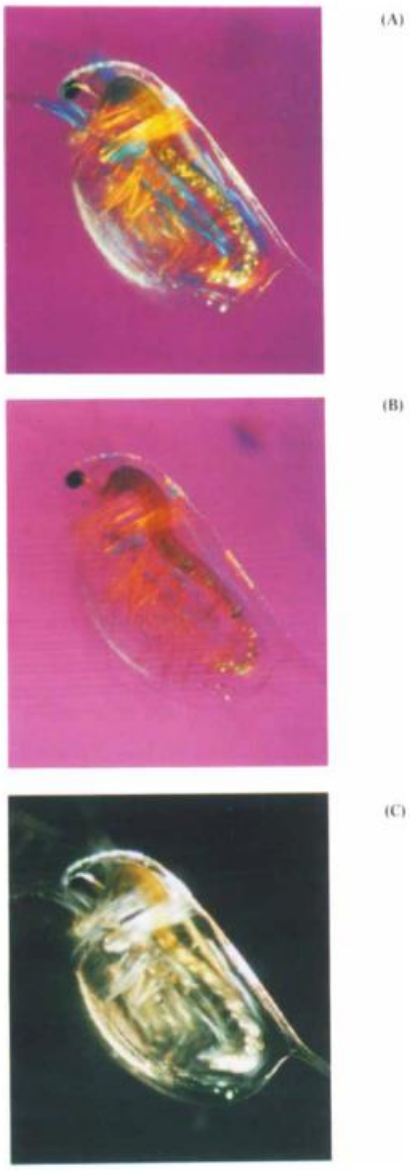

Figure 3-15. Daphnia viewed under a polarised light microscope.
Wave plate at 7.5° (a). Wave plate at conventional 45° (b). Polarised light image without wave plate (c). Reproduced from Newton, Haffegee et al. (1995)

With the above in mind, claims that birefringence has been observed in water samples at hydrophilic surfaces are of particular interest (Bunkin, Ignatiev et al. 2013, Pollack 2013). Figure 3-16 shows an example of such anisotropy observed in water adjacent to a hydrophilic material.

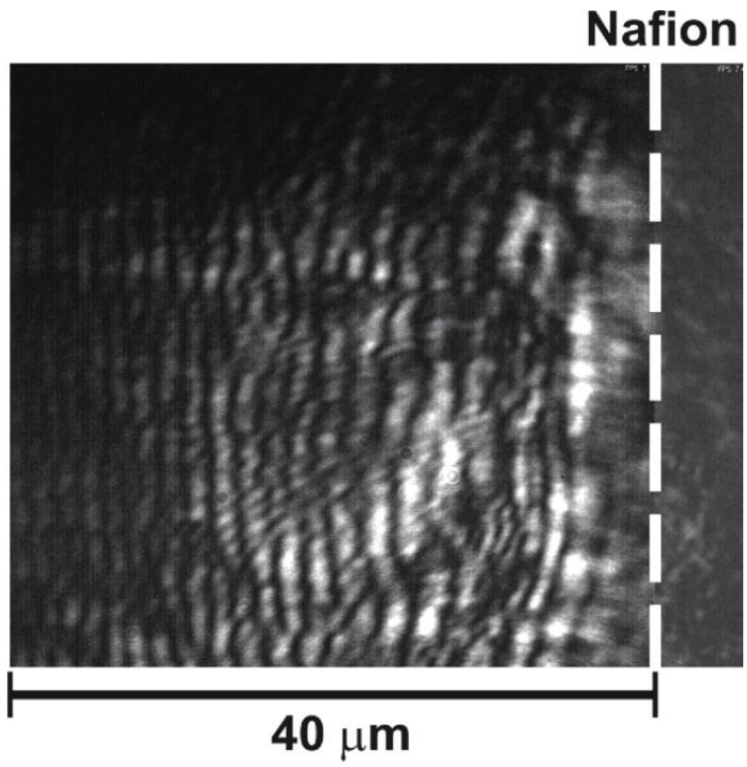

Figure 3-16. Anisotropic visual feature in water at the water-Nafion interface. (Bunkin, Ignatiev et al. 2013)

Such evidence of anisotropy is claimed to indicate long-range order in water. In order to examine this view the following experiment was conducted.

Materials and method

A polarised light microscope (Nikon Eclipse 50iPOL; Nikon Corporation, Japan) with mounted camera (Nikon DS-Fi1; Nikon Corporation, Japan) was used to view the samples. The standard ¼ wave plate was used to show birefringence. Although this plate is usually oriented at 45° to the fixed polariser, the birefringence enhancement technique developed by Newton, Haffegee et al. (1995) was employed. Thus the wave plate was rotated to 7.5° from the fixed polariser. This enhancement technique was applied in all views of birefringence in this study.

The water used in this study was obtained from a Milli-Q® Advantage A10 Water Purification System.

The samples consisted of: agar (2%; weight: 0.8 - 1.28 g; Difco, Maryland, USA;); agarose (5%; weight: 0.7 – 1.2 g; California, USA), Nafion 117 sheet (0.2 mm thick; weight: 0.058 – 0.108 g; Fuel Cells Etc.; Texas, USA), Aluminium foil (purity: >99.9%, thickness: 0.001”; weight: 0.0025 - 0.0053 g; ESPI Metals, Oregon, USA), Zinc wire (diameter: 0.020”, purity: >99.9%; weight: 0.06 –

0.08 g; Length: ~2.5 cm; ESPI Metals, Oregon, USA) and copper foil (thickness: 0.4 mm; Analar, British Drug Houses, England).

EZ's were visualized using a 1:500 suspension of 1.0 µm carboxylated solid-latex microspheres (Polyscience Inc., Pennsylvania, USA). Samples of various materials and substances were examined in both wet and dry conditions on a standard glass microscope slide (dimensions: 76.2 mm x 25.4 mm x 1.0 mm; Livingstone International Pty. Ltd., Australia) with a glass cover slip (dimensions: 50 mm x 22 mm x 0.16 mm; Ted Pella, Inc., California, USA), as well as on a modified slide as per figure 3-17a. The bottom cover slip was glued to the modified slide (figure 3-17b) using clear silicon adhesive (Handy Hardware brand; G&L Wholesalers Pty. Ltd., Australia). The modified slide allowed for thicker samples (~2 mm) as well as for thin strips of material to be turned on the side to view along the surface. The wet samples were examined with and without microspheres.

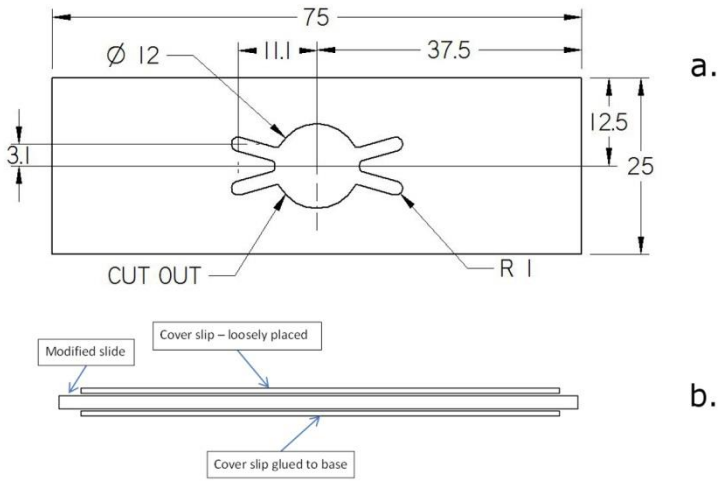

Figure 3-17. Modified microscope slide used for exclusion zone birefringence studies. Hole cut detail (a) and construction of the modified slide assembly (b).

Small portions of each material were cut to fit in the standard and modified slide arrangements.

Results

Of all the samples tested in this experiment no evidence of birefringence was detected emanating from the material edge into the bulk water in contrast to previous claims (see Appendix A). However, a significant degree of birefringence was observed at the edge of certain samples. These included Nafion, copper, zinc and aluminium. It was of great interest that birefringence could be detected on some edges more than others. Upon investigation it was found that the physical nature of the edge was the driving factor. That is, edges that were cut

using scissors appeared as peaks of varying size and shape when viewed through the microscope and yielded little birefringence. On the other hand, edges that were cut with a scalpel blade yielded significantly more birefringence (see figure 3-19).

Figure 3-18 shows single frame micrographs of a Nafion edge cut by blade (A) and scissors (B). In figure 3-18B we see the scissor cut producing an uneven edge consisting of peaks and troughs. Several of the peaks of six different images were measured using the image analysis program, Image J. Of the peaks measured the minimum and maximum were 0.501 and 4.611 μm respectively, and the average peak size was 2.382 μm.

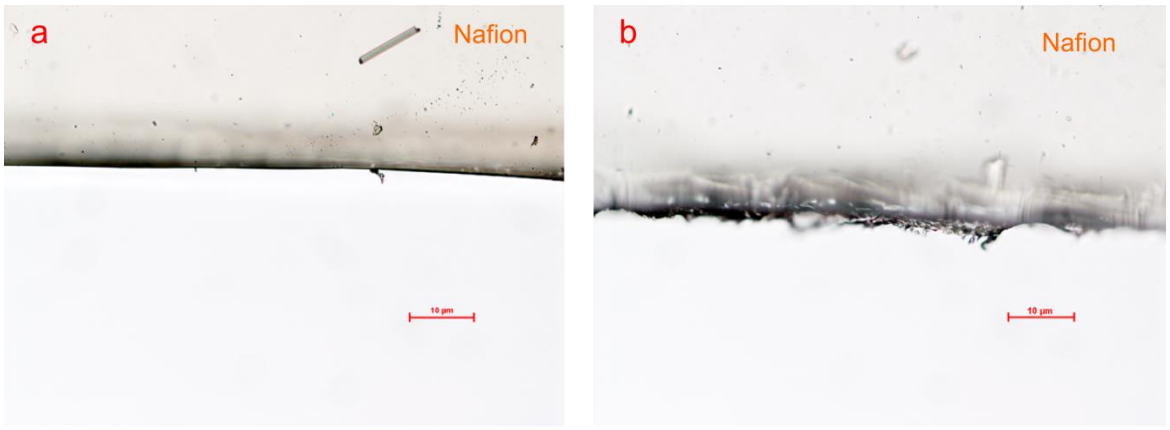

Figure 3-18. Micrographs of a Nafion edge cut by blade (A) and scissors (B).

Figure 3-19 shows a micrograph of a piece of Nafion in a microsphere suspension viewed through a polarised light microscope. Here the EZ can be seen (yellow arrows) but with birefringence evident only at the edge of the material. One edge was cut with a scalpel blade (a) at which birefringence is clearly seen, and the other was cut with scissors (b) where very little birefringence is evident. It is noted that the EZ is greater near the blade cut edge than the scissor cut edge. The reason for this is unknown and may require further study. However, the primary focus of this study is on investigating birefringence within the EZ and its cause.

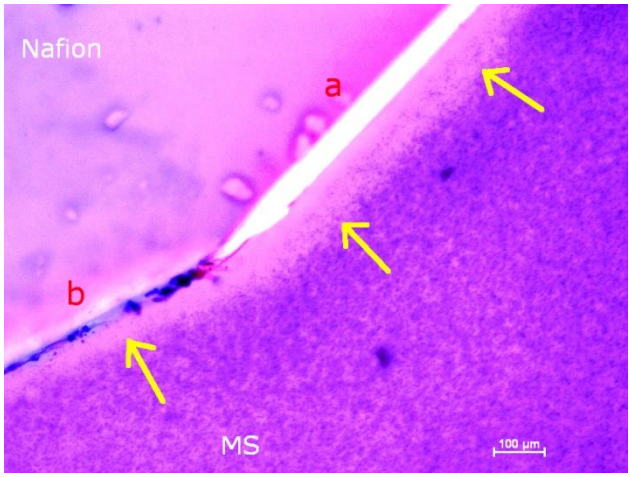

Figure 3-19. Exclusion Zone (EZ) evident adjacent to Nafion using a microsphere suspension (MS). EZ indicated by yellow arrows. One edge is cut with a scalpel blade (a), the other with scissors (b). Image is enhanced for print.

To further support the view that water was not a contributing factor to the observed birefringence the experiment was performed again without water and microsphere suspension (see figure 3-20).

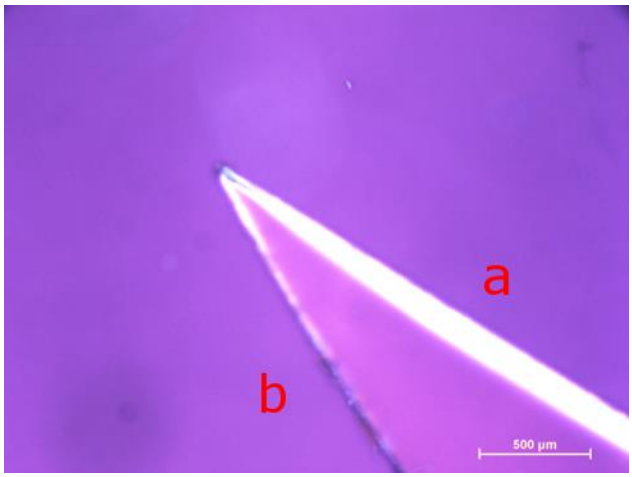

Figure 3-20. A dry spear-shaped piece of Nafion. Significantly brighter birefringence at the blade-cut edge (a) compared to the scissor-cut edge (b).

Here we see bright birefringence in the scalpel cut edge (a) and very little in the scissor cut edge (b).

Figure 3-21 shows a dry strip of aluminium foil (~2mm wide) turned on its side to allow viewing along the surface. As the sample is rotated from 0° (figure 3-21a) to 90° (figure 3-21b) the reflected light changes from yellow to blue. This is characteristic of birefringence.

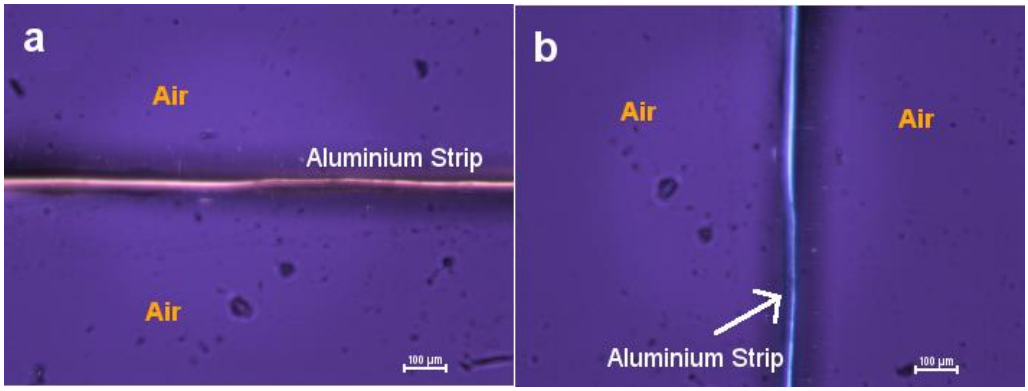

Figure 3-21. View of dry aluminium strip across the surface.
The sample appears yellow when horizontal (a) and blue when rotated 90° (b). Scale bar, 100 µm.

Figure 3-22 shows a strip of copper in a microsphere solution (figure 3-22a) and without water or microsphere solution (figure 3-22b). Here we can see bright birefringence at the material edge that appears to extend into the microsphere suspension. A birefringent edge can also be seen in the dry sample. It is of particular interest to note that an EZ is not evident in this image.

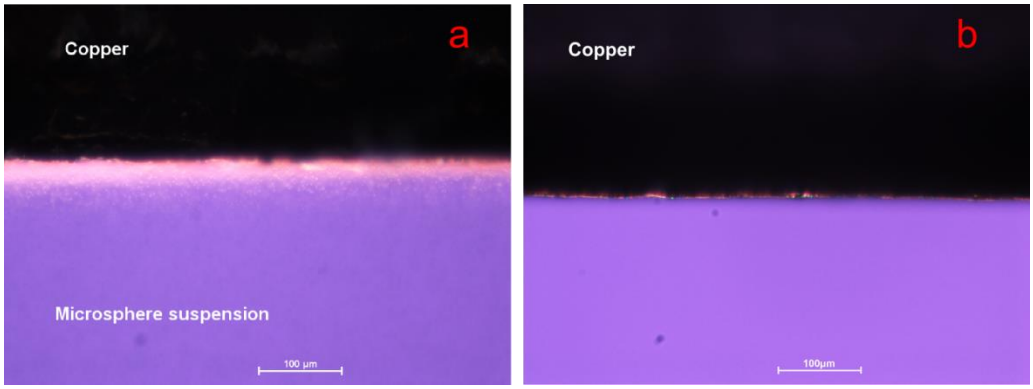

Figure 3-22. Copper foil viewed with a polarised light microscope.
Copper in microsphere suspension with brightly reflected birefringent edge visible at the copper-suspension interface (a). A thin region of birefringence is visible without the microsphere suspension (b).

Upon close inspection, zinc wire showed birefringence at its edge. Figure 3-23a shows birefringence at the zinc sample edge under typical lighting conditions. It is important to note that no water was used in this sample. Figure 3-23b shows the same sample with the light greatly reduced and image contrast enhanced.

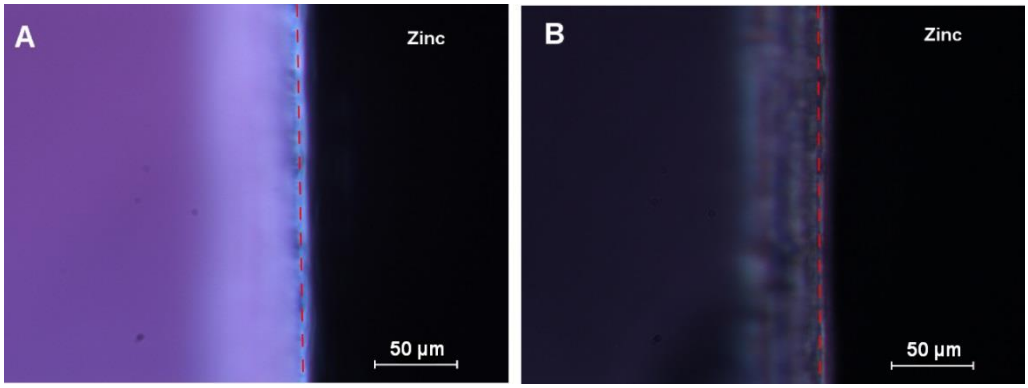

Figure 3-23. Dry zinc wire viewed with polarised light microscope.
A bright region is visible at the zinc edge with normal light settings (A). Decreasing light by reducing the aperture size reveals light and dark ridges (B).

Similarly, dry copper foil, viewed under a polarised light microscope also revealed light and dark ridges adjacent to its edge as seen in figure 3-24. In this case the ridges became more apparent when the image was enhanced by increasing the brightness and contrast.

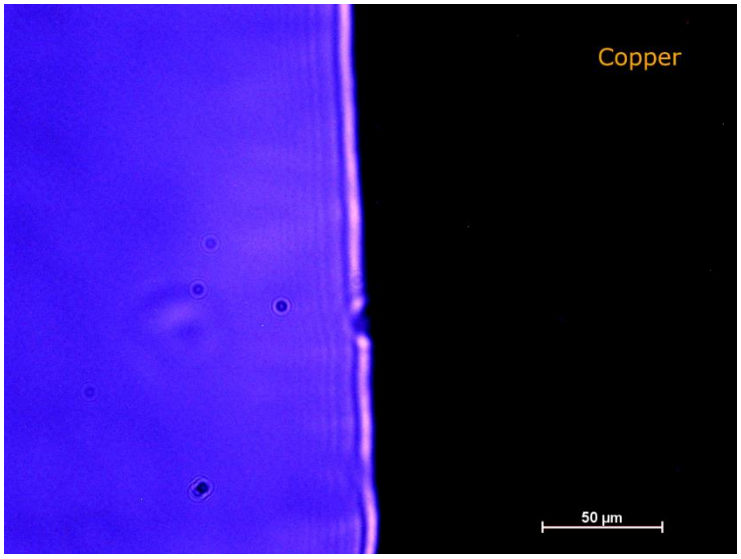

Figure 3-24 Dry copper foil viewed with polarised light microscope.
Light and dark ridges appear adjacent to the copper edge when image is enhanced by increasing brightness and contrast.

When viewing EZ's near Nafion samples it was noted that they varied as a function of height from the Nafion. Figure 3-25 shows an EZ adjacent to a piece of Nafion viewed from three focal planes as indicated in figure 3-25b. Figures 3-25ai (upper view) and 3-25aiii (lower view) showed all microspheres clearly but figure 3-25aii (middle view) showed a region of blurred microspheres further from the Nafion indicating they were located above and below the focal plane. The red rectangles indicate regions that have been enlarged and displayed beneath their

corresponding image. Thus the shape of the EZ is consistent with that indicated in figure 3-25b. The shape of the EZ appears consistent with the findings of Musa, Florea et al. (2013) who propose the EZ is generated by a flow of ions from Nafion into water.

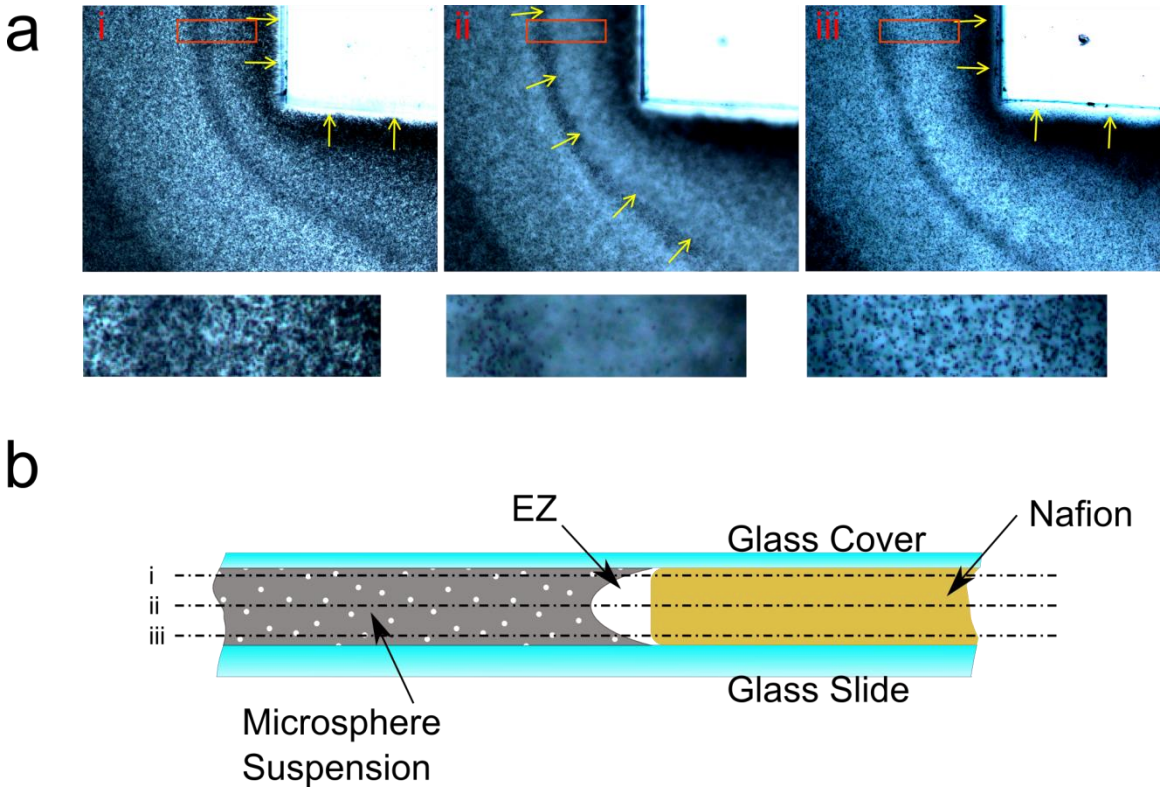

Figure 3-25. Shape of the EZ.
(a) Views of Nafion (upper right) in microsphere suspension at the three focal plains indicated in (b). Yellow arrows indicate the visible edges of the EZ from upper (i), middle (ii) and lower focal plains (iii). The images below ai, aii and aiii show enlarged sections outlined in red rectangles. Contrast and brightness of the micrographs are enhanced for print. (b) Diagrammatic representation of a typical EZ at the Nafion-water interface.

Preliminary Discussion

The evidence provided in this experiment clearly indicates that water was not a contributing factor in any of the observed birefringence. On the contrary, reflected light seemed to be the major contributor of birefringence. The details of reflected birefringence are beyond the scope of this study, however it is possible that low-angled reflection and internal reflection from the

blade-cut Nafion surface may contribute to the observed birefringence in other studies (Bunkin, Ignatiev et al. 2013, Pollack 2013, Bunkin, Gorelik et al. 2014) (see figure 3-26)

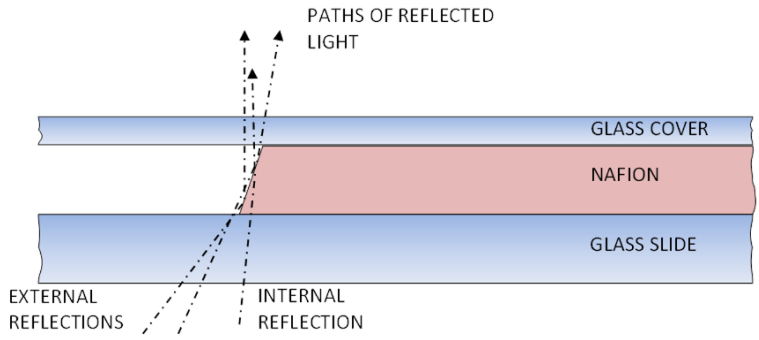

Figure 3-26. Proposed reflection detail describing low-angle internally and externally reflected light from the Nafion surface.

In support of this It is noted that Figures 3-23b and 3-24 show visual characteristics similar to that of Bunkin, Ignatiev et al. (figure 3-16). What is of particular interest here is that no water was necessary to generate these characteristics. When viewing EZ's at various depths (figure 3-24) it appears that the EZ extends further from the Nafion surface near the middle of the sample compared to the upper and lower regions. The shape of the EZ is consistent with that observed by Musa, Florea et al. (2013). This supports their view that EZ's may be generated by the diffusion of ions (protons) from the Nafion into the water. In their work they observe flow vortices in microsphere movement above and below the Nafion edge as shown in figure 3-27.

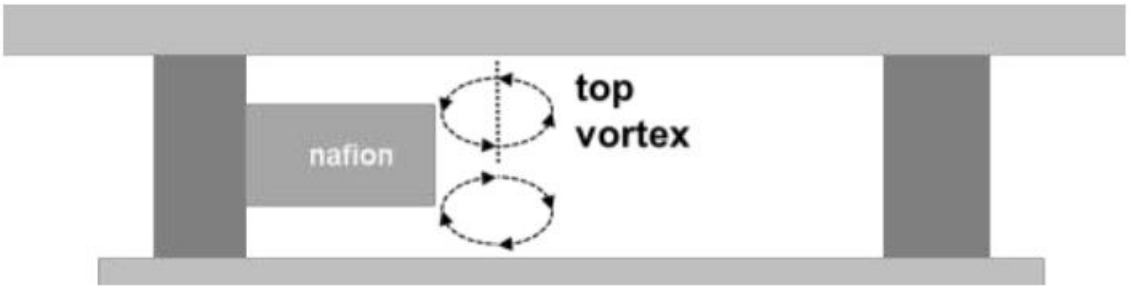

Figure 3-27. Flow vortices.
An illustration of microsphere movement above and below a Nafion sample during the formation of an EZ. Reproduced from Musa, Florea et al. (2013) with permission from ASCE.

3.4 EXPERIMENT 4; ELECTROCHEMICAL IMPEDANCE SPECTROSCOPY

Objective

It has been claimed that interface water can be detected using Electrochemical Impedance Spectroscopy (EIS) (Coster, Chilcott et al. 1996, Sistat, Kozmai et al. 2008). With this method an alternating current (A.C. signal) of small amplitude (~10 mV) is passed through a sample (cell) and the impedance of the current is measured. By this method, the capacitance and induction of a system (electrochemical circuit) respond differently with varying signal frequency. For example, any factor in the system that provides capacitance will impede low frequency A.C. current flow. Higher signal frequencies, however, will have less impedance. Also, an inductive factor will respond oppositely to a capacitor. That is, low frequencies will register less impedance than high frequencies. Therefore, with a set current over a range of frequencies the graphical plot of the impedance will indicate any change in electrochemical properties of the system such as capacitance and inductance.

It is theorised here that a pertinent instance of capacitance in this case is the double layer (interface water) capacitance (Sverjensky 2001, Park, Choi et al. 2006, Catalano 2011). This is caused by a build-up of ions on the electrode creating an insulating effect. Charges separated by an insulator form a capacitor. There are numerous factors affecting the value of the double layer capacitance. These include electrode potential, temperature, ionic concentration, types of ions, oxide layers, impurity absorption and size of electrode.

Magnetic fields are purported to alter the physicochemical properties of water due to a restructuring of the molecular clusters, and these changes are attributed to altered hydrogen bond strengths. If indeed this is the case then it may be reasonable to assume that such changes to hydrogen bonds may be evident in interface water. That is, strengthening or weakening hydrogen bonds may increase or decrease the number of bonds formed within a structured feature (i.e. cluster or ordered interface). This then may be expressed as changes to the extent of the double layer. This should, in turn, be indicated in the impedance plot as an increase or decrease of the capacitance of the system, i.e. change in the lower frequency impedance response.

This experiment aims to test the magnetic affect hypothesis and if changes are detected then a comparison can be made between magnetised and non-magnetised water. Figure 3-28 gives an indication of an expected difference between Bode impedance plots of magnetised and non-magnetised water. It is theorised here that magnetisation may lead to an increase of an ordered

region, such as the water-electrode interface, due to strengthening of the hydrogen bonds. With strengthening of the hydrogen bonds within the interface (double layer), the extent of this region may also increase. By increasing the extent of the interface layer it is expected the electrical capacitance of the layer would also increase. This would then be expressed as an increase in electrical impedance in the lower frequencies of an EIS plot.

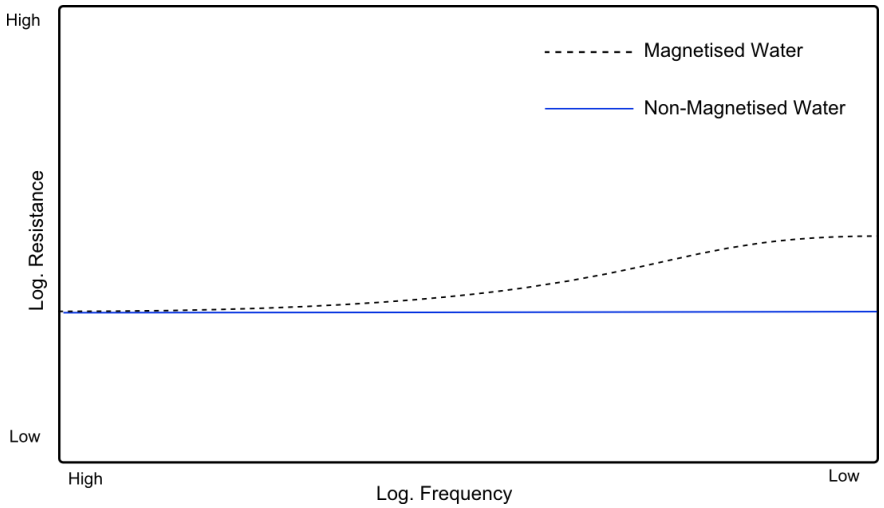

Figure 3-28. Predicted Bode impedance plots.
Magnetised water predicted to show greater impedance at low frequencies (dashed line) than non-magnetised water (solid line).

Design and procedure

This study consists of two apparatuses; 1/ a conductivity cell (Philips PW9512/01 cell with platinised platinum black electrodes) (apparatus 1; see figure 3-29); and, 2/ an apparatus made from 6mm clear acrylic sheet, designed specifically for this study (apparatus 2; see figure 3-30). This apparatus consists of multiple layers of acrylic sheet glued together to form two sides of a clamping arrangement. These sides are forced against either side of a layer (sample layer) with a central hole designed to be filled with a hydrogel. This layer is then sealed with O-rings to prevent leakage. Water is fed into the apparatus via the connecting nozzles. Electrodes are inserted into the openings at the top of each side as indicated (SECTION A-A).

Apparatus 2 allows for the inclusion of a boundary material or membrane to be inserted between the O-rings and the sample layer component in order to examine water-surface interface properties. In this study the hydrogels were Agar (5%, Oxoid Ltd., England) and membrane; Nafion 117 film (0.2 mm thick; Fuel Cells Etc.; Texas, USA).

The magnets used here were a ferrite block magnet (dimensions: 150 x 50 x 25.4 mm; Gauss: 1400; grade C8; The Aussie Magnet Company Pty. Ltd.; Australia – polarisation through 25.4 mm thickness) and six disc magnets (12 mm x 3 mm; Neodymium; combined Gauss: 670, grade N42, The Aussie Magnet Company Pty. Ltd., Australia). All magnetic Gauss strengths were measured at the magnet surface with a DC Gauss Meter (model GM-1-ST; Alpha Labs Ltd.; Salt Lake City; Utah, USA). These magnets were chosen due to magnets of similar strengths used by previous researchers (Toledo, Ramalho et al. 2008, Cai, Yang et al. 2009)

Both apparatuses were connected to a multichannel potentiostat (VSP; Biologic Science Instruments; France) running EC-Lab® software. The frequency range was from 20 Hz to 100 MHz. All water was obtained from an Elix® 100 Water Purification System supplier (Merck Millipore; Australia). The water was degassed by boiling in a sealed container and allowed to cool 24 hours prior to use.

A magnetic bridge was constructed from a 6 mm length of 75 mm x 75 mm x 5 mm square hollow steel tube and M10 steel nuts and bolts.

Figure 3-29. Philips PW9512/01 cell with platinised platinum black electrodes.

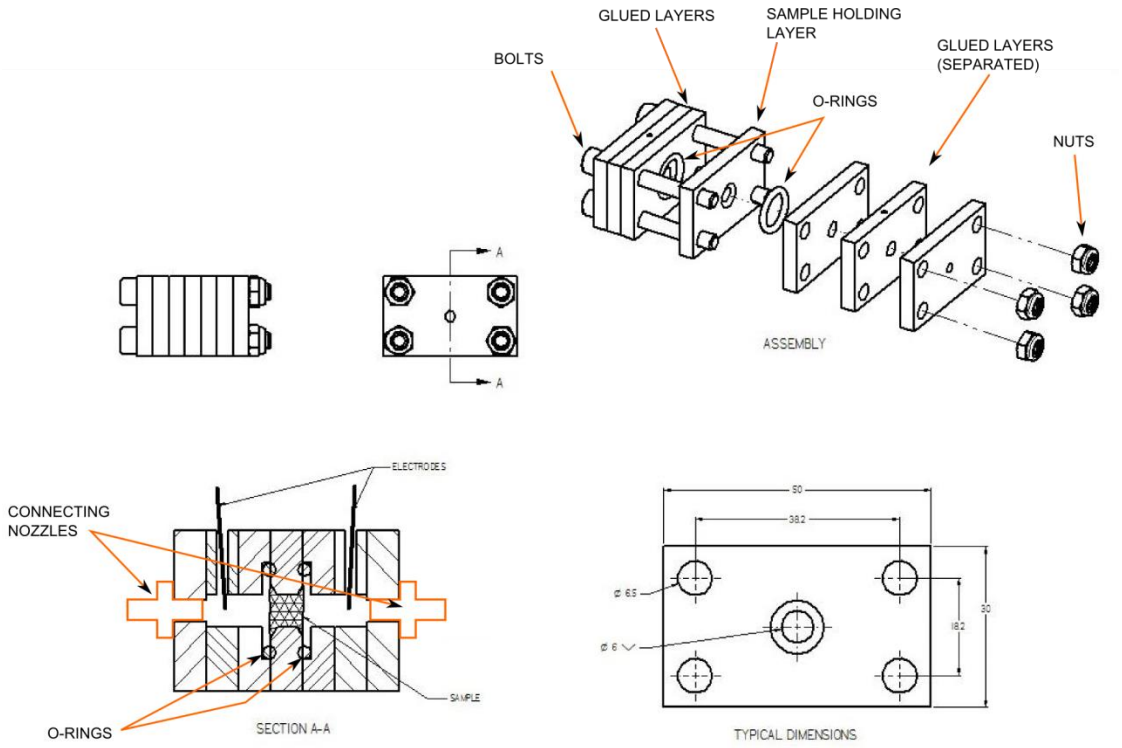

Figure 3-30. Construction diagram of apparatus 2.

Regarding the sensitivity of the equipment used in this experiment, the following studies give examples of relative changes in the properties of magnetically treated water compared to non-treated water.

Ghauri and Ansari (2006), examining the viscosity difference between magnetically treated and non-treated water, reported a relative increase in viscosity of 10^{-3} in a 7.5 KG strength transverse magnetic field. Hosoda, Mori et al. (2004) noted a ~0.1% increase in refractive index of water exposed to magnetic fields up to 10 T. Inaba, Saitou et al. (2004) noted an increase in melting temperature in H_2O and D_2O to 5.6 and 21.8 mK respectively when exposed to 6 T magnetic field compared to the non-exposed water. Higashitani and Oshitani (1998), using atomic force microscopy, investigated the adsorbed layers of electrolytes on mica surfaces within a 0.42 T static magnetic field. They reported a relative increase of adsorbed layers to 1.17 compared to that of non-treated solutions.

With the above in mind, and considering that the specifications of the potentiostat indicate the maximum resolution of the voltage and current measurements to be < 0.0033% of the range

(Biologic 2015), it is anticipated that the equipment is capable of detecting changes in the capacitance of the electrical double layer due to magnetic interaction.

Design and procedure

Apparatus 1 was placed in containers with water and sealed with Parafilm® to reduce atmospheric CO_2 infusion. Two different container configurations were used to examine water within an evenly directed magnetic flux (using the magnetic bridge) and exposed to an undirected magnetic pole (ferrite magnet).

The apparatus was then connected to the potentiostat with a two electrode configuration. Figure 3-31 shows the sample (water) between six disc magnets (three either side) held in a magnetic bridge to ensure an evenly directed magnetic flux. This is setup 1a.

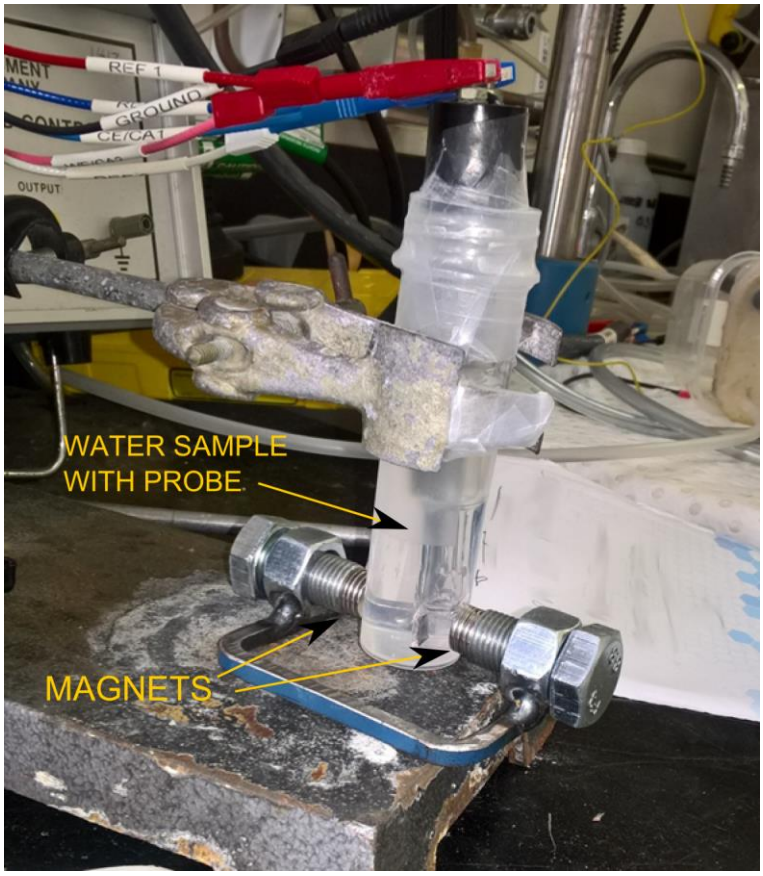

Figure 3-31. Probe and magnet apparatus 1a.
Philips cell in narrow container with water. Disc magnets in magnet bridge at base near electrodes.

Figure 3-32 shows the sample sitting approximately 7 mm above a ferrite block magnet. The magnetic field strength at this distance is calculated to be approximately 306 Gauss. This setup is similar to the method used by Toledo, Ramalho et al. (2008).

Measurements were taken periodically over a period of 30 minutes with and without magnetic field exposure.

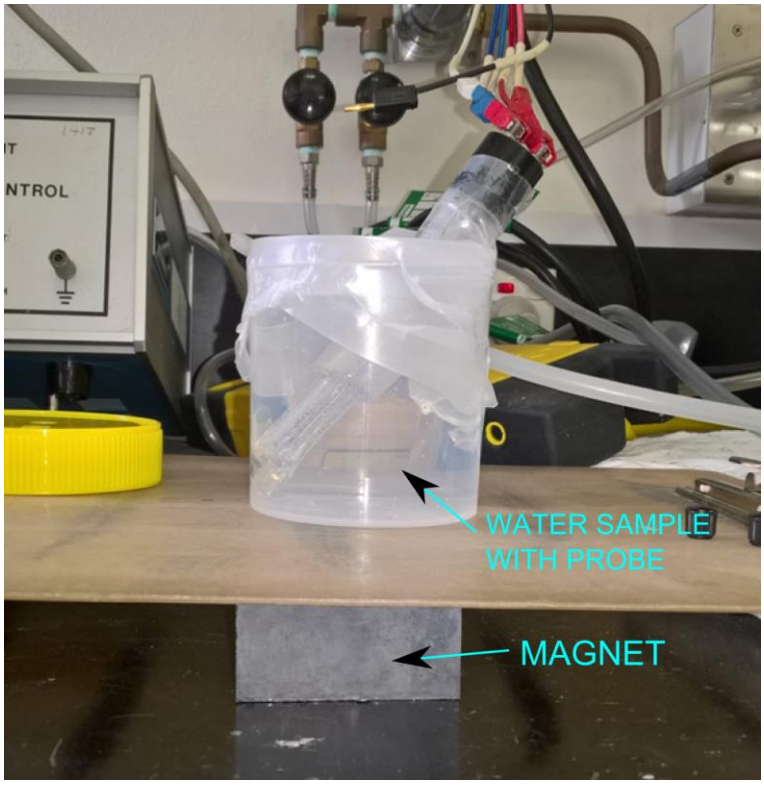

Figure 3-32. Probe and magnet apparatus 1b.
Philips cell in container with water. Ferrite magnet located beneath. Distance, magnet to probe ~7 mm.

Results

Figure 3-33 shows the Bode plots of two EIS experiments – magnetised and non-magnetised water samples. It shows the impedance with the log frequency plotted on the x-axis and the absolute impedance values on the y-axis. The magnetised and non-magnetised plots are labelled accordingly with the number of minutes from setup to plot in each plot label. The control plots of the magnetised samples (e.g. MAGNETISED-1 (CONTROL)) are non-magnetised. That is, the plots are taken prior to magnetic exposure. In this case the number following the plot name indicates the time in minutes from setup to plot.

The upper series of plots are taken from the non-magnetised samples and the lower series are from the magnetised samples. The non-magnetised sample plots are considered as a control run in that they are from a separate water sample examined over time.

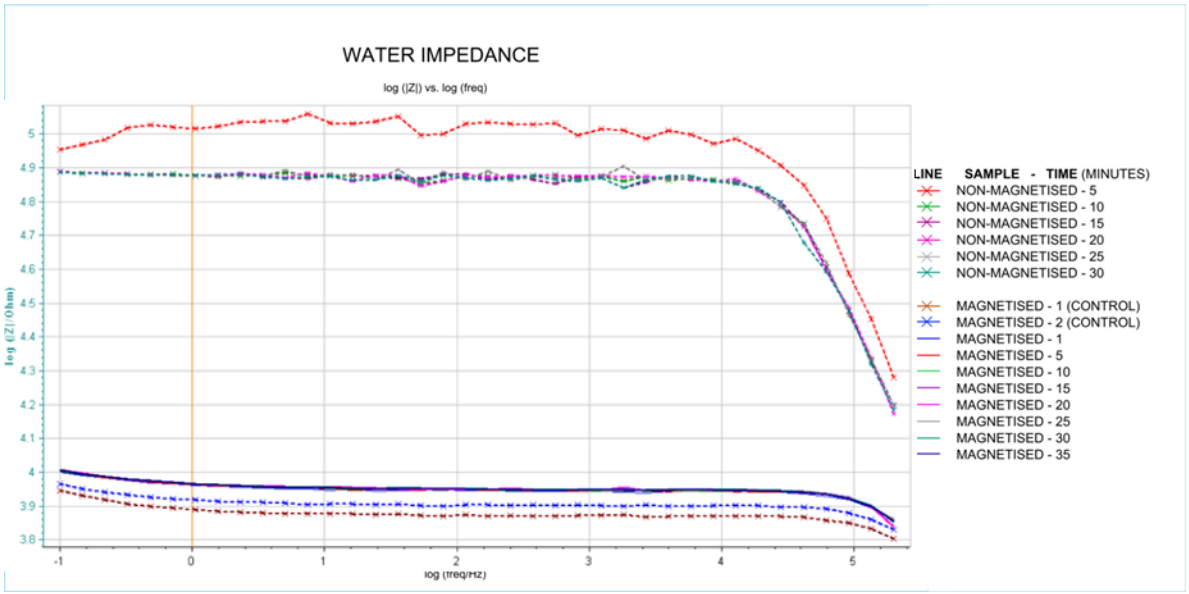

Figure 3-33. Bode plots of magnetised and non-magnetised water samples.
Names indicate condition of sample (magnetised/non-magnetised) and time start of experiment. Control samples in the magnetised sample plots are from the same water sample as magnetised but prior to application of magnets. The non-magnetised sample plots (upper) are from a separate water sample to the magnetised.

Here we can see a distinct difference between the magnetised and non-magnetised sample plots. However, it is important to note that of the magnetised sample plots, the control samples (no magnetic exposure) register lower impedance values to the subsequent magnetised plots. If considered alone this may indicate a distinct difference between control and magnetically exposed samples. But when compared to the non-magnetised plots (upper) it can be seen that the control plots are distinctively different to the non-magnetically exposed samples, even though they share the same conditions.

What can be deduced is that the plots taken within the first five minutes of each experiment show different values to the subsequent plots within the series. This is consistent with both magnetised and non-magnetised samples. This is most likely due to the dissolution of gases from the water that were introduced during the filling of the container and when inserting the probe.

The difference between the impedance readings of the two experiments may be due to a build-up of CO_2 or other atmospheric gases over the time between each experiment. Although the container from which the samples were decanted was sealed with a plastic lid, the brief period of exposure when decanting and the time elapsed between experiments, may have been enough

to expose the water to gaseous infusion. This may have sufficiently changed the chemical composition and electrochemical properties of the water.

Figures 3-34 and 3-35 show Bode plots of agar-in-water and Nafion-in-water experiments consecutively. In both these experiments it can be seen that even with the addition of a hydrophilic material there is no apparent difference in capacitance. This is evident by the similar values plotted in the lower frequencies (right-hand side). It is important to note that the impedance plots of the magnetised samples bear little difference to the non-magnetised samples.

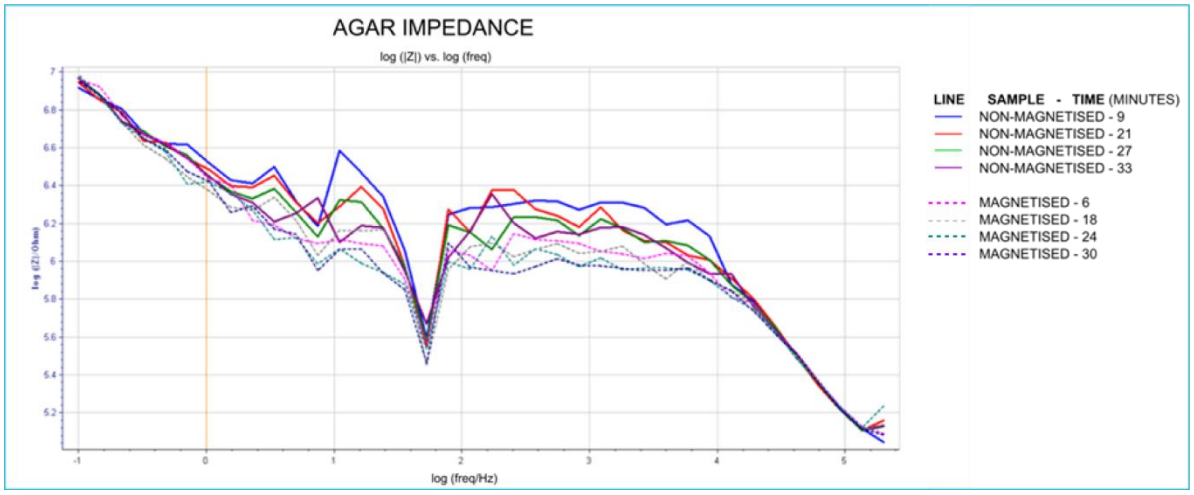

Figure 3-34. Bode plots of Agar-water sample over time.
Non-magnetised (solid lines) and magnetised (dashed lines). Number of minutes from setup indicated in graph legend. The same sample is used but with the introduction of a magnetic field after the initial non-magnetically exposed readings.

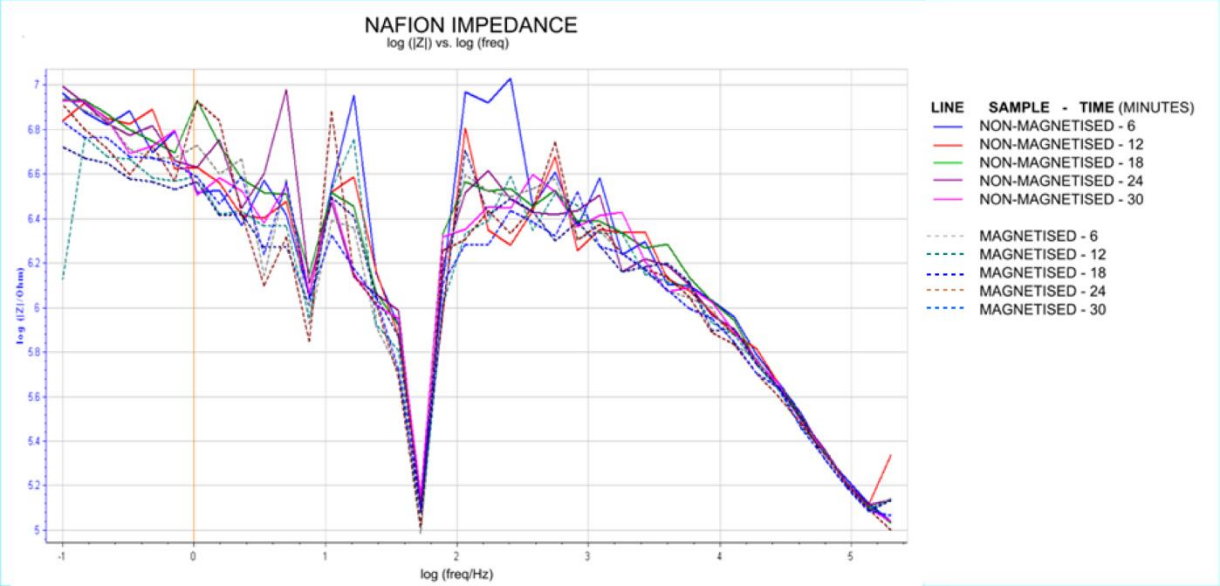

Figure 3-35. Bode plots of Nafion-water sample.

Non-magnetised (solid lines) and magnetised (dashed lines). Number of minutes from setup indicated in graph legend. The same sample is used but with the introduction of a magnetic field after the initial non-magnetically exposed readings.

3.5 EXPERIMENT 5; U.V. VISUAL SPECTROSCOPY

Objective and background

Vibrational spectroscopy techniques such as ultraviolet visual spectroscopy, infrared and Raman spectroscopies are useful in identifying the elementary atoms of a compound by identifying the bonds between atoms. Each bond type (e.g. carbon-oxygen, oxygen-hydrogen) vibrates within their own particular range of frequencies. In spectroscopic analysis techniques a light beam of a select frequency range (e.g. ultraviolet or infrared) is introduced to the sample and the light transmitted through the sample is then monitored. The vibrating bonds in the sample absorb the light frequencies corresponding to their own vibrational frequency.

It is by noting the frequencies (or range of frequencies) of the absorbed light that the bonds between particular atoms are identified. Not only are the elements within the sample identified but also the strength of the bonds give a clue to the number of bonds between the atoms. For example, a carbon atom can have 1 to 3 bonds with another carbon atom. The greater number of bonds lends to greater bond strength. The stronger bonds are shorter and vibrate at a higher vibrational frequency.

Changes to the molecular structure of the sample are reflected in changes to the bonds between the atoms. Such changes are expressed as increase or decrease in the amount of energy absorbed as well as shifts in absorption frequencies.

Not only are the elements, bond types and bond orientations identified using these techniques but also the polarisation of the molecules. This last factor has made vibrational spectroscopy useful in determining the level of molecular structuring within a sample.

A study by Pang and Deng (2008) gave dramatic examples of altered molecular structure in water as a result of exposure to magnetic fields. They argue that an externally applied magnetic field results in the changes of distribution and polarization of water molecules without changing the molecular constitutions. This work may provide useful insight into the study of magnetic fields and structured interfacial water.

Their study investigated the effects of magnetic fields on water structure using multiple vibrational spectroscopy techniques such as Raman and Infrared Spectroscopy and Ultraviolet Visual Spectroscopy (UV Vis). This latter technique was considered useful to this study as, according to Pang and Deng, increased polarisation in the atoms leads to increased transition dipole moments in the electrons. This in turn leads to increased radiation absorption. It is

claimed that magnetic fields enhance the clustering of water molecules whereby polarisation of atoms is also increased. This claim is supported by others (Chang and Weng 2006, Cai, Yang et al. 2009).

It is proposed here that if indeed magnetic fields alter hydrogen bond strength and molecular polarisation, then there should be a subsequent change in the ordered interface region. This altered molecular order should show as a change in UV light absorption.

A variation of Pang and Deng's experiment may include a hydrophilic membrane in dry, wet and wet-magnetised states. In this study, "wet" means immersed in water. It is hypothesised that a qualitative comparison of the absorption spectra of the wet and dry Nafion may give an indication of any structural difference in the water. This change may indicate interface water. Also, it is a simple matter to add magnetic fields to the experiment to observe any further alteration to the molecular structuring.

Materials and method

Samples were held in a standard quartz cuvette (10mm path length, quartz Q4, transmission > 80% @ 200 nm, Australian Scientific Pty. Ltd.) and ultraviolet absorption spectra measurements were obtained using a Cary 60 UV-Vis Spectrophotometer (Agilent Technologies, Australia). The frequency range was from 400 to 200 nm. The samples consisted of dry Nafion 117 film (8 mm x 30 mm x 0.2 mm strip; Fuel Cells Etc.; Texas, USA), pure water (with and without magnetic field) and Nafion in water (with and without magnetic field). The Nafion was soaked and rinsed for several weeks, and the water refreshed periodically, to deplete diffusible ions. This was to prevent the diffusion of ions creating an artefact in the experiment. The UV absorption spectra of each of the samples were recorded every five minutes over a period of up to thirty minutes. Magnets (2 x neodymium rods Ø12 x 20 mm, grade N42, Gauss = 6291, The Aussie Magnet Company Pty. Ltd.) were placed either side of the sample with N-S field configuration (see figure 3-36). The magnetic Gauss strength was measured at the magnet surface with a DC Gauss Meter (model GM-1-ST; Alpha Labs Ltd.; Salt Lake City; Utah, USA).

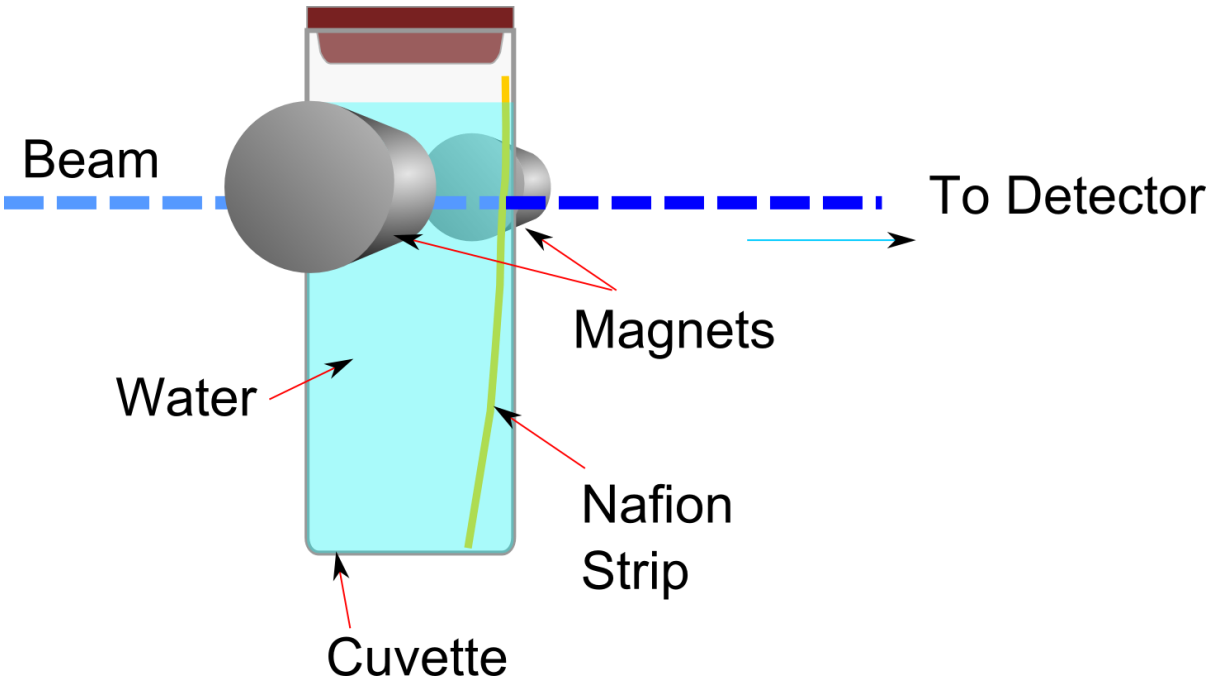

Figure 3-36 Cuvette sample and magnet setup for UV VIS experiment.

Results

Figure 3-37 shows the UV absorption spectra of non-magnetised water over the frequency range of 200 to 400 nm. Figures 3-38 and 3-39 show typical examples of the UV absorption spectra of water and Nafion immersed in water and exposed to magnetic fields over time. The time period between each plot in the magnetised experiments was five minutes. The magnetic affect was expected to increase with time as per previous research (Holysz, Szczes et al. 2007, Pang and Deng 2008, Cai, Yang et al. 2009, Szcześ, Chibowski et al. 2011).

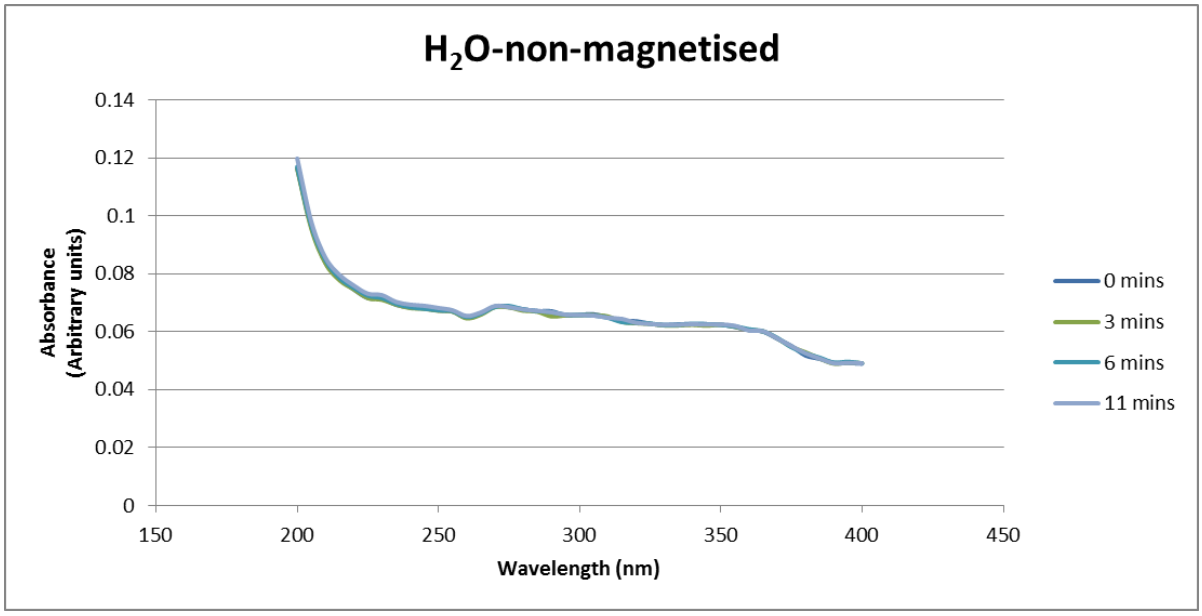

Figure 3-37 UV Absorption spectra of non-magnetised water over time.
Data collected at times indicated.

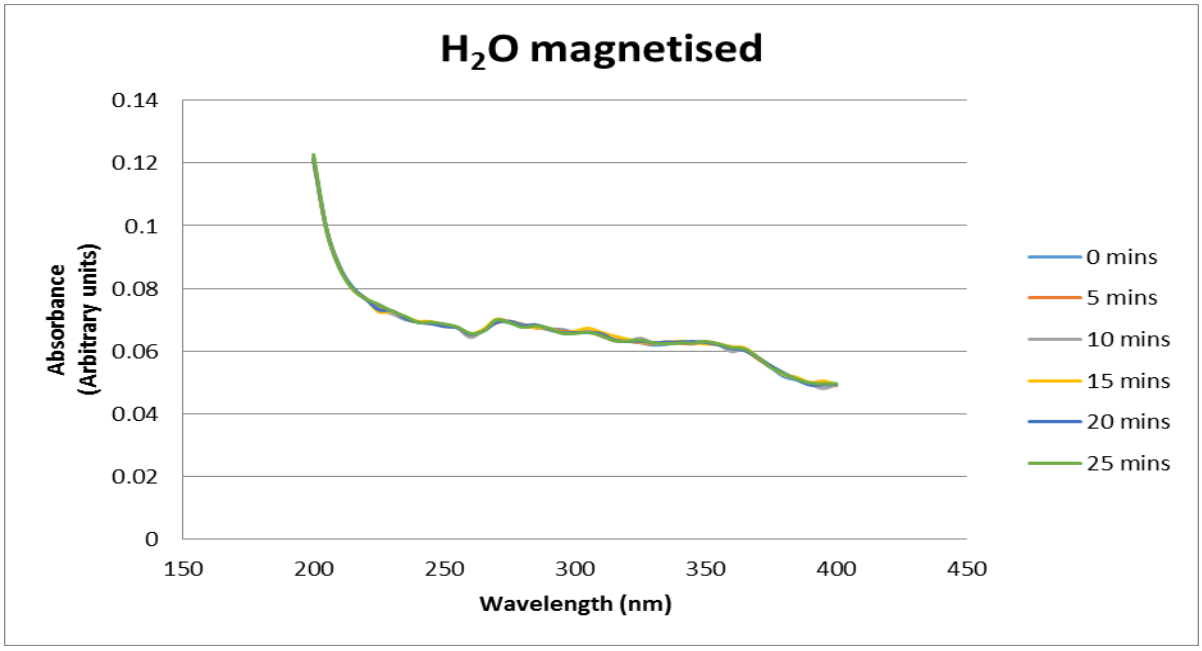

Figure 3-38. UV Absorption spectra of magnetised water over time.
Data collected every 5 minutes.

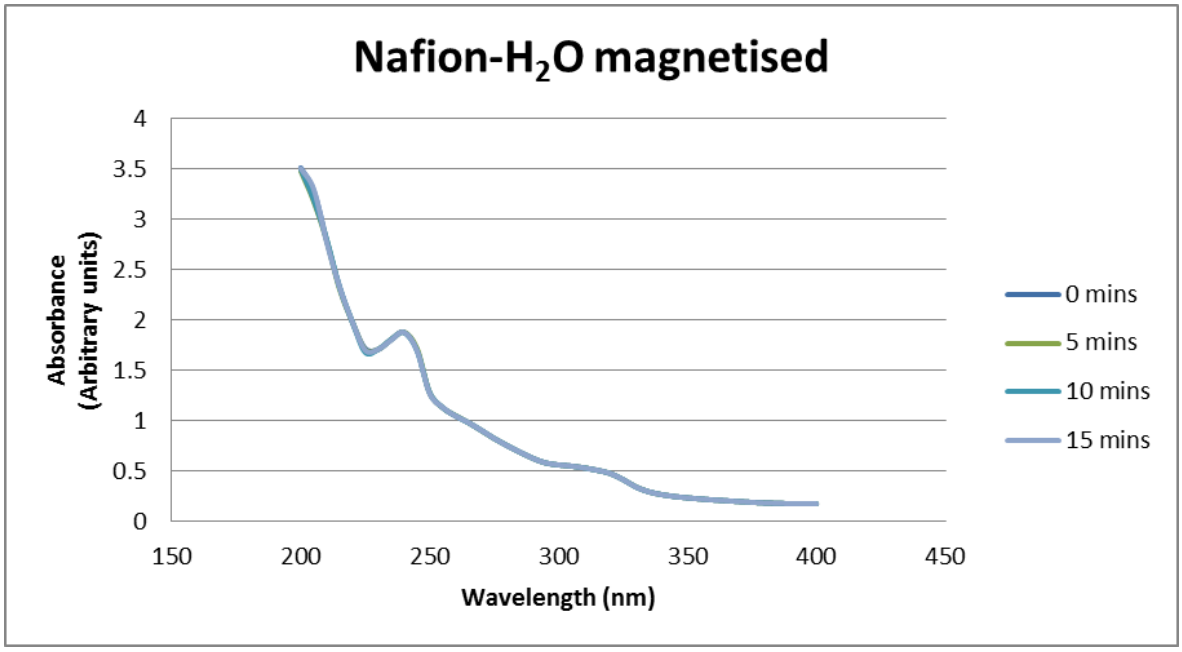

Figure 3-39. UV Absorption spectra of magnetised water and Nafion.
Data collected every 5 minutes.

These results are typical of three separate experiments of each type (H_2O and Nafion+H_2O). The arbitrary absorption units for H_2O range from 0.02 to 0.12 and for Nafion plus H_2O, from 0.04 to 3.5. This is as expected as Nafion has greater density and structure than water.

CHAPTER 4

Chapter 4 DISCUSSION/ANALYSIS

The molecular structure of water has been under investigation for almost a century. The evidence for the tendency towards structure in water has been attributed to the angularity of the hydrogen bonds (Frank and Wen 1957, Drost-Hansen 1969, Gragson and Richmond 1998, Chaplin 1999, Fenter and Sturchio 2004, Maccarini 2007). As hydrogen bonds are relatively weak they are short lived due to thermal perturbations (Chaplin 1999, Pal and Zewail 2004, Eftekhari-Bafrooei and Borguet 2010). There are some circumstances in which the hydrogen bonds persist longer giving rise to more observable structure. One such situation arises as water attaches to a hydrophilic surface (Fenter and Sturchio 2004, Zhang, Piatkowski et al. 2011). Evidence has also been presented that the molecular arrangement of the hydrophilic surface has a "templating" effect on the arrangement (structuring) of the attached water molecules (Fenter and Sturchio 2004, Verdaguer, Sacha et al. 2006, Maccarini 2007). The relatively locally constrained water molecules, coupled with highly directional hydrogen bonds may result in a more rigidly held and structured region of water due to localised protonation and deprotonation activity. Such activity would create a localised net electrical charge, with associated electric field, adding a polarising affect to several layers of water molecules. This argument has been used to support both theoretical and experimental evidence for long-range order at the water-hydrophilic surface interface (Shen and Ostroverkhov 2006, Catalano 2011) (Chaplin 2001, Eftekhari-Bafrooei and Borguet 2010). Other evidence suggests the interfacial water only extends to a few molecular layers as is consistent with the Double Layer theory (Fenter and Sturchio 2004).

A number of properties of this interface water have been identified including increased viscosity (Goertz, Houston et al. 2007) and density (Abraham 1978, Maccarini 2007) as well as thermal (Drost-Hansen 1969, Drost-Hansen 1973) and electrochemical differences (Choi, Park et al. 2002) compared to the bulk. Some have claimed that long-range order can be observed to as far as 300 μm using an optical microscope (Zheng and Pollack 2003, Zheng, Chin et al. 2006, Chai and Pollack 2010).

The hypothesis of experiment 1 is that, according to the above claims, EZ water should be detectable between the surfaces of hydrophilic material (in this case, Nafion), if the material surfaces are closer than 200 μm. Particularly as the EZ is reported to have greater density than bulk water and extend further than 100 μm (Chai, Zheng et al. 2008, Chai, Yoo et al. 2009). It was proposed that by combining two strips of Nafion the EZ between the strips would double,

thereby creating a large enough region to be seen at the resolution of the instrument (i.e. >200 μm).

Multiple images of each state of the experiment (e.g. empty cell, water-filled cell, cell with water and samples) were taken and "averaged" to create single images. These were then overlayed and "subtracted" to create an image showing only the differences between the states. If indeed the EZ water has greater density then this should have been evident in the final subtracted image.

No evidence of change in water density near the Nafion samples was detected. It is possible that a region of denser water did exist between the Nafion strips but was less than 50 μm, and therefore was undetectable by the instrument. Alternate possibilities are; 1/previous indications of increased density in the EZ are misinterpreted; 2/ the density difference between EZ water and bulk water was too subtle to be detected using this method; and 3/ the region known as EZ does not result from a change in the arrangement of water molecules. This last possibility is based on the idea that an ordered molecular arrangement would be structurally different to the relatively random bulk liquid. This would most likely be expressed as a difference in density (Totland, Lewis et al. 2013). For further investigation of the hypothesis of experiment 1 it is recommended that a higher resolution detection method be used.

Experiment 2 investigated the claims that observable physical phenomena (i.e. the exclusion of particulates from a hydrophilic surface – producing an EZ) can be attributed to the diffusion of ions from the material into the water. This is in opposition to the view that the EZ is caused by a structuring of water molecules adjacent to the material surface.

Of all the samples in this study only Nafion showed a change in pH, as is consistent with a diffusion of ions into the water. It is noted that the Nafion sample approached an equilibrium pH value between 3 and 4. This may indicate that the diffusible ions could be depleted from the Nafion material (Florea, Musa et al. 2014, Huszar, Martonfalvi et al. 2014).

Of the metals in this experiment, only zinc showed a notable indication of oxidation in the form of a whitish coating on the surface, typical of zinc oxide. Yet even so there was no notable net change in the pH of the surrounding water as a result of this chemical reaction. A similar experiment by Chai, Mahtani et al. (2012) noted an increase in pH of water adjacent to oxidising zinc foil using a universal pH indicator. It may be that the universal pH indicator contributed to the change in pH of the adjacent water by reacting with the metal.

The results from this experiment are consistent with the views of (Huszar, Martonfalvi et al. 2014). That is, Nafion does indeed diffuse ions (protons) into water and the resulting displacement of microspheres is misinterpreted as a difference in phase to that of the bulk. This was further supported by the serendipitous observation of the vertical shape of the EZ as seen in experiment 3 (see figure 3-24). As mentioned in the preliminary discussion, the shape of the EZ, when viewed at various depths, is consistent with the findings of Musa, Florea et al. (2013) that EZ's result from the flow of ions from the Nafion material into the water.

However, materials other than Nafion have been claimed to produce an EZ, in particular, zinc and aluminium (Chai, Mahtani et al. 2012). According to the study by Chai, Mahtani et al. pH changes were observed by a probe located 5 mm from the materials. It may well be that a region of differing pH remains localised to the materials in question and therefore not diffused into the bulk water. Such a situation would support the presence of a localised region adjacent to a material that maintains different properties to the bulk water. It may also be that the localised pH changes could be distributed throughout the bulk by time and agitation. However, as the present study was to examine the claims of Huszar, Martonfalvi et al. the location of the probe relative to the material was not taken into consideration, only the pH of the water in general.

For future study it is recommended two sets of samples be examined, one stirred and the other unstirred. The pH values of adjacent and bulk fluids should be measured and compared to determine if the changes in pH values are due to diffusion or localised phenomena.

Experiment 3 investigated the presence of birefringence at the material-water interface. As birefringence is normally associated with anisotropy in crystalline materials, its presence in water has been viewed as clear evidence of liquid-crystalline structuring of water molecules (Bunkin, Ignatiev et al. 2013, Pollack 2013, Bunkin, Gorelik et al. 2014). However, it is clear from the evidence presented that water was not a contributing factor in any observed birefringence. On the contrary, the light reflecting off the material surfaces seemed to be the main contributor. It also appears that in some cases microspheres reflect the birefringent light, thereby giving the appearance of a wide birefringent region extending from the material surface into the bulk water.

It is not clear how the relatively smooth surface of a blade-cut edge could create such distinct birefringence but surface shape and polarization by reflection may play a significant role (Filippov 2006, Shokr and Sinha 2015). This implies that the observance of birefringence in water adjacent to a Nafion surface does not necessarily indicate anisotropic properties in the water.

It may be that the observed light phenomenon is caused by reflective interference patterns similar to Newton's Rings. In this case it may be that light is reflected between the material surface and the glass microscope slide. As the light is reflected back and forth between the two surfaces it may interfere both constructively (creating bright lines) and destructively (creating darker lines). The resulting bright and dark lines are known as "interference fringes". It is important to point out that the light and dark fringes were observed in low light settings which may further support the notion of interference fringes as destructive interference (darker lines) which may be obscured by more intense light.

This study indicates that the previously observed birefringence at the hydrophilic surface-water interface do not necessarily indicate anisotropic properties in the water. Such phenomena could be ascribed to a number of causes other than a crystalline, ordered layer of water such as Newton's Rings-like phenomena and reflective birefringence. It is recommended that observation of birefringence in liquid adjacent to a surface be considered with these findings in mind.

Evidence of long-range order, as mentioned in this study, is seen to provide opportunities to not only observe the phenomena but also to determine whether they can be manipulated by external forces. In this study "manipulation" means to increase or decrease the extent of the observable phenomenon. This may also provide the opportunity to determine if the observable phenomenon can be contributed to factors other than long-range structure.

In searching for an appropriate external force for the manipulation of interfacial water it was determined that magnetic fields would be a promising candidate. This is because numerous studies have suggested that magnetic fields increase the hydrogen bond strength within water (Hosoda, Mori et al. 2004, Chang and Weng 2006, Ghauri and Ansari 2006, Cai, Yang et al. 2009, Szcześ, Chibowski et al. 2011). If such is the case then once the observable phenomena is confidently attributed to long-range order it would be a simple matter to apply a magnetic field and observe any changes. It is anticipated that with a change in hydrogen bond strength due to the magnetic field there would be an increase in the extent of the observable phenomena.

Experiment 4 sought to observe changes to the electrical properties of interfacial water known as double layer capacitance. However, the experiments showed no apparent difference between the magnetised and non-magnetised samples in the Bode plots over the period of testing. It may also be that the premise upon which this experiment is based is incorrect. That is, magnetic fields may not affect the size, and therefore electrical properties, of the structured interface layer. Although, multiple studies by others, using different techniques, indicate that there is

indeed an increase in interfacial structure, therefore such a dismissal of the magnetic effect may be unwarranted. It seems important to note that in studies where magnetic interfacial effects were reported the properties of the surfaces involved were crucial to the results. For example, the water-oxygen interface (Otsuka and Ozeki 2006, Ozeki and Otsuka 2006) and hydrophobic (weakly hydrogen bonded) surfaces (Ozeki, Wakai et al. 1991, Higashitani and Oshitani 1998). Therefore, it may be that the hydrophilic material used in this study does not provide a suitable interface to promote a magnetically enhanced structure.

It is recommended that future work on similar experiments may benefit from modifications of apparatus 2 to include a magnetic bridge. This would condense the magnetic field in proximity to the sample. Such modifications were not applied here due to time and funding limitations. Additionally, more powerful magnets (≥ 0.9 T) may yield different results as increased field strength may increase hydrogen bond strength (Ozeki, Wakai et al. 1991). This in turn may lead to increased ordering and an interface layer that extends further than that of lower strength magnets. However, this is not consistent with all the literature mentioned as some studies have achieved results with less powerful magnetic fields.

The results of experiment 5 showed no discernible difference to the UV absorption spectra over the period of magnetic exposure. This is demonstrated by there being no discernible difference between the magnetised and non-magnetised water experiments over the same frequency range. Also, the plot lines of each experiment overlap each other to the extent that they appear to be only one line, thereby indicating no change over the time of the experiments.

It appears that magnetic fields do not affect the UV absorption spectra of water. It may be that if structural changes do occur within waters molecular network it does present as a change in UV absorption spectra. It could also be that the changes to the sample were less than the limits of detection. Also, there may be a magnetic field strength threshold in that more powerful magnets (e.g. ≥ 0.5T) may be required to create a noticeable effect. The magnets used in this experiment were selected for size (to fit the UV-VIS sample environment) and strength similar to previous research (Toledo, Ramalho et al. 2008, Cai, Yang et al. 2009, Szcześ, Chibowski et al. 2011). To avoid possible damage by the larger magnets to the electronic workings of the UV visual spectrophotometer, a magnetic bridge may be employed. This will also ensure more direct Gauss lines and greater field concentration through the sample.

There is also the possibility that the research by So, Stahlberg et al. (2012), investigating the transition of ice to liquid water using UV-VIS, was based on a false premise that the interface water (referred to as EZ water) is liquid-crystalline in nature. In their work they noted that as

ice melts a transient 270 nm absorption phase occurs to which they attribute the presence of structure different to, and distinct from that of ice. To support this premise reference is made to the work of Gerald Pollack of Washington University and co-workers (Zheng, Chin et al. 2006). It is here that a 270 nm absorption peak is found in water in close proximity to a Nafion surface and attributed to a difference in molecular structure compared to that of the bulk. Consistent with similar experiments involving Nafion Pollack interprets the displacement of microspheres from hydrophilic surfaces as an indication of long-range structuring of water molecules. Other researchers, however, propose alternate interpretations such as the movement of the microspheres is the result of a diffusion of ions (protons) from the hydrophilic material (Nafion) (Schurr 2013, Florea, Musa et al. 2014, Huszar, Martonfalvi et al. 2014). This latter interpretation is supported by the findings of this study.

In the case of melting ice the contribution of protons from Nafion cannot be considered. However, as the 270 nm absorption peak was detected in the region of ion flow in the Zheng, Chin et al. study it may be that the same absorption peak found in melting ice can be attributed to a flow of water. Further study is required to support this hypothesis but it is suggested here that the attribution of the 270 nm absorption peak to alternately structured water lacks support.

Regarding previous studies on the effects of magnetic fields on the properties of water, the study by Pang and Deng (2008) used multiple techniques including IR and Ramen spectroscopy and UV Vis spectroscopy to show a clear distinction between magnetised and non-magnetised water.

However, their study has notable flaws. In their paper infrared absorption and Raman spectra data is presented with absorbance peaks reflecting the effect of magnetisation of water over time. It is noted that the non-magnetised water spectra (magnetic exposure time = 0) showed little resemblance to that of other researchers (Maréchal 1991, Max and Chapados 2002, Yan, Ou et al. 2014). This is demonstrated in figures 4-1 to 4-4.

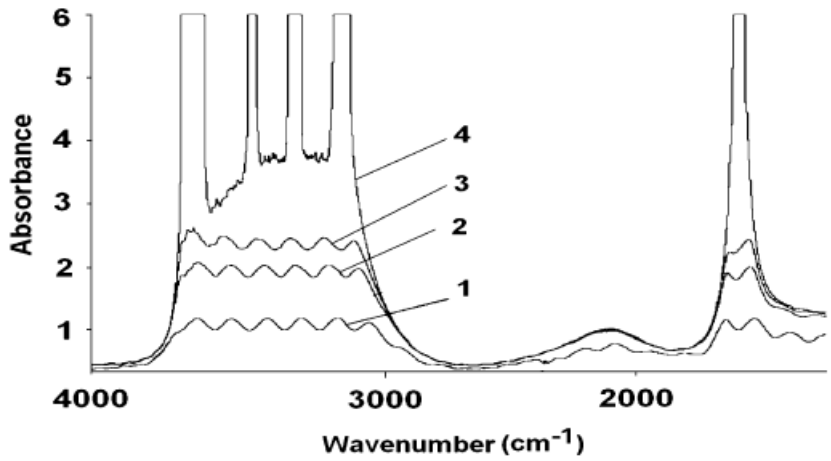

Figure 4-1. Infrared absorption spectra of water as reproduced from Pang and Deng (2008).
Curves numbered 1-4 indicate magnetisation times of 0, 10, 20 and 60 minutes respectively. Reprinted from Physica B: Condensed Matter 403(19–20): 3571-3577. Pang, X.-F. and B. Deng, "The changes of macroscopic features and microscopic structures of water under influence of magnetic field." Copyright 2008, with permission from Elsevier.

Figure 4-1 shows comparative IR absorbance spectra of water at different magnetic exposure times. Curves numbered 1 to 4 represent magnetic exposure time of 0, 10, 20 and 60 minutes respectively. For this argument attention is given to curve 1 (no magnetic exposure) and the peaks between wavenumbers 3000 cm-1 and 4000 cm-1. Here we can see a series of six peaks of similar value spanning wavenumbers from approximately 3100 cm-1 to 3650 cm-1. This is then compared with IR absorption spectra from Maréchal (1991) where a distinct broad peak is seen at around the 3400 cm-1 wavenumber without the additional peaks seen in the Pang and Deng paper (see figure 4-2).

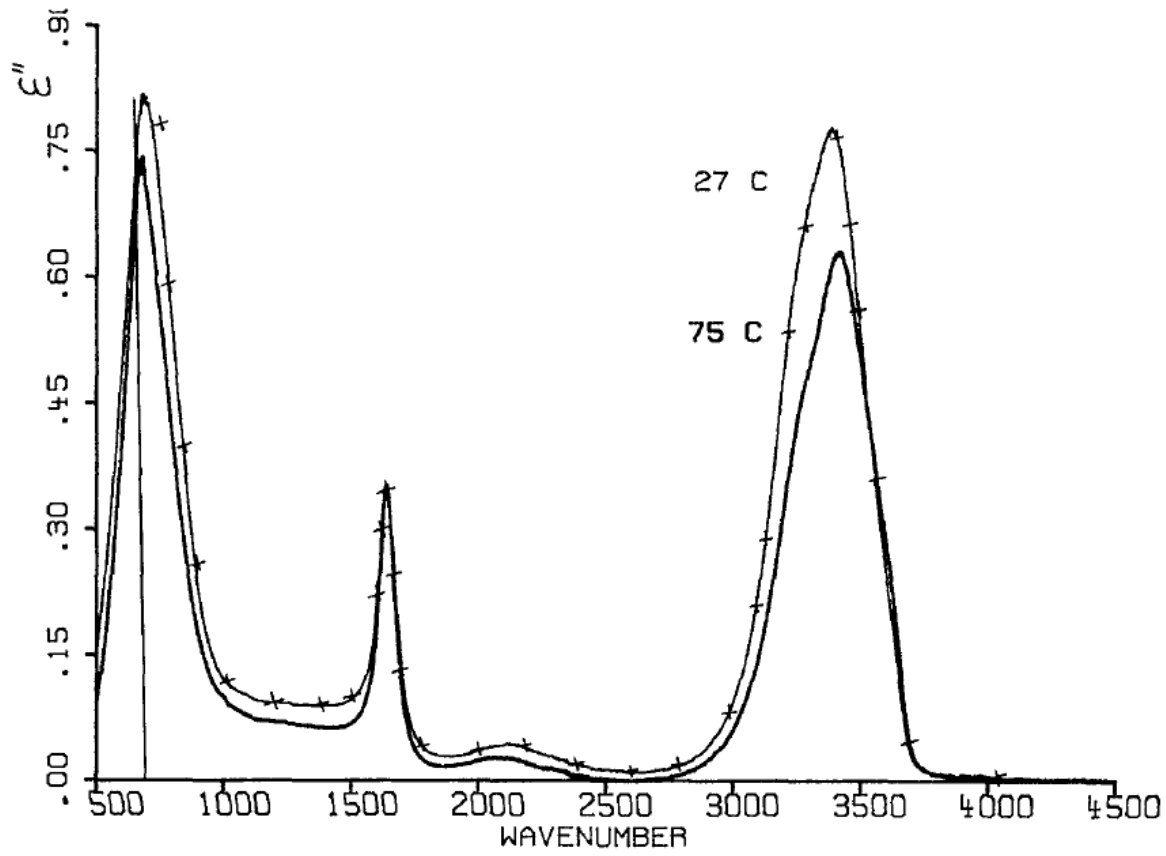

Figure 4-2. Infrared absorption spectra of water at 25° C and 75° C.
Reprinted from Maréchal (1991) with permission from AIP Publishing.

Similarly, figure 4-3 shows attenuated total reflection-IR spectra of H2O, HDO (mixture H2O + D2O) and D2O from Max and Chapados (2002) in which a distinct broad peak is also seen at around the 3400 cm-1 wavenumber.

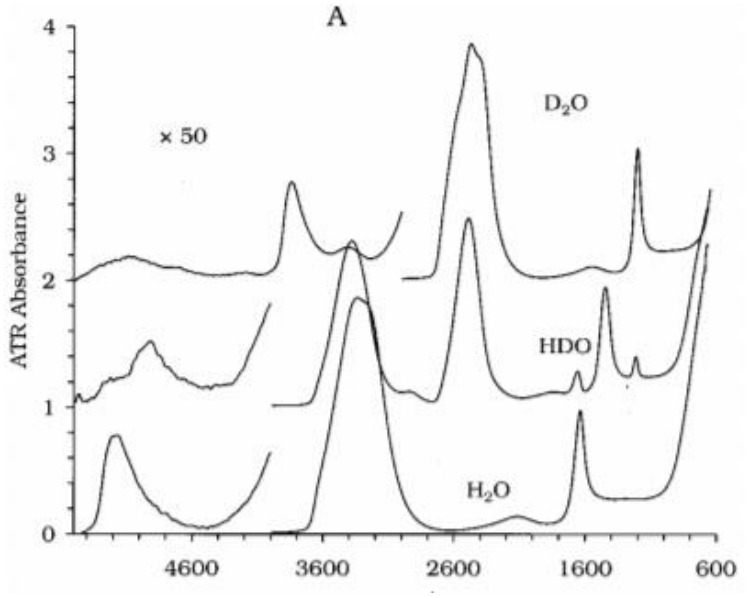

Figure 4-3. Attenuated total reflection-IR spectra of H_2O (bottom), HDO (mixture H_2O + D_2O) (middle) and D_2O.
Reprinted from Max and Chapados (2002) with the permission of AIP Publishing.

Again, Yan, Ou et al. (2014) show Raman spectra of a series of water samples at varying temperatures (figure 4-4) in which a distinct broad peak is seen at the 3400 cm-1 wavenumber without the additional peaks mentioned above.

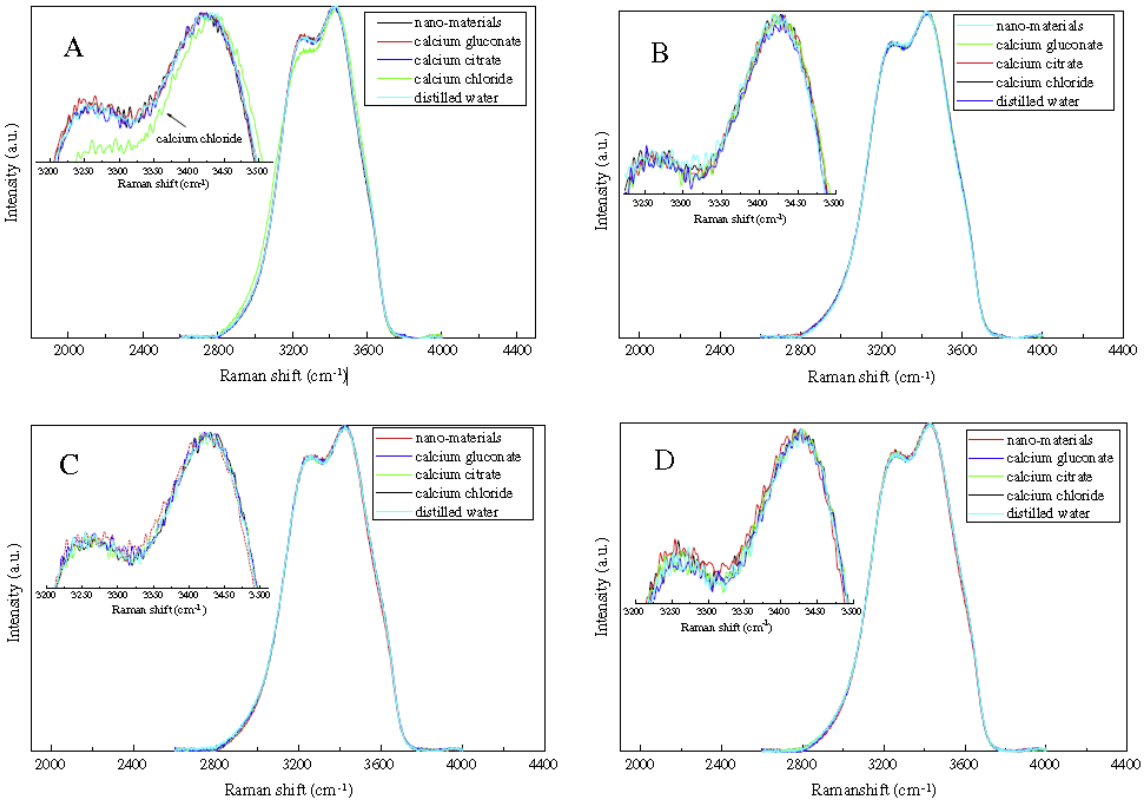

Figure 4-4. Raman spectra of different water samples normalized to the same peak height. Sample temperatures are (A) 30° C, (B) 45° C, (C) 65° C, and (D) 85° C. Reprinted from Journal of Molecular Structure, 1074: 310-314. Yan, Ou et al. (2014), "17O NMR and Raman spectra of water with different calcium salts." Copyright 2014 with permission from Elsevier.

This small sampling of available literature highlights the difference between the work of Pang and Deng (Pang and Deng 2008) and other researchers and calls into question the accuracy of their data concerning non-magnetised water.

Even more concerning is the comparison of Pang and Deng's results with that of Ozeki and Otsuka 2006) (2006) as shown in figure 4-5.

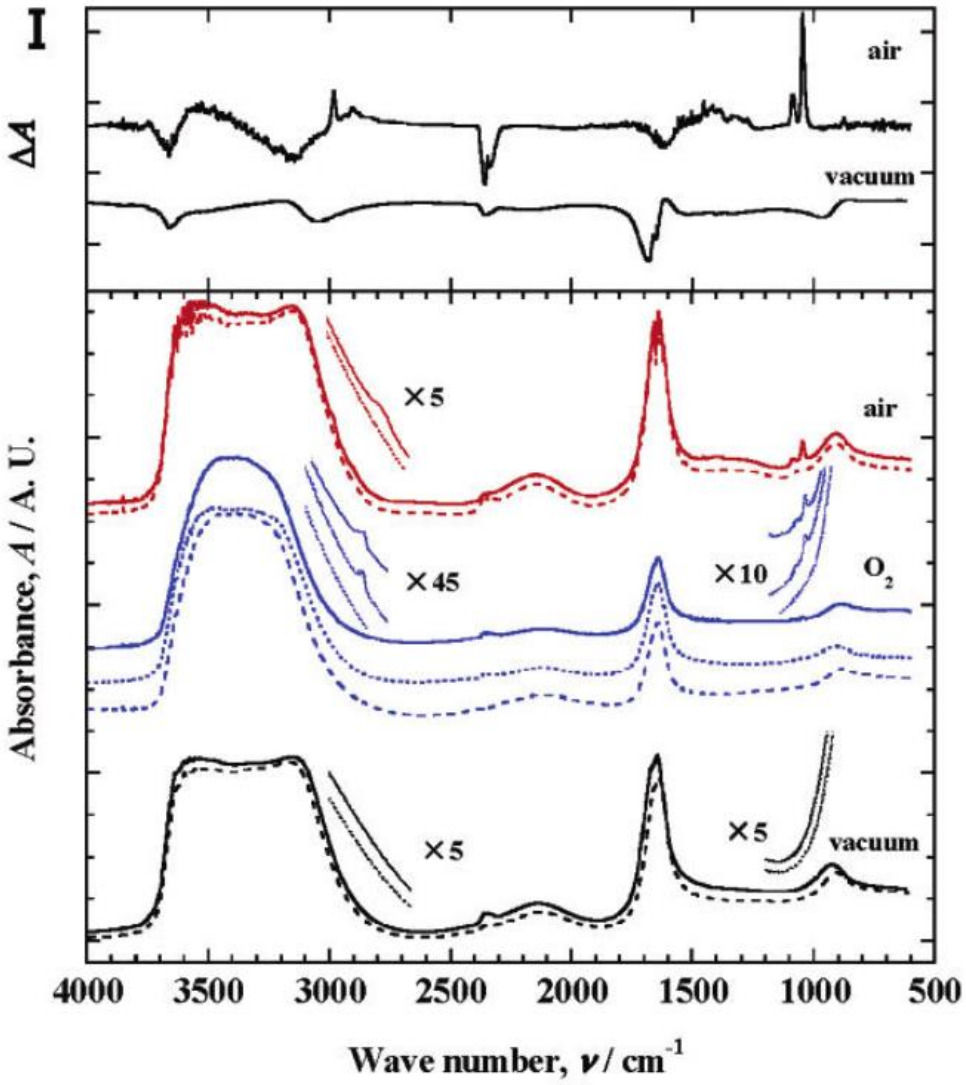

Figure 4-5. Magnetic treatment effects on IR spectra of water.
Upper section: Difference in IR absorption spectra between the magnetically treated and non-magnetically treated spectra (vacuum). Lower section: IR absorption spectra of vacuum-distilled water (bottom), distilled water exposed to oxygen (middle) of 98.2 Torr (broken and dotted) and 695 Torr (solid) and air of 1 atm (top) at 298 K. Solid and dotted lines, magnetic treatmen; broken line, non-magnetic treatment. Reprinted with permission from Ozeki and Otsuka (2006). Copyright 2006 American Chemical Society.

Here we see IR absorption spectra of water following 6T magnetic treatment. It is noted that even with magnetic treatment the data looks distinctly different to that of Pang and Deng.

The argument may then be presented that if the non-magnetised sample data is compromised then the magnetised data may be equally questionable as is evident in comparison with figure 4-5. With this in mind, and considering that their ultraviolet light absorption spectra data could not be replicated, it may be that this data is also flawed through experimental approach and analysis. That is, such a distinct change in the UV-VIS spectra from non-magnetised to

magnetised water is more consistent with a change in the chemical constituents of the sample rather than the polarisation of its molecules as claimed by Pang and Deng.

Also, such distinct changes to the molecular properties of water due to magnetic fields should be apparent in similar research regarding the magnetisation of water. However, as stated in chapter 2.5 the topic of magnetised water remains controversial due to the lack of reproducible results (Smothers 2001, Knez and Pohar 2005, Toledo, Ramalho et al. 2008).

During this study, some of the claims of long-range structure and magnetic effects on water have been subjected to testing in order to find a suitable path for more rigorous investigation. It was anticipated that evidence of molecular ordering, large enough to be detected with a microscope (i.e. the Exclusion Zone), would provide a convenient starting point. However, after some scrutiny, it appears that the proponents of this view (Pollack and co-workers) failed to adequately consider the chemical properties of their most prominent hydrophilic material, Nafion. That is, what is thought to be a region of molecular structuring is actually caused by diffusion of ions (protons) from the Nafion into the water. Indeed this interpretation is consistent with their own experiments showing differences in pH in water adjacent to Nafion (Klimov and Pollack 2007, Chai, Yoo et al. 2009, Das and Pollack 2013).

An interesting note about experiment 2 is that the increased acidity may be related to an accumulation of hydronium (H_3O+) ions. As these ions diffuse in water by proton transfer (structural diffusion) and not by hydrodynamics the question is where do these additional H3O+ ions come from? That is, protons are conducted through structured hydrogen networks (e.g. ice) rather than unstructured (liquid water). A review by Ball (Ball 2008) (and references therein) propose an extensive and complex cooperativity in the hydrogen bonded network takes place to facilitate proton migration. This encompasses both a reorganisation of the hydrogen bonded network and the creation of an intermediate Zundel cation: H_5O_2+. In this picture there are two classes of hydrogen bond that contribute to the process, those emanating from the protonated molecule stabilise the local hydrogen bond network and those pointing towards it destabilise. Thus the proton transfer is facilitated by destabilising hydrogen bonds in front of the protonated molecule causing them to part, and stabilising (closing) the bonds behind it. The Zundel cation may then diffuse to the hydronium ion further from the Nafion surface.

Thus with the transfer of protons from Nafion into the water it is likely that a region of small, localised structures would be created, however, these structures would be transient in nature and very short-lived. This is of particular interest as the transiently structured water adjacent to

a Nafion surface (proton donor) may be responsible for the 270 nm absorption peak found by Zheng, Chin et al. in their UV-VIS study (as mentioned above). In which case, any indication of structure may be the result of proton transfer rather than the hydrophilic surface itself. Further experimentation is required to confirm this theory.

Electrical Impedance Spectroscopy (EIS) held promise for investigating the size of an interfacial layer due to the difference in impedance at different frequencies. The results obtained had some inconsistencies due to experimental difficulties such as an inability to achieve a steady state. This may be due to the ease in which water absorbs atmospheric gases causing a drift in impedance values over time. Additionally, changes to the electrochemical properties of water due to magnetic fields could not be detected with the experimental setup used.

CHAPTER 5

CHAPTER 5 CONCLUSION

5.1 THE STUDY'S FINDINGS

Tetrahedrally coordinated structure in water molecules has been identified as far as 262 nm from a silicon surface using Infrared internal reflective spectroscopy (Yalamanchili, Atia et al. 1996). Nuclear magnetic resonance studies suggest surface induced water structure can extend to micrometres (Totland, Lewis et al. 2013). However, upon investigating some of the claims of molecular structure in water extending beyond these distances it appears the evidence presented may require alternate interpretations. Visual indication of liquid-crystallinity (birefringence) in interfacial water may result from reflection off adjacent surfaces and therefore do not support the claims of long-range order. Chemical diffusion of materials into the water and the dynamic nature of water itself appear to not have been adequately considered.

Magnetic fields of the strength used in this study did not produce any detectable effect on the size of any ordered layer in these experiments. Also, some of the evidence for change in molecular structure due to magnetic fields appears to be highly questionable.

From this study it appears that evidence of long-range order in interfacial water to distances beyond the few microns mentioned earlier can be dismissed.

As the magnetic field strengths used in this study did not produce any detectable effect on water structure, it may be that more powerful magnets may be required (e.g. >0.5 T). This may suggest a threshold factor that may be explored in future work.

5.2 SIGNIFICANCE OF THIS RESEARCH

Interfacial water has been under investigation for almost a century and much progress has been made. However, there still remains much uncertainty about the properties, structure and causes of interfacial water. As the physicochemical properties of interfacial water are significant to many areas of science, including biology, the studies in this field need to be accurate to ensure a useful outcome. The significance of this study is that it helps determine the limits of the magnitude of interfacial water and highlight shortcomings in current evidence that go beyond these limits. This research also clears the path of the disruptive influence of misinterpreted data. This particularly applies to the interpretation of EZ water as long-range molecular structuring.

From what can be determined this is the first body of research that seeks to influence interfacial water using an external field (i.e. magnetic field). This innovative approach may provoke new ideas in this field. Should other means of manipulation prove more successful they may be useful in a biological context, particularly in the treatment of cancer by manipulating intracellular water.

LIMITATIONS

Preliminary experiments with magnetic fields may have been limited by the strength of the available magnets. With the addition of more time and resources, stronger magnetic fields could be applied.

Progress in this field has been hampered by a lack of robust detection techniques. Continued development of novel and sensitive detection methods is required to address whether interfacial water exists and can be modulated.

FUTURE WORK

As previously mentioned, stronger magnetic fields may prove more effective in this research. If such is the case then this may indicate an effective field strength threshold. Such a finding could be of great importance in understanding the interface water phenomenon.

BIBLIOGRAPHY

Abraham, F. F. (1978). "The interfacial density profile of a Lennard-Jones fluid in contact with a (100) Lennard-Jones wall and its relationship to idealized fluid/wall systems: A Monte Carlo simulation." J. Chem. Phys. **68**(8): 3713-3716.

Abramczyk, H., B. Brozek-Pluska, M. Krzesniak, M. Kopec and A. Morawiec-Sztandera (2014). "The cellular environment of cancerous human tissue. Interfacial and dangling water as a "hydration fingerprint"." Spectrochim. Acta. A. **129**: 609-623.

Allan, B. D. and R. L. Norman (1973). "The characterization of Liquids in contact with high surface area materials." Ann. N. Y. Acad. Sci. **204**(1): 150-168.

Ambashta, R. D. and M. Sillanpää (2010). "Water purification using magnetic assistance: A review." J. Hazard. Mater. **180**(1–3): 38-49.

Baker, J. S. and S. J. Judd (1996). "Magnetic amelioration of scale formation." Water Res. **30**(2): 247-260.

Bakker, H. J. and H. K. Nienhuys (2002). "Delocalization of protons in liquid water. (Reports)." Science **297**: 587+.

Ball, P. (2008). "Water as an active constituent in cell biology." Chem. Rev. **108**(1): 74-108.

Ball, P. (2008 a). "Water as a biomolecule." Chemphyschem **9**(18): 2677-2685.

Barrett, R. A. and S. A. Parsons (1998). "The influence of magnetic fields on calcium carbonate precipitation." Water Res. **32**(3): 609-612.

Bartha, F., O. Kapuy, C. Kozmutza and C. Van Alsenoy (2003). "Analysis of weakly bound structures: hydrogen bond and the electron density in a water dimer." J. Mol. Struct. **666**: 117-122.

Benson, S. W. and E. D. Siebert (1992). "A Simple Two-Structure Model for Liquid Water." J. Am. Chem. Soc. **114**(11): 4269-4276.

Besseling, N. A. M. (1997). "Theory of hydration forces between surfaces." Langmuir **13**(7): 2113-2122.

Biologic. (2015). Retrieved August 6th, 2018, from http://www.bio-logic.net/wp-content/uploads/2015-bio-logic-vsp300.pdf.

Biryukov, A. S., V. F. Gavrikov, L. O. Nikiforova and V. A. Shcheglov (2005). "New physical methods of disinfection of water." J. Russ. Laser Res. **26**(1): 13-25.

Bunkin, N. F., V. S. Gorelik, V. A. Kozlov, A. V. Shkirin and N. V. Suyazov (2014). "Colloidal crystal formation at the "Nafion-water" interface." J. Phys. Chem. B **118**(12): 3372.

Bunkin, N. F., P. S. Ignatiev, V. A. Kozlov, A. V. Shkirin, S. D. Zakharov and A. A. Zinchenko (2013). "Study of the Phase States of Water Close to Nafion Interface." Water-Sui. **4**: 129-154.

Cai, R., H. Yang, J. He and W. Zhu (2009). "The effects of magnetic fields on water molecular hydrogen bonds." J. Mol. Struct. **938**(1–3): 15-19.

Catalano, J. G. (2011). "Weak interfacial water ordering on isostructural hematite and corundum (0 0 1) surfaces." Geochim. Cosmochim. Ac. **75**(8): 2062-2071.

Chai, B.-H., J.-M. Zheng, Q. Zhao and G. H. Pollack (2008). "Spectroscopic Studies of Solutes in Aqueous Solution." J. Phys. Chem. A. **112**(11): 2242-2247.

Chai, B., A. G. Mahtani and G. H. Pollack (2012). "Unexpected Presence of Solute-Free Zones at Metal-Water Interfaces." Contemp. Mater. **3**(1): 1-12.

Chai, B. and G. H. Pollack (2010). "Solute-free interfacial zones in polar liquids." J. Phys. Chem. B **114**(16): 5371-5375.

Chai, B., H. Yoo and G. H. Pollack (2009). "Effect of radiant energy on near-surface water." J. Phys. Chem. B **113**(42): 13953-13958.

Chang, K.-T. and C.-I. Weng (2006). "The effect of an external magnetic field on the structure of liquid water using molecular dynamics simulation." J. Appl. Phys. **104**(4): 043917-043917-043916.

Chaplin, M. (2006). "Do we underestimate the importance of water in cell biology?" Nat. Rev. Mol. Cell Biol. **7**(11): 861-866.

Chaplin, M. (2017 a). "Water Structure and Science: Hexagonal Ice (ice Ih)." Retrieved 16 September, 2017, from http://www1.lsbu.ac.uk/water/hexagonal_ice.html.

Chaplin, M. F. (1999). "A proposal for the structuring of water." Biophy. Chem. **83**(3): 211-221.

Chaplin, M. F. (2001). "Water: its importance to life." Biochem. Mol. Biol. Educ. **29**(2): 54-59.

Chaplin, M. F. (2017 b). "Water Structure and Science: Water Molecule and Structure." Retrieved 3 September 2017, from http://www1.lsbu.ac.uk/water/water_molecule.html#lp.

Chaplin, M. F. (2017 c). "Hexagonal Ice (ice Ih)." Retrieved 27 November 2017, from http://www1.lsbu.ac.uk/water/hexagonal_ice.html.

Chaplin, M. F. (2017 d). "Water Phase Diagram." Retrieved 18 November, 2015, from http://www1.lsbu.ac.uk/water/water_phase_diagram.html#all.

Chaplin, M. F. (2018). "Hydrogen bonding and information transfer (2)." Retrieved July 18, 2018, from http://www1.lsbu.ac.uk/water/hydrogen_bonding.html.

Chibowski, E. and A. Szcześ (2018). "Magnetic water treatment–A review of the latest approaches." Chemosphere **203**: 54-67.

Choi, J.-H., J.-S. Park and S.-H. Moon (2002). "Direct Measurement of Concentration Distribution within the Boundary Layer of an Ion-Exchange Membrane." J. Colloid. Interf. Sci. **251**(2): 311-317.

Clark, G. N., C. D. Cappa, J. D. Smith, R. J. Saykally and T. Head-Gordon (2010). "The structure of ambient water." Molecular Physics **108**(11): 1415-1433.

Coey, J. M. D. and S. Cass (2000). "Magnetic water treatment." J. Magn. Magn. Mater. **209**(1): 71-74.

Coster, H., T. Chilcott and A. Coster (1996). "Impedance spectroscopy of interfaces, membranes and ultrastructures." Bioelectroch. Bioener. **40**(2): 79-98.

Damadian, R. (1971). "Tumor Detection by Nuclear Magnetic Resonance." Science **171**(3976): 1151-1153.

Damadian, R., K. Zaner, D. Hor and T. DiMaio (1974). "Human tumors detected by nuclear magnetic resonance." Proc. Natl. Acad. Sci. U. S. A. **71**(4): 1471-1473.

Das, R. and G. H. Pollack (2013). "Charge-based forces at the Nafion-water interface." Langmuir **29**(8): 2651-2658.

Dickey, A. N. and M. J. Stevens (2012). "Site-dipole field and vortices in confined water." Phys. Rev. E. **86**(5): 051601.

Drost-Hansen, W. (1969). "Structure of water near solid interfaces." Ind. Eng. Chem. **61**(11): 10-10.

Drost-Hansen, W. (1973). "Phase transitions in biological systems: Manifestations of cooperative processes in vicinal water." Ann. N. Y. Acad. Sci. **204**(1): 100-112.

Ebbinghaus, S., S. J. Kim, M. Heyden, X. Yu, U. Heugen, M. Gruebele, D. M. Leitner and M. Havenith (2007). "An extended dynamical hydration shell around proteins." P. Natl. Acad. Sci. USA **104**(52): 20749-20752.

Eftekhari-Bafrooei, A. and E. Borguet (2010). "Effect of hydrogen-bond strength on the vibrational relaxation of interfacial water." J. Am. Chem. Soc. **132**(11): 3756.

Eisenberg, D. S. and W. Kauzmann (2005). The structure and properties of water. Oxford, Oxford University Press.

Emilio Del, G., T. Alberto, V. Giuseppe and V. Vladimir (2013). "Coherent structures in liquid water close to hydrophilic surfaces." J. Phys. Conf. Ser. **442**(1): 012028.

Etzler, F. M. and D. M. Fagundus (1987). "The extent of vicinal water: Implications from the density of water in silica pores." J. Colloid Interf. Sci. **115**(2): 513-519.

Fenter, P. and N. C. Sturchio (2004). "Mineral–water interfacial structures revealed by synchrotron X-ray scattering." Prog. Surf. Sci. **77**(5): 171-258.

Filippov, V. V. (2006). "Double reflection and birefringence of a wave incident on the crystal boundary under the conditions of internal conical refraction." Crystallogr. Rep. **51**(4): 636-639.

Florea, D. D., S. S. Musa, J. J. Huyghe and H. M. H. Wyss (2014). "Long-range repulsion of colloids driven by ion-exchange and diffusiophoresis." P. Natl. Acad. Sci. USA **111**(18): 6554-6559.

Frank, H. S. and W.-Y. Wen (1957). "Ion-solvent interaction. Structural aspects of ion-solvent interaction in aqueous solutions: a suggested picture of water structure." Discuss. Faraday Soc. **24**(0): 133-140.

Frauenfelder, H., G. Chen, J. Berendzen, P. W. Fenimore, H. Jansson, xe, B. H. McMahon, I. R. Stroe, J. Swenson and R. D. Young (2009). "A Unified Model of Protein Dynamics." P. Natl. Acad. Sci. USA **106**(13): 5129-5134.

Fröhlich, H. (1975). "The extraordinary dielectric properties of biological materials and the action of enzymes." P. Natl. Acad. Sci. USA **72**(11): 4211-4215.

Gehr, R., Z. A. Zhai, J. A. Finch and S. R. Rao (1995). "Reduction of soluble mineral concentrations in CaSO 4 saturated water using a magnetic field." Water Res. **29**(3): 933-940.

Geiger, A., F. Sciortino and H. E. Stanley (1991). "Effect of defects on molecular mobility in liquid water." Nature **354**(6350): 218-221.

Ghauri, S. A. and M. S. Ansari (2006). "Increase of water viscosity under the influence of magnetic field." J. Appl. Phys. **104**(6): 066101-066101-066102.

Goertz, M. P., J. E. Houston and X. Y. Zhu (2007). "Hydrophilicity and the viscosity of interfacial water." Langmuir **23**(10): 5491-5497.

Gragson, D. E. and G. L. Richmond (1998). "Investigations of the Structure and Hydrogen Bonding of Water Molecules at Liquid Surfaces by Vibrational Sum Frequency Spectroscopy." J. Phys. Chem. B **102**(20): 3847-3861.

Gun'ko, V. M., V. V. Turov, V. M. Bogatyrev, V. I. Zarko, R. Leboda, E. V. Goncharuk, A. A. Novza, A. V. Turov and A. A. Chuiko (2005). "Unusual properties of water at hydrophilic/hydrophobic interfaces." Adv. Colloid Interfac. **118**(1–3): 125-172.

Hakala, M., K. Nygård, S. Manninen, S. Huotari, T. Buslaps, A. Nilsson, L. G. M. Pettersson and K. Hämäläinen (2006). "Correlation of hydrogen bond lengths and angles in liquid water based on Compton scattering." J. Chem. Phys. **125**(8): 084504.

Hardy, W. B. (1912). "The Tension of Composite Fluid Surfaces and the Mechanical Stability of Films of Fluid." P. R. Soc. Lond. A-Conta. **86**(591): 610-635.

Head-Gordon, T. and G. Hura (2002). "Water structure from scattering experiments and simulation." Chem. Rev. **102**(8): 2651-2670.

Henao, A., S. Busch, E. Guardia, J. L. Tamarit and L. C. Pardo (2016). "The structure of liquid water beyond the first hydration shell." Phys. Chem. Chem. Phys. **18**(28): 19420-19425.

Henniker, J. C. (1949). "The depth of the surface zone of a liquid." Rev. Mod. Phys. **21**(2): 322-341.

Higashitani, K., A. Kage, S. Katamura, K. Imai and S. Hatade (1993). "Effects of a Magnetic Field on the Formation of CaCO3 Particles." J. Colloid. Interf. Sci. **156**(1): 90-95.

Higashitani, K. and J. Oshitani (1998). "Magnetic Effects on Thickness of Adsorbed Layer in Aqueous Solutions Evaluated Directly by Atomic Force Microscope." J. Colloid Interf. Sci. **204**(2): 363-368.

Higo, J., M. Sasai, H. Shirai, H. Nakamura and T. Kugimiya (2001). "Large Vortex-like Structure of Dipole Field in Computer Models of Liquid Water and Dipole-Bridge between Biomolecules." P. Natl. Acad. Sci. USA **98**(11): 5961-5964.

Hodgson, A. and S. Haq (2009). "Water adsorption and the wetting of metal surfaces." Surf. Sci. Rep. **64**(9): 381-451.

Holysz, L., A. Szczes and E. Chibowski (2007). "Effects of a static magnetic field on water and electrolyte solutions." J. Colloid. Interf. Sci. **316**(2): 996-1002.

Hosoda, H., H. Mori, N. Sogoshi, A. Nagasawa and S. Nakabayashi (2004). "Refractive indices of water and aqueous electrolyte solutions under high magnetic fields." J. Phys. Chem. A **108**(9): 1461-1464.

Huszar, I. N., Z. Martonfalvi, A. J. Laki, K. Ivan and M. Kellermayer (2014). "Exclusion-Zone Dynamics Explored with Microfluidics and Optical Tweezers." Entropy **16**(8): 4322-4337.

Inaba, H., T. Saitou, K.-i. Tozaki and H. Hayashi (2004). "Effect of the magnetic field on the melting transition of H2O and D2O measured by a high resolution and supersensitive differential scanning calorimeter." J. Appl. Phys. **96**(11): 6127-6132.

Israelachvili, J. and R. Pashley (1982). "The hydrophobic interaction is long range, decaying exponentially with distance." Nature **300**(5890): 341.

Israelachvili, J. N. and G. E. Adams (1978). "Measurement of forces between two mica surfaces in aqueous electrolyte solutions in the range 0–100 nm." J. Chem. Soc. Farad. T. 1 **74**: 975-1001.

Jasnin, M., M. Moulin, M. Haertlein, G. Zaccai and M. Tehei (2008). "Down to atomic-scale intracellular water dynamics." Embo. J. **9**(6): 543-547.

Jena, K. C. and D. K. Hore (2010). "Water structure at solid surfaces and its implications for biomolecule adsorption." Phys. Chem. Chem. Phys. **12**(43): 14383-11444.

Ji-Xin, C., P. Sophie, A. W. David and X. S. Xie (2003). "Ordering of water molecules between phospholipid bilayers visualized by coherent anti-Stokes Raman scattering microscopy." P. Natl. Acad. Sci. USA **100**(17): 9826.

Kim, B. I., R. D. Boehm and J. R. Bonander (2013). "Direct observation of self-assembled chain-like water structures in a nanoscopic water meniscus." J. Chem. Phys. **139**(5).

Klimov, A. and G. H. Pollack (2007). "Visualization of charge-carrier propagation in water." Langmuir **23**(23): 11890-11895.

Knez, S. and C. Pohar (2005). "The magnetic field influence on the polymorph composition of CaCO3 precipitated from carbonized aqueous solutions." J. Colloid. Interf. Sci. **281**(2): 377-388.

Korson, L., W. Drost-Hansen and F. J. Millero (1969). "Viscosity of water at various temperatures." J. Phys. Chem. **73**(1): 34-39.

Le Bihan, D. and H. Fukuyama (2016). Water: The Forgotten Biological Molecule. Great Britian, Pan Stanford.

Lee, S. H., S. I. Jeon, Y. S. Kim and S. K. Lee (2013). "Changes in the electrical conductivity, infrared absorption, and surface tension of partially-degassed and magnetically-treated water." J. Mol. Liq. **187**: 230-237.

Li, T.-D., J. Gao, R. Szoszkiewicz, U. Landman and E. Riedo (2007). "Structured and viscous water in subnanometer gaps." Phys. Rev. B **75**(11): 115415.

Ling, G. N. (1964). "The Association-Induction Hypothesis." Tex. Rep. Biol. Med. **22**: 244-265.

Ling, G. N. (1965). "The physical state of water in living cell and model systems." Ann N Y Acad Sci **125**(2): 401-417.

Ling, G. N. (2003). "A new theoretical foundation for the polarized-oriented multilayer theory of cell water and for inanimate systems demonstrating long-range dynamic structuring of water molecules." Physiol. Chem. Phys. & Med. NMR **35**: 91-130.

Ling, G. N., C. Miller and M. M. Ochsenfeld (1973). "The physical state of solutes and water in living cells according to the association-induction hypothesis." Ann. N. Y. Acad. Sci. **204**(1): 6-47.

Lum, K. (1998). Hydrophobicity at small and large length scales. D. Chandler, ProQuest Dissertations Publishing.

Lyapin, A. G., O. V. Stal'gorova, E. L. Gromnitskaya and V. V. Brazhkin (2002). "Crossover between the thermodynamic and nonequilibrium scenarios of structural transformations of H2O Ih ice during compression." J. Exp. Theor. Phys+ **94**(2): 283-292.

Maccarini, M. (2007). "Water at solid surfaces: A review of selected theoretical aspects and experiments on the subject." Biointerphases **2**(3): MR1-MR15.

Madsen, H. E. L. (1995). "Influence of magnetic field on the precipitation of some inorganic salts." J. Cryst. Growth **152**(1): 94-100.

Mahmoud, B., M. Yosra and A. Nadia (2016). "Effects of magnetic treatment on scaling power of hard waters." Sep. Purif. Technol. **171**: 88-92.

Major, R. C., J. E. Houston, M. J. McGrath, J. I. Siepmann and X. Y. Zhu (2006). "Viscous water meniscus under nanoconfinement." Phys. Rev. Lett. **96**(17): 177803.

Maréchal, Y. (1991). "Infrared spectra of water. I. Effect of temperature and of H/D isotopic dilution." J. Chem. Phys. **95**(8): 5565-5573.

Max, J.-J. and C. Chapados (2002). "Isotope effects in liquid water by infrared spectroscopy." J. Chem. Phys. **116**(11): 4626-4642.

McIntyre, G. I. (2006). "Cell hydration as the primary factor in carcinogenesis: A unifying concept." Med. Hypotheses **66**(3): 518-526.

Milischuk, A. A. and B. M. Ladanyi (2011). "Structure and dynamics of water confined in silica nanopores." J. Chem. Phys. **135**(17): 174709.

Mills, M., B. G. Orr, M. M. Banaszak Holl and I. Andricioaei (2013). "Attractive hydration forces in DNA-dendrimer interactions on the nanometer scale." J. Phys. Chem. B **117**(4): 973-981.

Musa, S., D. Florea, S. V. Loon, H. Wyss and J. M. Huyghe (2013). Interfacial Water: Unexplained Phenomena. Poromechanics**:** 2086-2092.

Nakagawa, J., N. Hirota, K. Kitazawa and M. Shoda (1999). "Magnetic field enhancement of water vaporization." J. Appl. Phys. **86**(5): 2923-2925.

Newton, R. H., J. P. Haffegee and M. W. Ho (1995). "Polarized light microscopy of weakly birefringent biological specimens." J. Microsc. - Oxford **180**(2): 127-130.

Nilsson, A. and L. G. M. Pettersson (2015). "The structural origin of anomalous properties of liquid water." Nat. Commun. **6**: 8998.

Novoa, J. J., F. Mota, C. Perez del Valle and M. Planas (1997). "Structure of the First Solvation Shell of the Hydroxide Anion. A Model Study Using OH-(H2O)n (n = 4, 5, 6, 7, 11, 17) Clusters." J. Phys. Chem. A **101**(42): 7842-7853.

Oehr, K. and P. LeMay (2014). "The Case for Tetrahedral Oxy-subhydride (TOSH) Structures in the Exclusion Zones of Anchored Polar Solvents Including Water." Entropy **16**(11): 5712.

Otsuka, I. and S. Ozeki (2006). "Does magnetic treatment of water change its properties?" J. Phys. Chem. B **110**(4): 1509.

Ozeki, S. and I. Otsuka (2006). "Transient oxygen clathrate-like hydrate and water networks induced by magnetic fields." J. Phys. Chem. B **110**(41): 20067.

Ozeki, S., C. Wakai and S. Ono (1991). "Is a magnetic effect on water adsorption possible?" J. Phys. Chem. **95**(26): 10557-10559.

Pal, S. K. and A. H. Zewail (2004). "Dynamics of water in biological recognition." Chem. Rev. **104**(4): 2099-2124.

Pang, X.-F. and B. Deng (2008). "The changes of macroscopic features and microscopic structures of water under influence of magnetic field." Physica. B **403**(19–20): 3571-3577.

Pang, X. and B. Deng (2008). "Investigation of changes in properties of water under the action of a magnetic field." Sci. China Ser. G-Phys. Mech. Astron. **51**(11): 1621-1632.

Pang, X. F. (2006). "The conductivity properties of protons in ice and mechanism of magnetization of liquid water." Eur. Phys. J. B **49**(1): 5-23.

Park, J.-S., J.-H. Choi, J.-J. Woo and S.-H. Moon (2006). "An electrical impedance spectroscopic (EIS) study on transport characteristics of ion-exchange membrane systems." J. Colloid. Interf. Sci. **300**(2): 655-662.

Peschel, G., P. Belouschek, M. M. Müller, M. R. Müller and R. König (1982). "The interaction of solid surfaces in aqueous systems." Colloid Polym. Sci. **260**(4): 444-451.

Peter, R. C. G., R. Pethig and A. Szent-Gyorgyi (1981). "Water Structure-Dependent Charge Transport in Proteins." P. Natl. Acad. Sci. USA **78**(1): 261-265.

Pokorný, J. (2004). "Excitation of vibrations in microtubules in living cells." Bioelectrochemistry **63**(1): 321-326.

Pokorný, J. (2011). "Electrodynamic activity of healthy and cancer cells." J. Phys. Conf. Ser. **329**(1): 012007.

Pokorný, J., C. Vedruccio, M. Cifra and O. Kučera (2011). "Cancer physics: diagnostics based on damped cellular elastoelectrical vibrations in microtubules." Eur. Biophys. J. **40**(6): 747-759.

Pollack, G. H. (2013). The Fourth Phase of Water: Beyond Solid, Liquid, and Vapor. D. Scott. Seattle, WA, Ebner and Sons Publishers.

Pollack, G. H., I. L. Cameron and D. N. Wheatley (2006). Water and the cell. Dordrecht, Springer Verlag.

Robinson, P. C. and M. W. Davidson. (2000). "Introduction to Polarized Light Microscopy." Retrieved January 24th, 2016, from http://www.microscopyu.com/articles/polarized/polarizedintro.html.

Samal, S. and K. E. Geckeler (2001). "Unexpected solute aggregation in water on dilution." Chem. Commun.(21): 2224-2225.

Schurr, J. M. (2013). "Phenomena Associated with Gel–Water Interfaces. Analyses and Alternatives to the Long-Range Ordered Water Hypothesis." J. Phys. Chem. B **117**(25): 7653-7674.

Segtnan, V. H., S. Sasić, T. Isaksson and Y. Ozaki (2001). "Studies on the structure of water using two-dimensional near-infrared correlation spectroscopy and principal component analysis." Anal. Chem. **73**(13): 3153.

Shelton, D. P. (2014). "Long-range orientation correlation in water." J. Chem. Phys. **141**(22): 224506.

Shen, Y. R. and V. Ostroverkhov (2006). "Sum-frequency vibrational spectroscopy on water interfaces: polar orientation of water molecules at interfaces." Chem. Rev. **106**(4): 1140.

Shokr, M. and N. Sinha (2015). Laboratory Techniques for Revealing the Structure of Polycrystalline Ice. Sea Ice, John Wiley & Sons, Inc**:** 231-269.

Silva, I. B., J. C. Queiroz Neto and D. F. S. Petri (2015). "The effect of magnetic field on ion hydration and sulfate scale formation." Colloid. Surface A **465**: 175-183.

Sistat, P., A. Kozmai, N. Pismenskaya, C. Larchet, G. Pourcelly and V. Nikonenko (2008). "Low-frequency impedance of an ion-exchange membrane system." Electrochim. Acta **53**(22): 6380-6390.

Smothers, K. W. C., Charles D. ; Gard, Brian T. ; Strauss, Robert H. ; Hock, Vincent F. (2001). "Demonstration and Evaluation of Magnetic Descalers." Retrieved March 22, 2017, from http://oai.dtic.mil/oai/oai?verb=getRecord&metadataPrefix=html&identifier=ADA399455.

So, E., R. Stahlberg and G. Pollack (2012). Exclusion zone as intermediate between ice and water, WIT Press: Southampton, UK.

Stillinger, F. H. (1980). "Water revisited." Science **209**(4455): 451-457.

Summers, V. E. (2015, September 30). "I See Double! The Birefringence or Double Refraction of Calcite." Retrieved March 15, 2017, from http://www.quirkyscience.com/i-see-double-the-birefringence-or-double-refraction-of-calcite/.

Sun, Q. (2009). "The Raman OH stretching bands of liquid water." Vib. Spectrosc. **51**(2): 213-217.

Sverjensky, D. A. (2001). "Interpretation and prediction of triple-layer model capacitances and the structure of the oxide-electrolyte-water interface." Geochim. Cosmochim. Ac. **65**(21): 3643-3655.

Szcześ, A., E. Chibowski, L. Hołysz and P. Rafalski (2011). "Effects of static magnetic field on water at kinetic condition." Chem. Eng. Process. **50**(1): 124-127.

Takei, T., K. Mukasa, M. Kofuji, M. Fuji, T. Watanabe, M. Chikazawa and T. Kanazawa (2000). "Changes in density and surface tension of water in silica pores." Colloid and Polymer Science **278**(5): 475-480.

Takenaka, N., K. Sugimoto, S. Takami, K. Sugioka, T. Tsukada, T. Adschiri and Y. Saito (2013). "Application of Neutron Radiography to Flow Visualization in Supercritical Water." Physcs. Proc. **43**: 264-268.

Toledo, E. J. L., T. C. Ramalho and Z. M. Magriotis (2008). "Influence of magnetic field on physical–chemical properties of the liquid water: Insights from experimental and theoretical models." J. Mol. Struct. **888**(1–3): 409-415.

Totland, C., R. T. Lewis and W. Nerdal (2013). "Long-range surface-induced water structures and the effect of 1-butanol studied by 1H nuclear magnetic resonance." Langmuir **29**(35): 11055.

Verdaguer, A., G. M. Sacha, H. Bluhm and M. Salmeron (2006). "Molecular structure of water at interfaces: wetting at the nanometer scale." Chem. Rev. **106**(4): 1478-1510.

Vogler, E. A. (1998). "Structure and reactivity of water at biomaterial surfaces." Adv. Colloid Interfac. **74**(1–3): 69-117.

Wahlstrom, E. E. (1954). Optical crystallography. New York, J. Wiley & sons, inc.

Walker, D. (2004). "Examples of the animation of macro and microscopy subjects using sequential jpeg images." Retrieved 23rd January, 2016, from http://www.microscopy-uk.org.uk/mag/indexmag.html?http://www.microscopy-uk.org.uk/mag/artmay04/dwjpegcyc.html.

Wernet, P., D. Nordlund, U. Bergmann, M. Cavalleri, M. Odelius, H. Ogasawara, L. A. Naslund, T. K. Hirsch, L. Ojamae, P. Glatzel, L. G. Pettersson and A. Nilsson (2004). "The structure of the first coordination shell in liquid water." Science **304**(5673): 995-999.

Wiggins, P. M. and R. T. Van Ryn (1986). "The Solvent Properties of Water in Desalination Membranes." J. Macromol. Sci. A **23**(7): 875-903.

Yalamanchili, M. R., A. A. Atia and J. D. Miller (1996). "Analysis of interfacial water at a hydrophilic silicon surface by in-situ FTIR/internal reflection spectroscopy." Langmuir **12**(17): 4176-4184.

Yan, Y., X.-x. Ou and H.-p. Zhang (2014). "17O NMR and Raman spectra of water with different calcium salts." J. Mol. Struct. **1074**: 310-314.

Yoo, H., R. Paranji and G. H. Pollack (2011). "Impact of hydrophilic surfaces on interfacial water dynamics probed with N M R spectroscopy." J. Phys. Chem. Lett. **2**(6): 532-536.

Zhang, Z., L. Piatkowski, H. J. Bakker and M. Bonn (2011). "Communication: interfacial water structure revealed by ultrafast two-dimensional surface vibrational spectroscopy." J. Chem. Phys. **135**(2): 021101-021101.

Zheng, J.-M. and G. H. Pollack (2003). "Long-range forces extending from polymer-gel surfaces." Phys. Rev. E. **68**(3 Pt 1): 031408.

Zheng, J. M., W. C. Chin, E. Khijniak, E. Khijniak, Jr. and G. H. Pollack (2006). "Surfaces and interfacial water: evidence that hydrophilic surfaces have long-range impact." Adv. Colloid Interfac. **127**(1): 19-27.

Zheng, J. M., W. C. Chin, E. Khijniak, E. Khijniak, Jr. and G. H. Pollack (2006). "Surfaces and interfacial water: evidence that hydrophilic surfaces have long-range impact." Adv Colloid Interface Sci **127**(1): 19-27.

APPENDIX A

The following images are typical examples of materials in a microsphere suspension showing no EZ.

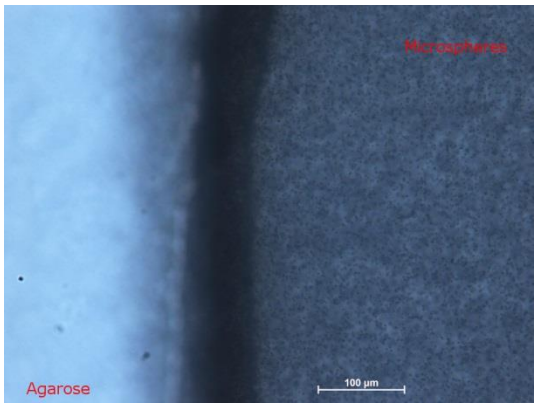

Figure 0-1 Agarose and microsphere suspension

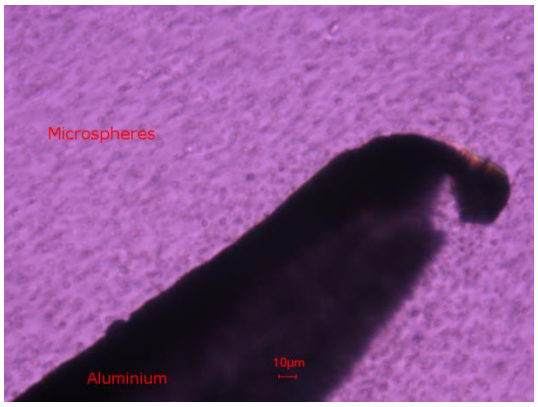

Figure 0-2 Aluminium and microsphere suspension

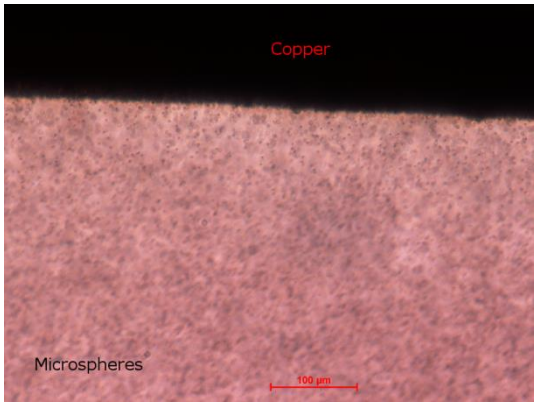

Figure 0-3 Copper and microsphere suspension

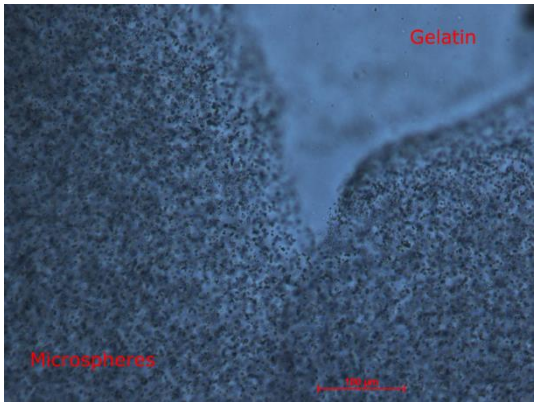

Figure 0-4 Gelatin and microsphere suspension

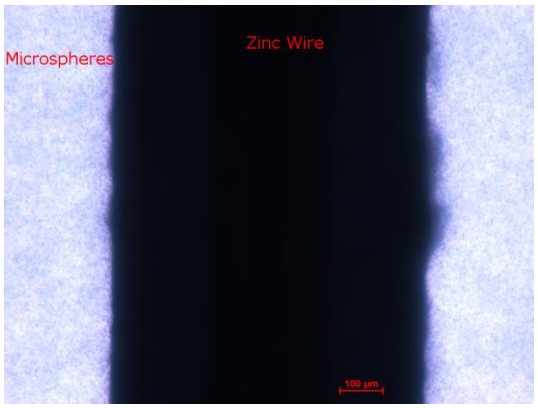

Figure 0-5 Zinc Wire and microsphere suspension